

# **The Jan Mayen Microcontinent Project Database and Seafloor Mapping of the Dreki Area**

**Input Data, Geological and  
Geomorphological Mapping and Analysis**

Anett Blischke  
Ögmundur Erlendsson  
Gunnlaugur M. Einarsson  
Víkingur L. Ásgeirsson  
Sigurveig Árnadóttir

Prepared for Orkustofnun  
National Energy Authority of Iceland

ÍSOR-2017/055

**ICELAND GEOSURVEY**

**Reykjavík:** Orkugardur, Grensásvegur 9, 108 Reykjavík, Iceland - Tel.: 528 1500 - Fax: 528 1699

**Akureyri:** Rangárvellir, P.O. Box 30, 602 Akureyri, Iceland - Tel.: 528 1500 - Fax: 528 1599

**isor@isor.is - www.isor.is**

# The Jan Mayen Microcontinent Project Database and Seafloor Mapping of the Dreki Area


## Input Data, Geological and Geomorphological Mapping and Analysis

Anett Blischke  
Ögmundur Erlendsson  
Gunnlaugur M. Einarsson  
Víkingur L. Ásgeirsson  
Sigurveig Árnadóttir

Prepared for Orkustofnun /  
National Energy Authority of Iceland





Report no. ÍSOR-2017/055	Date September 2017	Distribution <input type="checkbox"/> Open <input checked="" type="checkbox"/> Closed to Sept. 2020
Report name / Main and subheadings The Jan Mayen Microcontinent Project Database and Seafloor Mapping of the Dreki Area. Input Data, Geological and Geomorphological Mapping and Analysis.		Number of copies 4
		Number of pages 79 + Appendices A to J
Authors Anett Blischke, Ögmundur Erlendsson, Gunnlaugur M. Einarsson, Víkingur L. Ásgeirsson and Sigurveig Árnadóttir		Project manager Anett Blischke
Classification of report Confidential data analysis report		Project no. 16-0039 / 17-0021
Prepared for Orkustofnun / National Energy Authority of Iceland		
Cooperators		
Abstract <p>This project is part of a regional exploration study for assessing the possibility of hydrocarbon resources in the area, and is conducted for the National Energy Authority of Iceland (NEA) with its focus on the development of the Jan Mayen Micro-Continent (JMMC) and its southern continuation into the northeastern Iceland Plateau. The study was initiated in 2008 with a thorough database review and compilation as a digital dataset in the GIS ArcMap (ESRI) and Petrel (Schlumberger) project environments, in order to form a basis to build on existing geophysical, geological and geochemical databases for seafloor research. The purpose of this report is to summarize data, research conducted and interpretations in regards to all available information for the region, such as bathymetry, gravity, and magnetic data, as well as sub-surface seismic refraction and multi-channel reflection seismic data, etc. Seafloor data is a fundamental and first observation for any following geological and geophysical mapping interpretations. Here, shallow processes that affect the individual ridge segments of the JMMC were investigated. Resulting observations are key elements for further structural elements work, studying structural processes and possible outcrop characteristics, planning of seafloor sampling campaigns, and seafloor risk analysis.</p>		
Key words Jan Mayen Ridge, microcontinent, Dreki, database, seafloor sampling, reflection seismic, magnetic, gravity, multibeam, backscatter, gravity coring, ROV sampling, Orkustofnun, ÍSOR		ISBN-number
		Project manager's signature 
		Reviewed by Sigvaldi Thordarson



## Table of contents

<b>1</b>	<b>Introduction</b>	<b>9</b>
<b>2</b>	<b>Geophysical subsea database</b>	<b>9</b>
2.1	Gravity and magnetic data sets	13
2.2	2D multi-channel reflection seismic data	15
2.3	Seismic refraction data	20
2.4	Satellite analysis and remote sensing for oil seepage data	22
2.4.1	University of Iceland oil slick data surveys in 2006, 2007 & 2008	22
2.4.2	NPA oil slick data survey in 2009	23
<b>3</b>	<b>Bathymetry</b>	<b>24</b>
3.1	Multibeam – initial high resolution data set analysis	29
3.1.1	Submarine landslides and slump – slump faulting	31
3.1.2	Normal faulting	36
3.1.3	Strike-slip faulting	37
3.1.4	Channelling and water current erosion	41
3.1.5	Ice plough marks	42
3.1.6	Pockmarks	44
3.1.7	Polygonal fault pattern	49
3.2	Multibeam backscatter	52
<b>4</b>	<b>Borehole and seafloor sampling database</b>	<b>55</b>
4.1	Boreholes	55
4.1.1	The Jan Mayen Ridge wells - DSDP boreholes, 1974	56
4.2	Seafloor sampling and benthic surveys	58
4.2.1	NEA-NPD, Dreki Sea floor sampling campaign 2010	61
4.2.2	NPD seafloor sampling survey, 2011 & 2012	64
4.2.3	TGS-VPBR seafloor sampling survey, 2011	66
<b>5</b>	<b>Conclusion &amp; future recommendation for seafloor research</b>	<b>72</b>
<b>6</b>	<b>References</b>	<b>74</b>
<b>7</b>	<b>Additional references</b>	<b>78</b>
	<b>Appendix A: Jan Mayen microcontinent bathymetry data interpretation</b>	
	<b>Appendix B: Scanned hardcopy displays</b>	
	<b>Appendix C: Scanning list</b>	
	<b>Appendix D: Project 2DMCS digital database list until 2010</b>	
	<b>Appendix E: Regional 2DMCS data prior 2001</b>	
	<b>Appendix F: 2DMCS data 2001-2012</b>	
	<b>Appendix G: Seismic refraction data listing</b>	

<b>Appendix H: Map displays of additional examples of gravitational seafloor structures and sea current features .....</b>	
<b>Appendix I: Map displays of additional examples for fault structures encountered at seafloor.....</b>	
<b>Appendix J: Additional map displays for multibeam- and amplitude features in regards to sediment type and alteration .....</b>	

## List of tables

Table 1. <i>Listing of pre-2008 surveys in the Jan Mayen area. ....</i>	11
Table 2. <i>Listing of surveys on the Jan Mayen area since 2008. ....</i>	13
Table 3. <i>Data sources for bathymetry and elevation datasets of the NAGTEC project .....</i>	25
Table 4. <i>Boreholes in the Jan Mayen area, drilled during Leg 38 of the Deep Sea Drilling Project in 1974.....</i>	56
Table 5. <i>A11-2010 Piston coring survey samples, supervised and analysed by Fugro Norway. ....</i>	62

## List of figures

Figure 1. <i>Project area location and exploration licenses .....</i>	10
Figure 2. <i>Data coverage of the Jan Mayen extended regional project .....</i>	12
Figure 3. <i>Free air gravity data for the Middle East-Greenland-JMMC-Norway shelf corridor .....</i>	14
Figure 4. <i>Magnetic Anomaly data for the Middle East-Greenland-JMMC-Norway shelf corridor and Iceland .....</i>	14
Figure 5. <i>Magnetic survey data coverage for the JMMC and Norway basin areas .....</i>	15
Figure 6. <i>2D multi-channel seismic reflection (2DMCS) data line display for the project area for data prior to 2001. ....</i>	16
Figure 7. <i>Bathymetry map showing shallow borehole locations and 2D MCS data within the study area .....</i>	17
Figure 8. <i>NPD 2D multichannel surveys 2011 &amp; 2012 .....</i>	18
Figure 9. <i>JMR15 multichannel survey operated by CNOOC and conducted by CGG-Veritas in September 2015.....</i>	19
Figure 10. <i>Refraction data locations in and around the JMMC area for OBS seismic surveys .....</i>	21
Figure 11. <i>Herring ships and associated slick on June 18th 2007 .....</i>	22
Figure 12. <i>NPA oil seep data interpretations in 2009 with red polygons of satellite image coverage and image id .....</i>	23
Figure 13. <i>Bathymetry data coverage for the central North Atlantic of the NAGTEC projec .</i>	26

Figure 14. Bathymetry grid data layer for the Jan Mayen Ridge within the Iceland Continental Shelf Portal, based on the bathymetry map by Åkermoen (1989).....	26
Figure 15. Overview of the A8-2008 bathymetry data in the Iceland Continental Shelf Portal. ....	27
Figure 16. Overview map (ÍSOR, 2010) of the A11-2010 bathymetry data acquired during the seafloor sampling campaign of NEA, NPD & MRI. ....	28
Figure 17. Location map for the A8-2008 & A11-2010 surveys data displays and 2D seismic reflection line locations. ....	30
Figure 18. The larger of the two landslides has an area of approx. 28.35 km <sup>2</sup> and is located to the north of Buðli Knoll .....	31
Figure 19. The smaller landslide, with an area of approx. 3.98 km <sup>2</sup> , is located on the eastern flank of Lyngvi's southern tip.....	32
Figure 20. Seismic profile showing gravitational slumping on Sigurður Knoll near CDP 4360.....	33
Figure 21. Seismic profile of Sigurður Knoll showing slumping due to subsidence along the eastern flank of the JMMC from CDP 7000 to the east. ....	34
Figure 22. The eastern flank of Otur Ridge is dominated by slumps and their seafloor surface edges are here marked with black lines.....	35
Figure 23. Seismic profile showing normal faulting, slightly transpressional fault sets, slump faulting and sliding plain, or scouring and sediment drift surfaces on top of the Sigurður Knoll, along 2D seismic reflection profile JM-11-0020-NPD2011.....	36
Figure 24. Normal faults on the Sigurður (NE) and Reginn (SW) knolls .....	37
Figure 25. Regional transfer systems that affected the flanks of the JMMC during at least 5 stages.....	38
Figure 26. Regional transfer systems affecting the central area of the microcontinent. ....	39
Figure 27. Borehole DSDP 38-350 tie-line showing fault trends that indicate at least 2 structural events .....	40
Figure 28. Left: Locations of the CTD-stations that record conductivity, temperature at water depth with the associated water depth pressure, and the three moorings across the Jan Mayen Ridge area. Right: Average velocities at 50 m depth and near bottom.....	42
Figure 29. Very large ice plough marks on the Otur Ridge plateau, the largest of which has a maximum width of around 400 m.....	43
Figure 30. The Lyngvi Ridge plateau has a high density of ice plough marks .....	44
Figure 31. A11-2010 multibeam data review in comparison to the 1989 point features assumed to be pock marks, which are related to ice plough and erosional marks.....	45
Figure 32. Possible pockmark locations based on the original 1985 2D multi-channel seismic reflection data and coarse gridded bathymetry data.....	46
Figure 33. Seismic section example over a pockmark.....	47
Figure 34. Line JM-85-14, 5 pockmarks on top of the Jan Mayen Ridge were interpreted on this line but the data quality makes an interpretation inconclusive, especially with the deeper apparent faulting and possible slumping at the edge of the structure. ....	47

Figure 35. Sea floor surface marks showing primarily a small scale popup-fault structure at the centre of the ridge. ....	48
Figure 36. Pockmark-like depressions on the ridge structure in Fáfnisrenna Channel .....	48
Figure 37. Pockmark-like depressions on Otur Ridge.....	49
Figure 38. Dewhurst et al. (1999) published an analogue case of polygon faulting .....	50
Figure 39. JMMC example of polygonal faults (yellow box) vs. structural faults (light blue box) within the southeastern most data extent of the Dreki area, along line IS-JMR-01-80 (vertical scale is in two-way travel time and the exaggeration is 4). For location, see Figure 17.....	50
Figure 40. Overview map of the polygonal fault pattern areas.....	51
Figure 41. Overview map of the backscatter amplitude .....	52
Figure 42. The amplitude data contained linear artefacts correlating with the survey vessel's (inferred) sailing route and possible "edge effects" indicating that there was not enough overlap between the data sweeps .....	53
Figure 43. Reginn Knoll showing high amplitude values on its slopes .....	53
Figure 44. Low amplitude values can be seen clearly in Fáfnisrenna Channel and at the southern margin of the Völsungur area .....	54
Figures 45. Location of the DSDP and ODP boreholes for the East Greenland - Jan Mayen - Norway Basin corridor. ....	55
Figure 46. Jan Mayen Ridge well correlation panel tied to the JM-85 seismic data set.....	57
Figure 47. Location map of gas measurements during the 1971 and 1973 surveys. ....	59
Figure 48. Location of samples taken in MRI's benthic survey .....	60
Figure 49. Sample sites locations of the 2010 seafloor sampling campaign, with the Russian seafloor samples for comparison, and the Dreki licensing area outline.....	61
Figure 50. NPD sampling stations for ROV surveys in 2011 and 2012.....	65
Figure 51. Outcrop correlations within the Icelandic sector of the Jan Mayen Ridge of the 2012 ROV samples and the NPD2011 2D reflection seismic data.....	66
Figure 52. Local setting of the A8-2011 seafloor sampling profile by VPBR-TGS, just south of a slope spur, and possibly a large slumped block. ....	68
Figure 53. Northeast to southwest 2DMCS profile for the NE Dreki sampling sites NPD-VPBR .....	69
Figure 54. Local setting of the A8-2011 seafloor sampling campaign by VPBR-TGS viewing the sampling site looking east onto the fault escarpment and well visible spur just north of the sampling profile.....	70
Figure 55. Interpretation comparison for the NPD, VPBR and ÍSOR-OS cases .....	71

# 1 Introduction

This project is part of a regional exploration study for assessing the possibility of hydrocarbon resources in the area, and is conducted for the National Energy Authority of Iceland (NEA), see Figure 1. A key part here is the study of the Jan Mayen Micro-Continent (JMMC) and its southern continuation into the north-eastern Iceland Plateau using bathymetry, gravity, and magnetic data, as well as sub-surface seismic refraction and multi-channel reflection seismic data to conduct sequence stratigraphy and tectonic research, including basin and petroleum systems analysis.

The purpose of this report is to summarize data, research conducted and interpretations in regards to the seafloor in the greater Jan Mayen Ridge area. Bathymetry data is a fundamental and first observation (Hopper et al., 2014) that is needed for basic geological and geophysical mapping and interpretations, especially to understand the shallowest processes of the individual ridge segments.

The study was initiated in 2008 with a thorough database review (Appendix B & C) and compilation of a digital dataset in the ArcView (ESRI) and Petrel (Schlumberger) environments, in order to form a basis for seafloor research, which is built on existing geophysical, geological and geochemical databases.

Seafloor data and observations are key elements for planning seafloor sampling campaigns, performing seafloor risk analysis, or when conducting further structural elements work by studying structural processes and possible outcrop characteristics that would be based on the compiled high-resolution datasets.

## 2 Geophysical subsea database

Considerable data compilations was carried out between 2008–2011, both for data and interpretative data of the initial research stage that was conducted in the 1980's and early 1990's (Gunnarsson et al., 1989). In 2011 a large scale data compilation project started, which was conducted by the Northeast Atlantic Geoscience Tectono-stratigraphic Atlas (NAGTEC) research group (<http://www.nagtec.org/home.seam>), operated by the geo-surveys bordering the North Atlantic region on the European side (GEUS, NGU, BGS, Jarðfeingi, TNO, ÍSOR, GSI and GSNI). The compilation is proprietary until June 2016 for the paper Atlas and June 2019 for the digital dataset.

The NAGTEC Atlas project enabled us to include up to date regional gravity and magnetic anomaly data sets as well (Hopper et al., 2014), see Figure 2 to Figure 4.



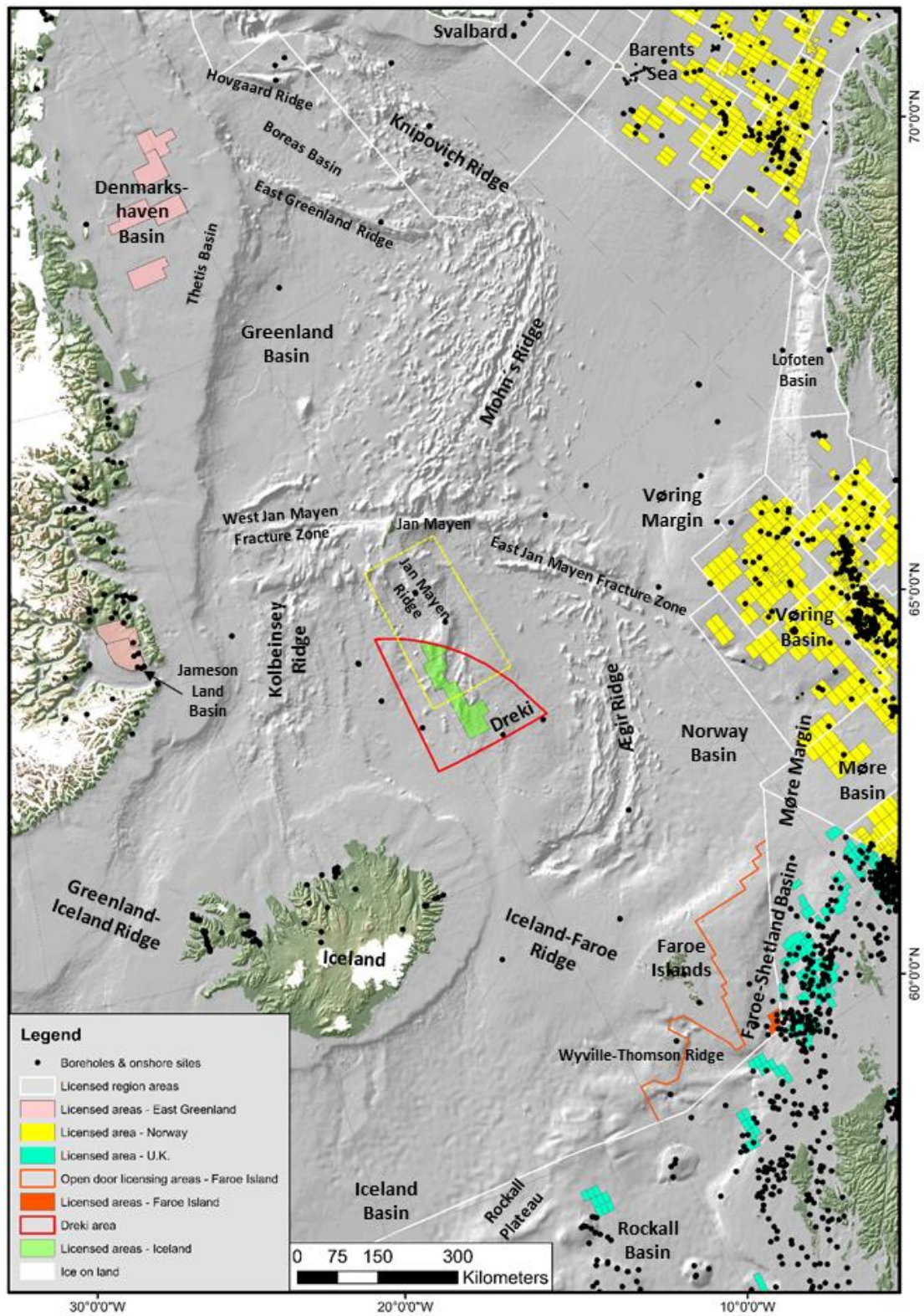


**Figure 1.** Project area location and exploration licenses. The Møre-Vøring Basins of the Norwegian margin and the Faroe-Shetland Basin are proven hydrocarbon provinces to the east and southeast of the JMMC area.



**Table 1.** Listing of pre-2008 surveys in the Jan Mayen area.

Year	Survey ID	Acquisition	Country	Repository	Data types
1957		NAVO	USA		Aeromagnetic
1961-1971	V2304/V2703/ V2803	L-DGO	USA	NGDC	Bathymetry; Magnetics; Gravity; Seismic
1973	V3010	L-DEO	Norway		Bathymetry; Magnetics; Gravity; Seismic
1974	DSDP Leg 38	DSDP		IODP	Borehole logging & coring
1975	CEPAN-75	CNEXO	France	Ifremer	Bathymetry; Magnetics; Gravity; Seismic
1975	BGR-75	BGR	Germany	BGR	Seismic
1976	BGR-76	BGR	Germany	BGR	Seismic
1976	CGG-76	NPD/CGG	Norway		Aeromagnetic
1977	IOS-77	UD/IOS	England	NGDC	Seismic
1978	UiB-78	UiB	Norway	UiB	Seismic
1978	RC2114	L-DGO	USA	MGDS	Bathymetry; Magnetics; Gravity; Seismic
1978	WGC-78		USA	WesternGeco	Seismic
1979	J-79	NPD	Norway	NPD	Bathymetry; Magnetics; Gravity; Seismic
1980	Cruise 10	PAH/SGC	USSR		Seafloor sampling
1983	NGT83 / RC2412	L-DGO/BGR	USA/Germany		Seismic, ESP, WA, CDP
1983	RC2412	L-DEO	Norway		Seismic (MCS & SCS), Gravimeter, Magnetometer, Sonar-Echosounder
1984	Arktis II/5	UHH	Germany		Refraction seismic
1985	JM-85	NPD; NEA	Norway	NPD	Bathymetry; Magnetics; Free Air Gravity; Bouguer Gravity; Seismic
1985	ODP Leg 104	ODP			Boreholes
1986	UiO-86	UiO	Norway	NPD	Seismic
1987	ESP	IFP	France		ESP; Velocity; Gravity
1988	JM-88	NPD/NEA	Norway	NPD	Bathymetry; Magnetics; Gravity; Seismic
1993	ODP Leg 151	ODP	U.S.A.	IODP	Borehole logging & coring
1995	JMKR-95	UoB & Hokkaido	Norway	UoB	Refraction seismic
1995	ODP Leg 162	ODP	U.S.A.	IODP	Borehole logging & coring
2000	KRISE	UoB et al.	Norway	UoI (Bryndís Brandsdóttir)	Ocean Bottom Seismographs (OBS)
2000	OBS 2000	UoB e al.	Norway	UoB	Refraction seismic; Ocean Bottom Seismographs (OBS)
2001	IS-JMR-01	InSeis	Norway	CGGVeritas	Seismic
2002	ICE-02	TGS-Nopec	Iceland	TGS-NOPEC	Seismic; Gravity
2003	EW0307	L-DEO	USA	MGDS	Seismic; Gravity; Bathymetry; Cores
2005	JAS-05	NGU	Norway	NGU	Aeromagnetic
2006	OBS-JM-2006	UoB	Norway	UoB (Kandilarov)	Refraction seismic; Ocean Bottom Seismographs (OBS)
2006	OBS-JM-06	UiB/Geomar	Norway/Germany	UiB	Seismic, gravity, magnetics
2007	NB-07	NGU	Norway	NGU	Aeromagnetic

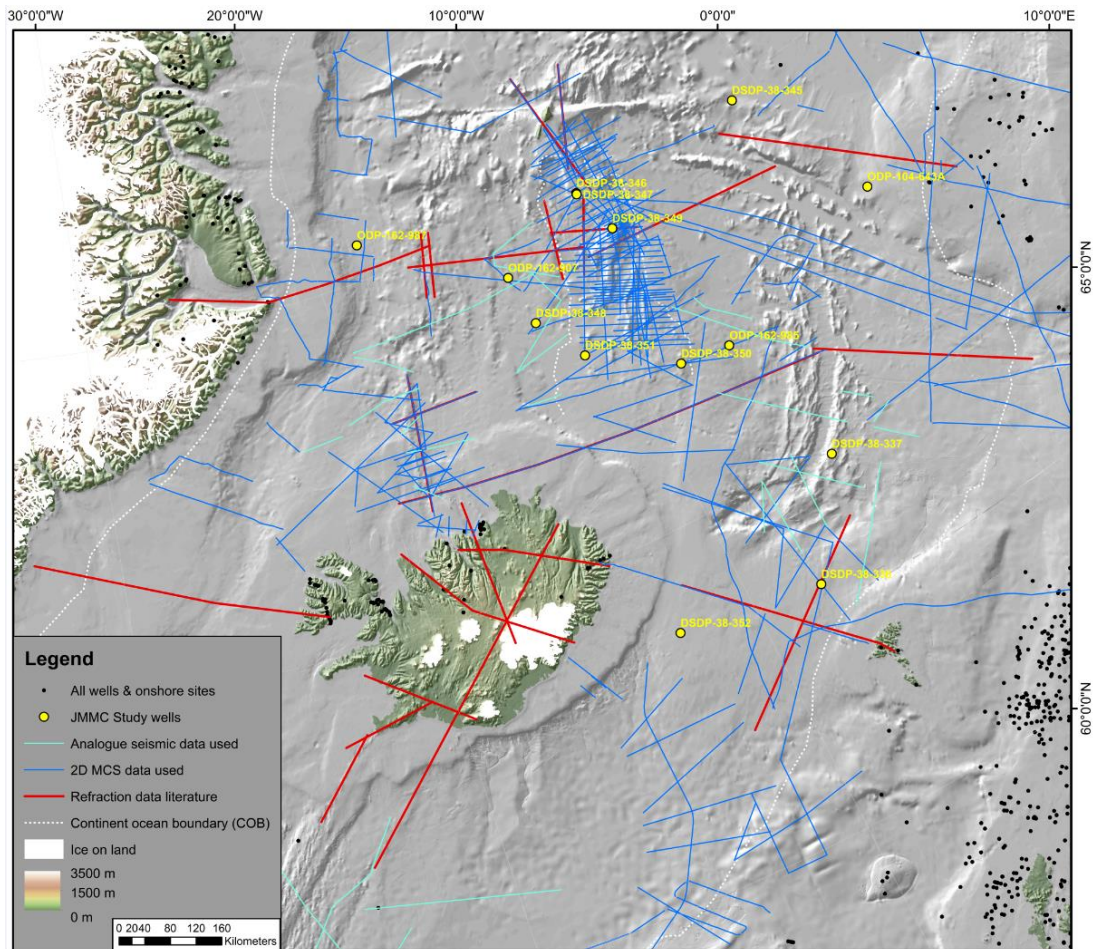


**Figure 2.** Data coverage of the Jan Mayen extended regional project. Displayed blue lines are 2D multi-channel seismic reflection line data prior to 2009, turquoise lines are analogue reflection seismic data, red lines are seismic refraction data, black dots represent offshore boreholes and onshore site locations, and yellow dots mark the key offshore well control.

For the Jan Mayen study (Figure 1 & Figure 2) we use primarily digital datasets of bathymetry and multibeam sonar data that were cross-checked with existing 2D multi-channel reflection seismic data surveys from 1978, 1979, 1985, 1988, 2001, 2002, 2008, 2011 & 2012, refraction seismic data surveys from 1995, 2000 and 2006, analogue single channel seismic reflection data of various vintages, shallow borehole data acquired through the DSDP and ODP program in 1974, 1993 and 1995, and seafloor samples obtained in 2010–2012.

Since 2008 (Table 2) the focus has been to implement a digital database, which did not exist, and to improve the data quality, add new quality data, and add to the understanding of the micro-continent. This was accomplished not only by running up to date reflection seismic surveys with the aim to improve the understanding of the sub-basalt stratigraphy, but also by reprocessing vintage seismic reflection data, e.g. JM-85-88-2009 (Table 2), and obtaining direct evidence in the form of seafloor samples taken at seafloor outcroppings, which show stratigraphy layers. High-resolution magnetic surveys were added in the Norway basin in 2005 (JAS-05), 2007 (JAS-07), and in 2012 (JAS-12) that improve considerably the geochronological interpretation of the area east of the micro-continent and better define its eastern limit.

**Table 2.** *Listing of surveys on the Jan Mayen area since 2008.*

Year	Survey ID	Conducted by	Country	Data repository	Data types
2008	WI-JMR-08	InSeis	Norway	CGGVeritas	Seismic
2008	A8-2008	NEA & MRI	Iceland	MRI	Multibeam bathymetry
2008	B11-2008	MRI	Iceland	MRI	Benthic survey
2009	JM-85-88-2009	Spectrum	Norway	Spectrum AS	Reprocessed seismic
2009	OS-2009	NEA & UoI	Iceland	UoI	Oil slick survey
2010	A201011	NPD/NEA	Iceland-Norway	NPD & MRI	Multibeam bathymetry
2010	A11-2010	NEA/NPD	Iceland-Norway	Fugro	Seafloor sampling
2011	ROV 2011	NPD	Norway	NPD	Seafloor sampling
2011	JMRS11	TGS-VPBR	Norway	TGS-VPBR	Seafloor sampling
2011	NPD 2011	NPD	Norway	NPD	Bathymetry; Magnetics; Free Air Gravity; Seismic
2012	NPD 2012	NPD	Norway	NPD	Bathymetry; Magnetics; Free Air Gravity; Seismic
2012	ROV 2012	NPD	Norway	NPD	Seafloor sampling
2012	JAS-12	NGU	Norway	NGU	Magnetic survey
2015	JMR15	CGG-Veritas	China	CNOOC	Bathymetry; Magnetics; Free Air Gravity; Seismic

## 2.1 Gravity and magnetic data sets

Prior to the NAGTEC Atlas project, which enabled us to include up to date North Atlantic regional gravity and magnetic anomaly data sets (Hopper et al., 2014), see Figure 3 & Figure 4, the Jan Mayen project had limited regional data available. Gravity and magnetic data in the pre-2011 JMMC database, was primarily collected as line data acquisitions accompanying the seismic reflection surveys in 1988 & 1989.

The first gravity and magnetic studies in the area were conducted by Talwani & Udintsev (1976), Talwani & Eldholm (1977), Grönlie et al. (1979) and Vogt et al. (1980), who pointed out that the magnetic anomaly over the Jan Mayen area is relatively calm compared to surrounding areas, thus highlighting the area for further studies and investigations.



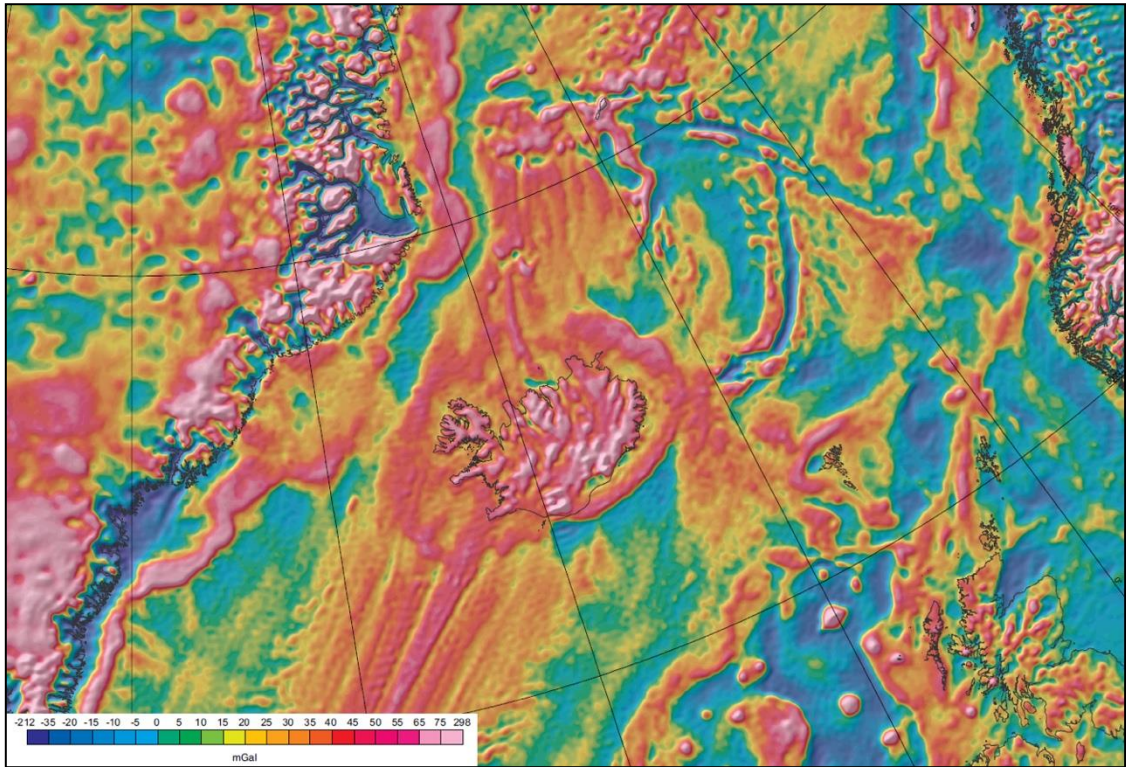


**Figure 3.** Free air gravity data for the Middle East-Greenland-JMMC-Norway shelf corridor (NAGTEC Atlas, Hopper et al., 2014).

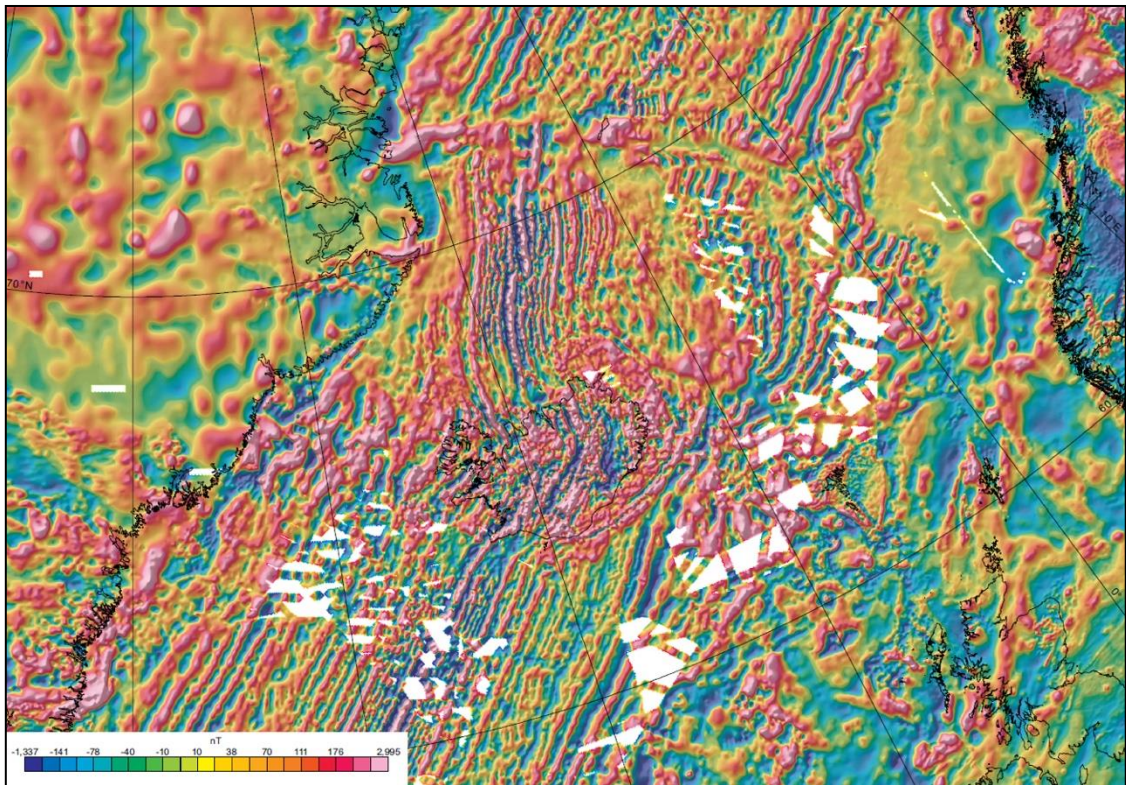


**Figure 4.** Magnetic Anomaly data for the Middle East-Greenland-JMMC-Norway shelf corridor and Iceland (NAGTEC Atlas, Hopper et al., 2014).

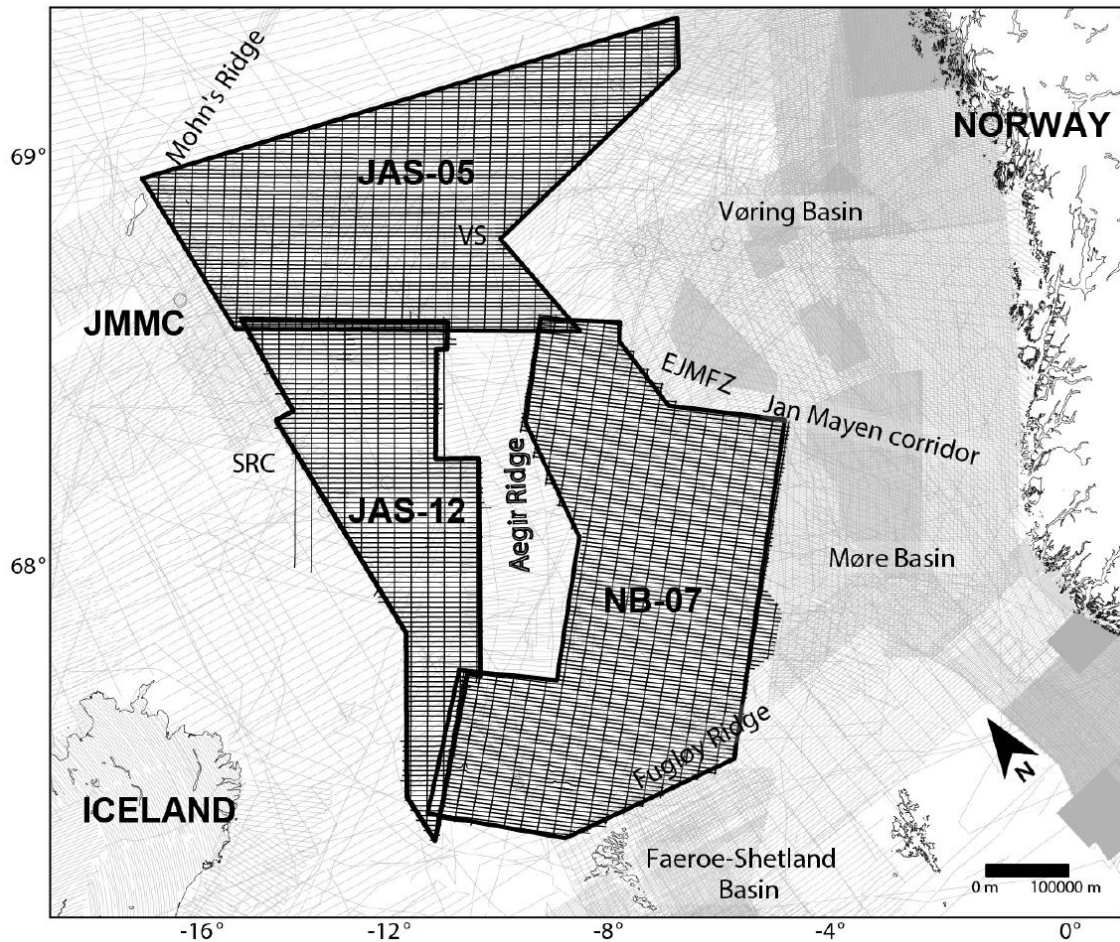


**Figure 5.** Magnetic survey data coverage for the JMMC and Norway basin areas (Gernigon et al., 2014), see Table 1 and Table 2 for survey details. NGU surveys JAS-05 (2005) and NB-07 (2007) were included in the compilation by Gernigon et al. (2015).

Since then, the area has been re-visited repeatedly, especially by NGU, to map the eastern flank of the JMMC within the Ægir ridge system and the Norwegian shelf (Figure 5). These new high-resolution magnetic grid data sets helped to better understand the breakup and ridge forming processes of the eastern flank of the JMMC within the Ægir ridge system and the Norwegian shelf. Proprietary study results (Gernigon et al., 2014, 2015) are helpful in assisting with the clarification of the micro-continent extent.

## 2.2 2D multi-channel reflection seismic data

2D multi-channel reflection seismic (MCS) surveys were available in paper, film, or digital format for the data set prior to 2001 (Table 1, Figure 6 & Appendix D & E). The primary digital datasets used for the JMMC area are shown in Figure 7 to Figure 9 and are listed in Table 1 & Table 2. Detailed line information is given in Appendices E & F.



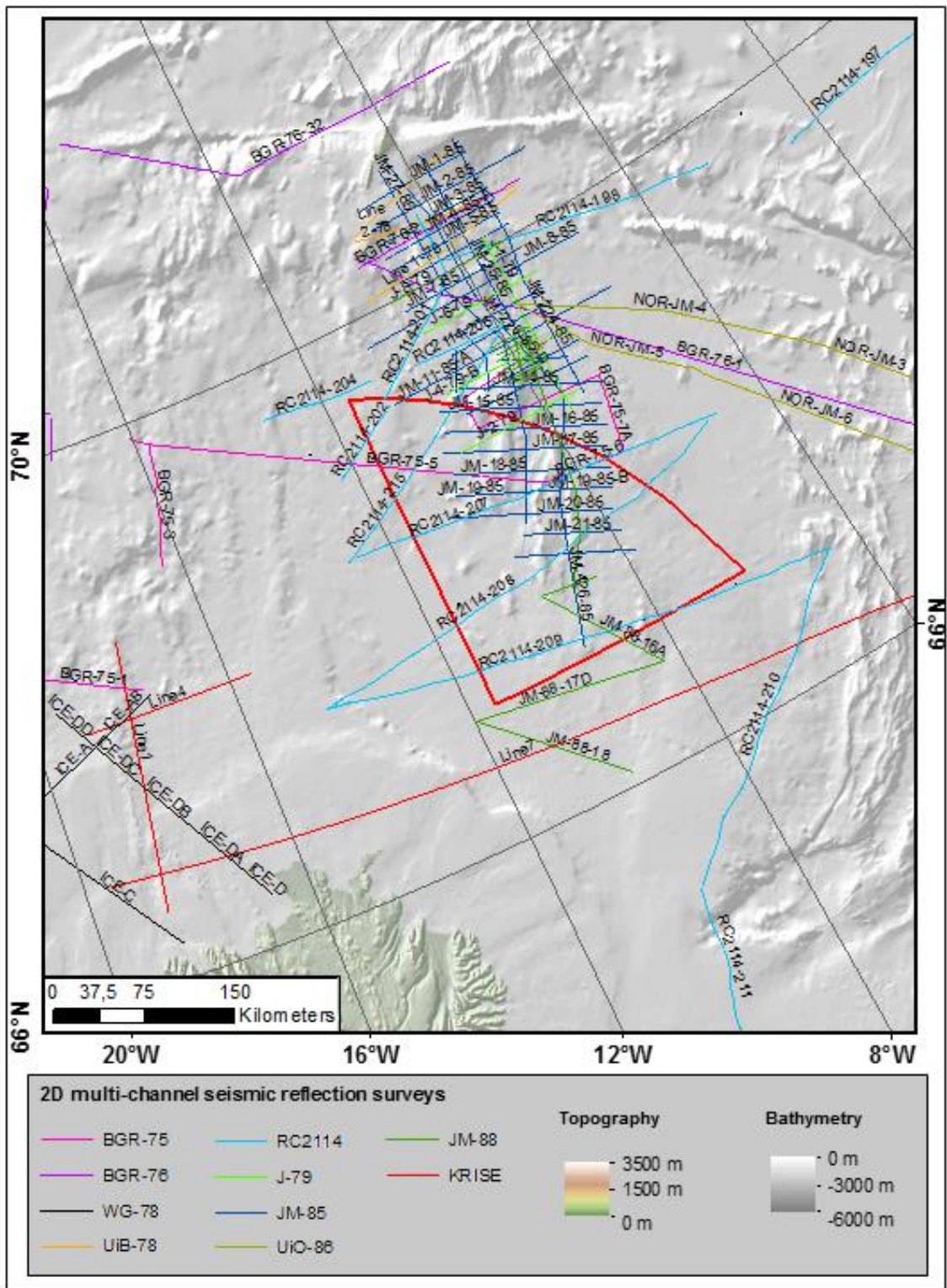


**Figure 6.** 2D multi-channel seismic reflection (2DMCS) data line display for the project area for data prior to 2001.

Most of that data used for the Jan Mayen exploration project are the data acquired and reprocessed since 2008, as data quality has improved a lot, especially for deeper section imaging. The latest surveys by NPD (in 2011 & 2012) have improved the quality of the Tertiary

section considerably, but still have not solved the sub-basalt imaging issues for the youngest (Late Oligocene – Early Miocene) flood basalt cover over the flank areas of the micro-continent. The most recent survey was conducted in September 2015 by CGG-Veritas for CNOOC (Figure 9), and its processing stage was finished in 2016. This dataset shows promising sub-basalt images along the Jan Mayen Trough, and east and west Jan Mayen Ridge flank areas of the micro-continent.

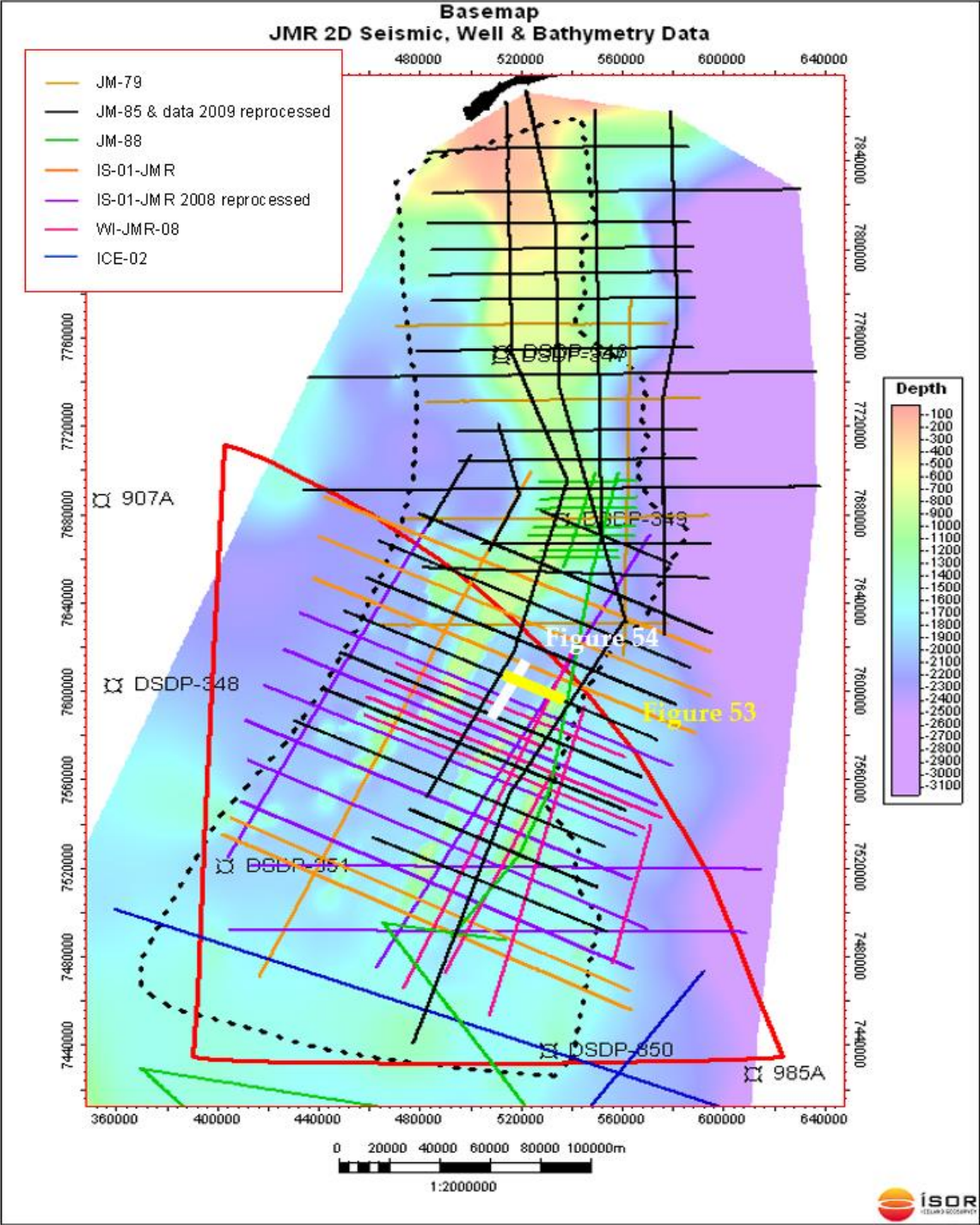


**Figure 7.** Bathymetry map showing shallow borehole locations and 2D MCS data within the study area. The black dashed line marks the extent of the JMMC based on presently analysed data and the red polygon represents the outline for the Dreki area.



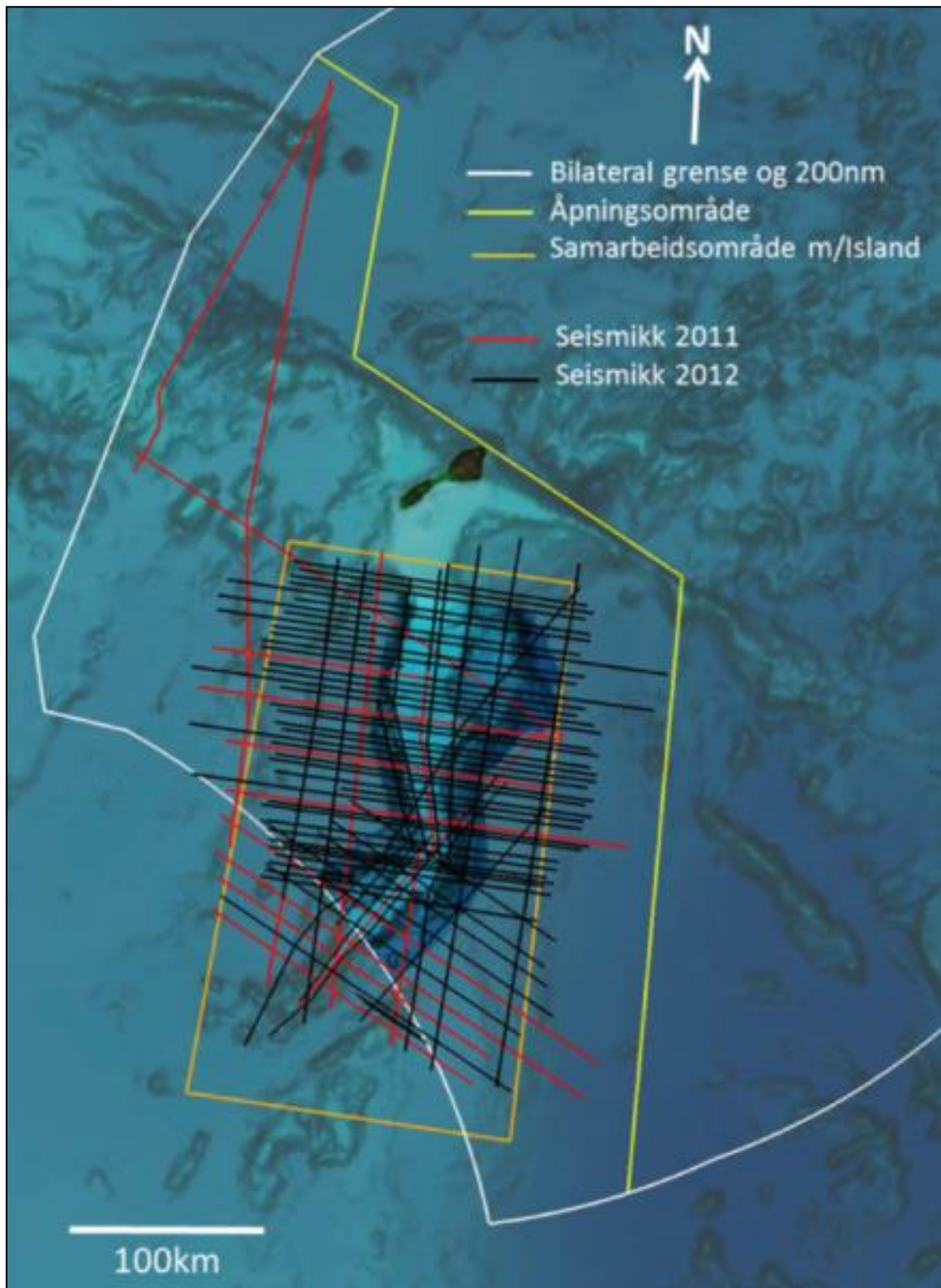


**Figure 8.** NPD 2D multichannel surveys 2011 & 2012 (Sandstå et al., 2013).



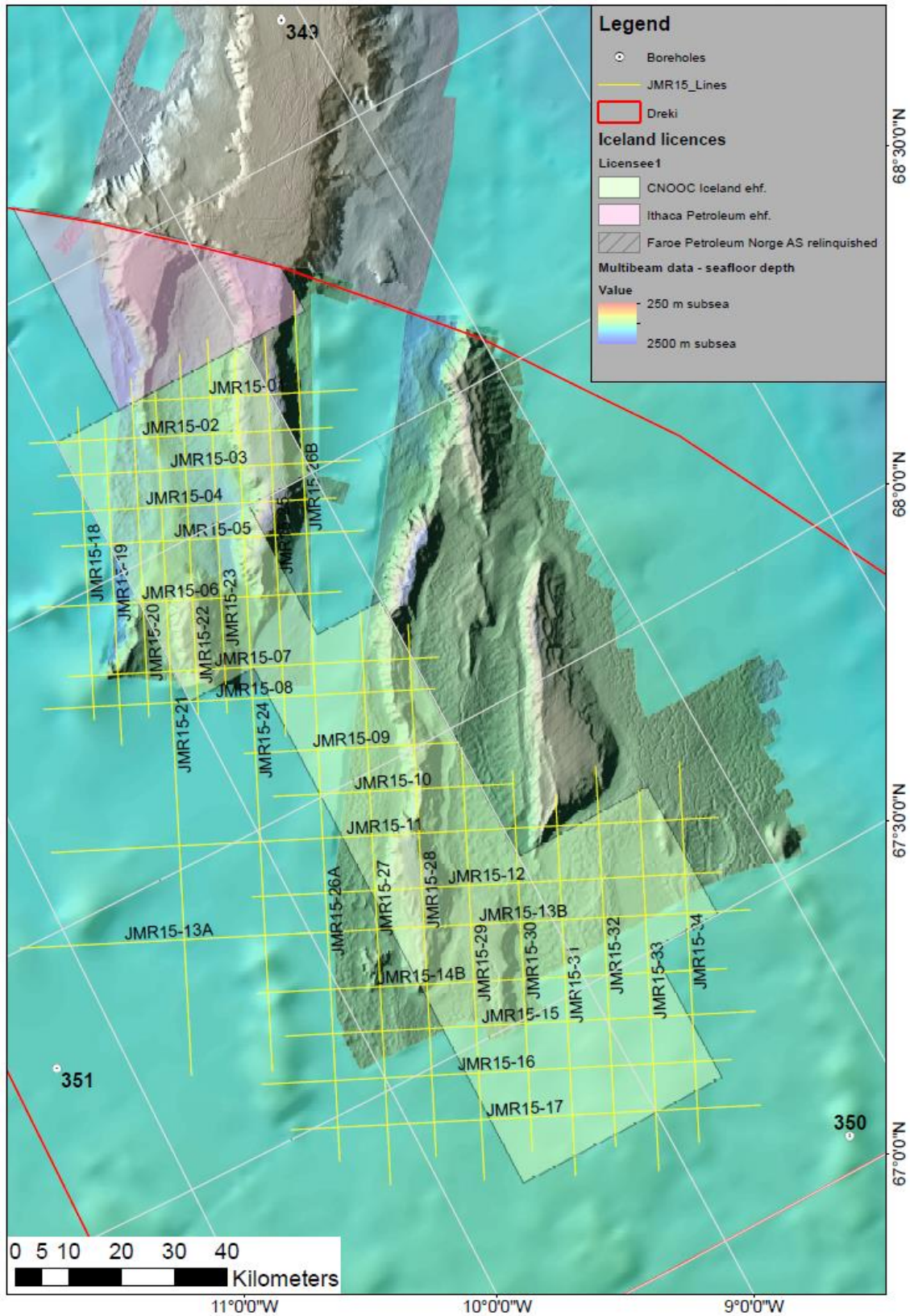


Figure 9. JMR15 multichannel survey operated by CNOOC and conducted by CGG-Veritas in September 2015.

The first multi-channel seismic reflection survey (CEPAN-75 in Table 1) was carried out in 1975 and survey results were published by Gairaud et al. (1978). This dataset exists in paper and film format only and line location data could unfortunately not be recovered.

Some early regional 2D multi-channel seismic reflection surveys were conducted for the greater Northeast Atlantic region, some of which crossed the JMMC area, mainly the surveys BGR-75, BGR-76 (Hinz & Schlüter, 1979), and RC2114 (Talwani et al., 1981; Mutter et al., 1984; Shipley et al., 2012) and are listed in Table 1, Figure 7 to Figure 9.

The first datasets that focused on the JMMC (J-79, JM-85 & JM-88; Table 1 & Figure 7) were acquired and interpreted by Åkermoen (1989), Gunnarsson et al. (1989) and Gunnarsson (1995), both to document data coverage and quality in the greater JMMC region at the time, and to describe the general structural build-up of the micro-continent and define the primary stratigraphic sequences.

In 2009, reprocessed 2D seismic reflection data of surveys JM-85 & 88 was reviewed and interpreted by Erlendsson (2010) as part of a MSc. study. The original and original JM-85 and JM-88 datasets in combination with the IS-JMR-01 (2001) data, were reviewed and interpreted by Peron-Pinvidic in 2012 (a, b) for a tectonostratigraphic analysis of the area.

Since 2011, the NPD high resolution datasets enable a considerable improvement of structural and facies interpretations, also over a much larger area by combining the datasets and interpretation of vintage data (pre-2000) with the more recent surveys that included the IS-JMR-01 (2001), ICE-02 (2002), WI-JMR-08 (2008), NPD-11 (2011), and the NPD-12 (2012). This led to a composite JMMC area analysis that is conducted in an ongoing study (Blichke et al., 2016) for detailed volcano-stratigraphic seismic characterizations, which facilitated mapping and identification of structural elements, sedimentary sequences, seaward dipping reflector sequences, and sill and dyke complexes.

The JMR15 seismic reflection dataset is the most recent proprietary dataset and was acquired by CGG-Veritas for CNOOC in 2015. The dataset is presently in review and being interpreted for the National Energy Authority of Iceland.

### **2.3 Seismic refraction data**

Several Ocean bottom seismic (OBS), sonobuoy, and expanded seismic profiling (ESP) refraction surveys and experiments have been conducted in and around the area since 1985 (Johansen et al., 1988; Olafsson & Gunnarsson, 1989; Kodaira et al., 1998; Mjelde et al., 2002; 2007; Breivik et al., 2012; Kandilarov et al., 2012; Brandsdóttir et al., 2015) (Figure 10 & Table 1). A more detailed line information is listed in Appendix G.

The JMKR-95 survey included east-west and southwest-northeast oriented profiles (Kodaira et al., 1998), of which profile line 4 crossed the Jan Mayen Ridge. OBS2000 survey line number 8 (Mjelde et al., 2002; 2007; Breivik et al., 2006, 2012) crosses the southwest end of the JMMC, and the northwestern end of the EJMFZ. The southern extent of the JMMC onto the Iceland Plateau was investigated as part of the KRISE survey in 2000 by line 7 (Hooft et al. 2006; Brandsdóttir et al., 2015).

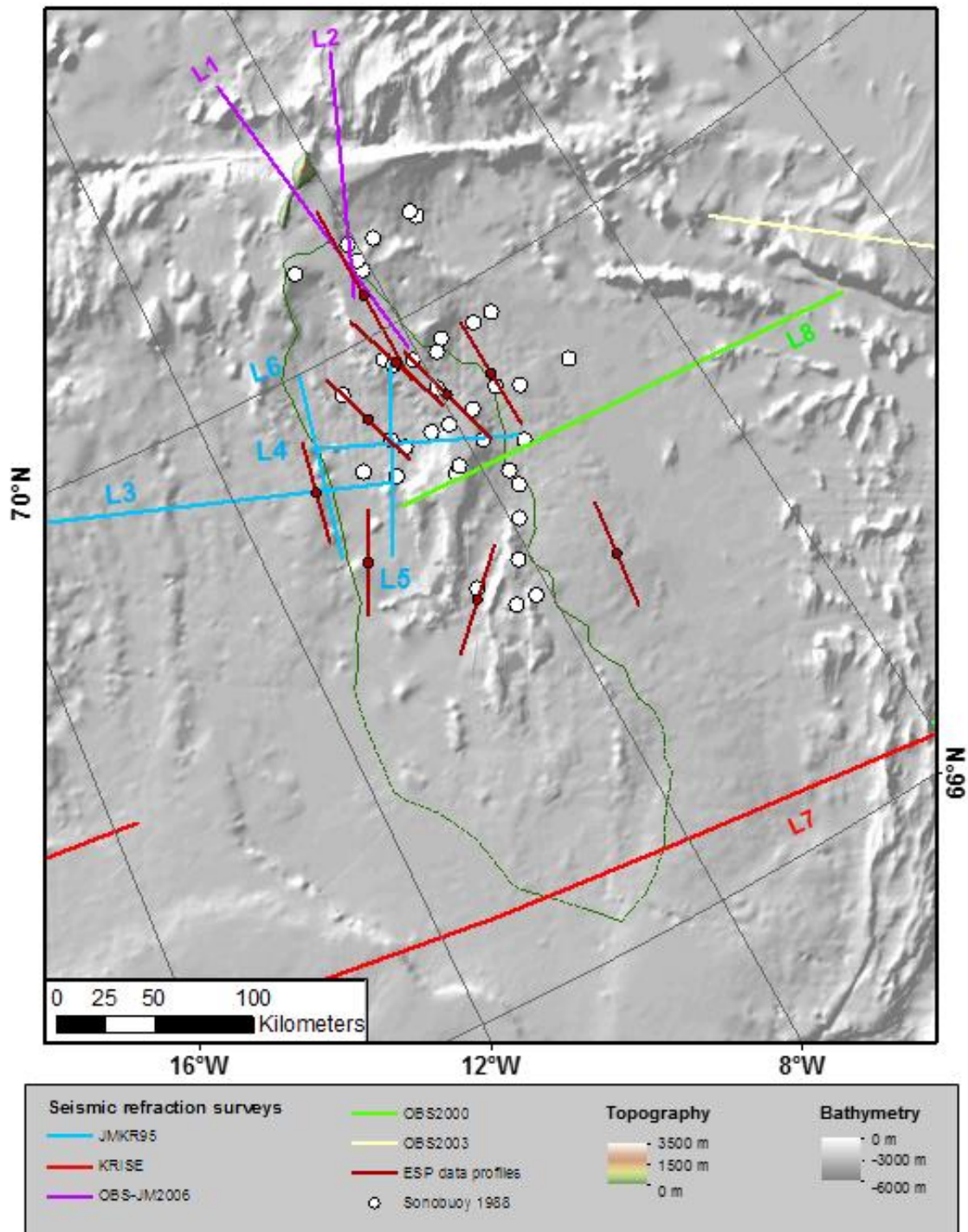


**Figure 10.** Refraction data locations in and around the JMMC area for OBS seismic surveys with line numbers referenced as “L” and the corresponding number. Additionally are shown sonobuoy (Johansen et al. 1988; Olafsson & Gunnarsson, 1989) and ESP seismic survey (unpublished data after Eldholm 1988) locations.

OBS-JM2006 survey focused on the northern region of the JMMC, consisting of NW-SE (L1) and N-S profile (L2) across the Jan Mayen Island (Kandilarov et al., 2012). Refraction data from all these surveys were used to constrain the southern extent of the JMMC.



Sonobuoys deployed during the JM-85 seismic reflection survey provide velocity information of the upper layers of the JMMC microcontinent (Olafsson & Gunnarsson, 1989), and utilized to better constrain the igneous crust of the continent-ocean transition (Blischke et al., 2016).

## 2.4 Satellite analysis and remote sensing for oil seepage data

Natural oil seepage can indicate accumulations of hydrocarbon deposits and can be observed in synthetic aperture radar images (SAR).

### 2.4.1 University of Iceland oil slick data surveys in 2006, 2007 & 2008

The first results of an oil seepage study across the Dreki area were reported in 2009 by Jónsdóttir & Valdimarsson (2009) (Figure 11). The project was carried out at the University of Iceland, Faculty of Earth Sciences, and the objective was to examine signs of natural oil seepage in the Dreki area, possibly indicating oil fields beneath the ocean floor. During the study, SAR images from the ENVISAT satellite were used in order to observe oil slicks, and the report presented results on a monthly basis for the year 2008.

The main conclusion was that no clear seeps were detected and higher resolution satellite image analysis was suggested in a calmer wind period over the area. Still, single spots of calmer waters were observed that were not connected to shipping activities or weather pattern observations.

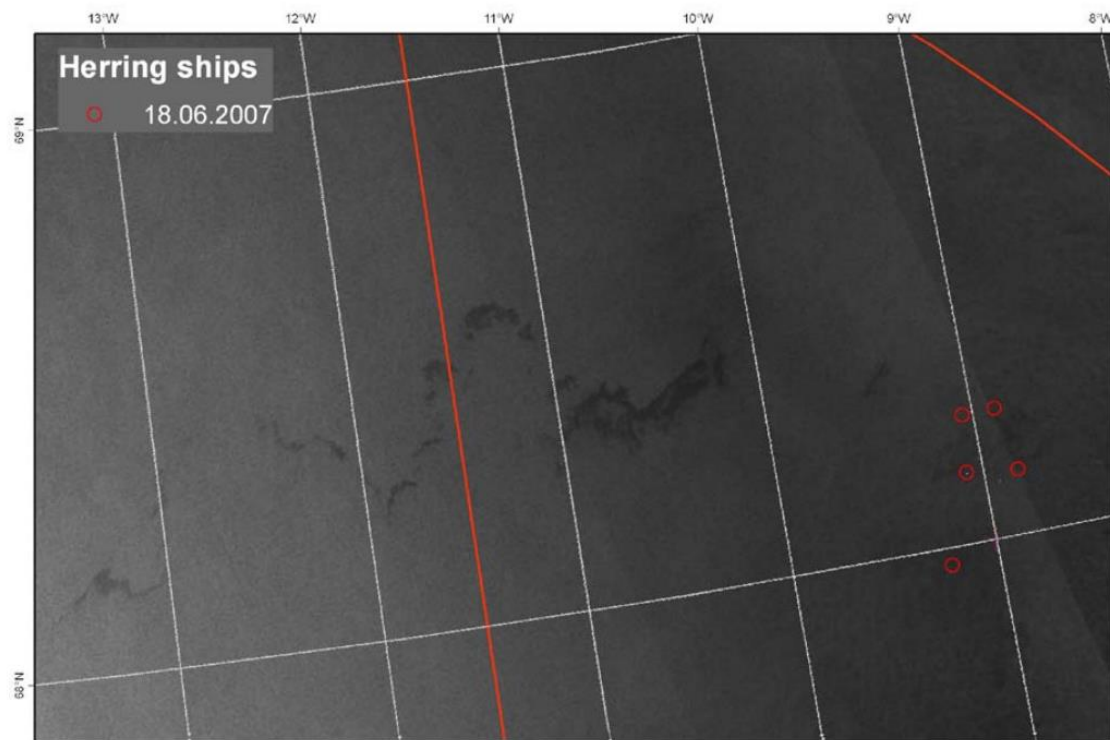


**Figure 11.** *Herring ships and associated slick on June 18th 2007 (Jónsdóttir & Valdimarsson, 2009), red outline is the Dreki licensing area and white polygons are the licensing blocks.*

**2.4.2 NPA oil slick data survey in 2009**

In 2009, Fugro NPA performed a Satellite Synthetic Aperture Radar (SAR) seep study across the Dreki area. The objective was to map potential surface oil seeps and provide indication of the existence of black oil petroleum systems. 186 slicks were mapped, with 8 higher confidence seepage slicks identified (see Figure 12).

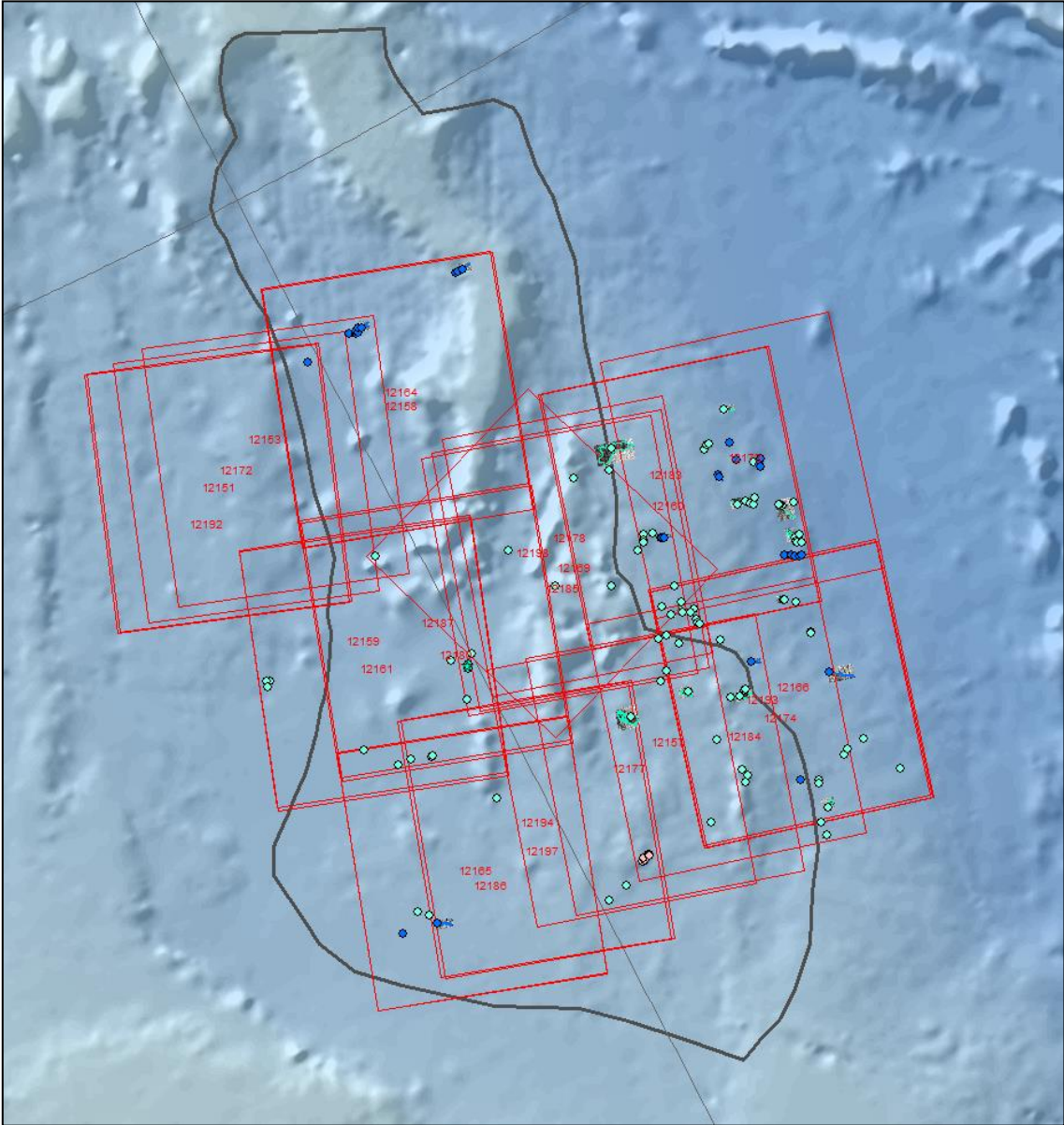


**Figure 12.** NPA oil seep data interpretations in 2009 with red polygons of satellite image coverage and image id, unassigned slicks are marked in light green, priority unassigned slicks are marked in blue, and 70–78% score percentage cluster seepage slicks of third rank are marked in pink.

### 3 Bathymetry

The primary regional bathymetry grid compilation with a 500 m x 500 m resolution that was produced by the NAGTEC Atlas group (Hopper et al., 2014), see Table 3 & Figure 13, is used for this exploration project.

An initial bathymetry map was compiled during the original JM-85 & 88 2D MCS surveys using the ship track and first seafloor arrival incidences (Åkermoen 1989; Gunnarsson et al., 1989) (Figure 14).

In 2008 the A8-2008 survey was conducted by the ocean research vessel Árni Friðriksson that set out on an 18-day expedition in June 2008 to the Dreki area to obtain detailed information of the seafloor with multibeam echo-sounder, and to do sea-current measurements. The survey area for the multibeam measurements was planned in cooperation with the National Energy Authority, NEA. The ship was equipped with a multibeam echo sounder (Simrad EM 300, 30 kHz, 2° x 2°), operating at peak performance in the depth range 100–3000 m, which made it possible to map the seabed with much greater precision than possible with previously used bathymetry acquisition tools for the Jan Mayen area (Helgadóttir, 2008a). In addition to collecting the depth data, the backscatter signals were also recorded for this survey.

The backscatter data of the multibeam data were processed with the open-source software package MB-system (<http://www.Ideo.columbia.edu/res/pi/MB-System/>) in order to map the hardness variations, which potentially represent differences in sediment or rock types at the seafloor( this is described in more detailed in section 3.2). The MB-system uses a single backscatter echo intensity value for each beam. The EM300 system produces "seabed image" datagrams as well, containing a time series of samples for each beam adjusting for the water column. This is the information used in the Geocoder-version used in CARIS-HIPS/SIPS. Unfortunately, for large parts of the survey in the Dreki-area in 2008, much of the seabed image datagrams are missing. In Geocoder/CARIS a beam-angle response is estimated from a homogenous soft seafloor. The resulting function is used in the following compensation of the backscatter as a function of the grazing angle (angle of incidence). A comparison of MB-system and Geocoder has been made on other EM300 data, giving quite similar results.

An average grazing angle response, using 2° bins, was calculated by using a "sliding window" of 250 pings along the vessel track. The across swath bottom slope was incorporated into the grazing angle estimation. This was done separately for the starboard and port side of the swath. The resulting averaged data sets were used to compensate the backscatter amplitudes for every angle bin in each window. A 30° angle was chosen as a reference for the compensation procedure. No filtering of the data was carried out beforehand. Outliers were simply excluded afterwards by using an upper and lower threshold. Excluding angles close to the nadir beams as well as the outermost beams did not affect the resulting backscatter image to any significant degree, although the along-track artefacts did not fully diminish.

In 2010 the Marine Research Institute (MRI) carried out a cruise (A11-2010) on behalf of NEA and NDP. The cruise was split into two parts:

1. Piston corer sampling cruise over selected sites on both sides of the Icelandic economic zone, i.e. in Icelandic and Norwegian sectors.

This part was led by Þórarinn Sveinn Arnarson.

2. Multibeam and sub-bottom measurements in the Norwegian sector (i.e. outside the Icelandic economic zone) using Simrad EM300 echo-sounder and Bathy 2010 3.5 kHz sub-bottom profiler respectively. These instruments were also active in part 1 of the survey.

The second part was led by Guðrún Helgadóttir.

The two proprietary and high resolution multibeam surveys were used from the survey *A8-2008* with a resulting 50m x 50m grid spacing (Helgadóttir, 2008a), see Figure 15, and *A11-2010* with a resulting 50m x 50m grid spacing (Helgadóttir & Reynisson, 2010), see Figure 16 and Appendix A, for the Dreki area and the main Jan Mayen Ridge.

**Table 3.** *Data sources for bathymetry and elevation datasets of the NAGTEC project (Hopper et al., 2014).*

Grid, Area, or Dataset	Original Resolution	References and Links
EMODnet, Celtic Seas	500x500 m	<a href="http://www.emodnet-hydrography.eu">http://www.emodnet-hydrography.eu</a>
EMODnet, North Sea	500x500 m	<a href="http://www.emodnet-hydrography.eu">http://www.emodnet-hydrography.eu</a>
ETOPO1	1 arc-minute	Amante and Eakins, 2009 <a href="http://www.ngdc.noaa.gov/mgg/global/global.html">http://www.ngdc.noaa.gov/mgg/global/global.html</a>
Faroese Shelf, LOS 05	100x100 m	Contributed by Jarðfeingi
Faroese Shelf, LOS 08	100x100 m	Contributed by Jarðfeingi
Faroese Shelf, LOS 11	100x100 m	Contributed by GEUS
GMTED (land areas, excluding Greenland)	15 arc-seconds	Danielson and Gesch, 2011
IBCAO 3.0	500x500 m	Jakobsson et al, 2012 <a href="http://www.ibcao.org">http://www.ibcao.org</a>
Iceland, Arnarfjörður	20x20 m	Marine Research Institute, Iceland <a href="http://www.hafro.is/undir.php?REFID=10&amp;ID=190&amp;REF=2">http://www.hafro.is/undir.php?REFID=10&amp;ID=190&amp;REF=2</a>
Iceland, Ísafjarðardjúp	20x20 m	Marine Research Institute, Iceland <a href="http://www.hafro.is/undir.php?REFID=10&amp;ID=231&amp;REF=2">http://www.hafro.is/undir.php?REFID=10&amp;ID=231&amp;REF=2</a>
Iceland, Kötluhyggir	100x100 m	Marine Research Institute, Iceland <a href="http://www.hafro.is/undir.php?REFID=10&amp;ID=232&amp;REF=2">http://www.hafro.is/undir.php?REFID=10&amp;ID=232&amp;REF=2</a>
Iceland, Lónsdjúp	30x30 m	Marine Research Institute, Iceland <a href="http://www.hafro.is/undir.php?REFID=10&amp;ID=192&amp;REF=2">http://www.hafro.is/undir.php?REFID=10&amp;ID=192&amp;REF=2</a>
Iceland, Reykjanes Ridge and surroundings	50x50 m	Marine Research Institute, Iceland <a href="http://www.hafro.is/undir.php?REFID=10&amp;ID=198&amp;REF=2">http://www.hafro.is/undir.php?REFID=10&amp;ID=198&amp;REF=2</a>
Iceland, Víkuráll	30x30 m	Marine Research Institute, Iceland <a href="http://www.hafro.is/undir.php?REFID=10&amp;ID=193&amp;REF=2">http://www.hafro.is/undir.php?REFID=10&amp;ID=193&amp;REF=2</a>
Jan Mayen, Dreki region	50x50 m	NEA, Iceland and ÍSOR
Norwegian shelf	250x250 m	Olesen et al., (2010)



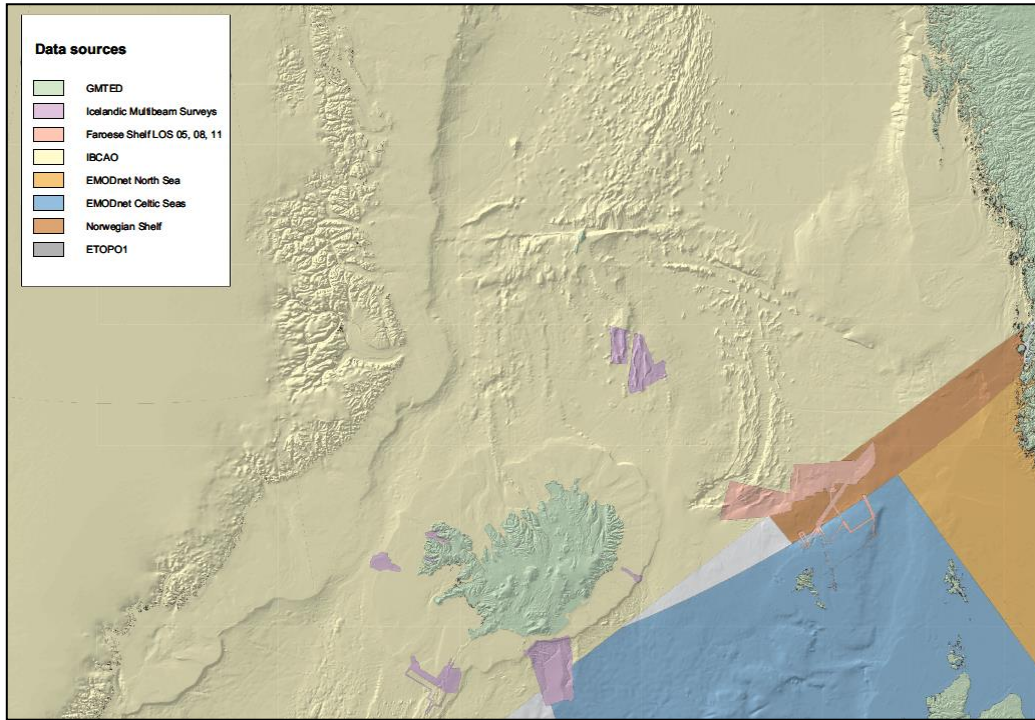


**Figure 13.** Bathymetry data coverage for the central North Atlantic of the NAGTEC project (Hopper *et al.*, 2014), survey list see Table 3.

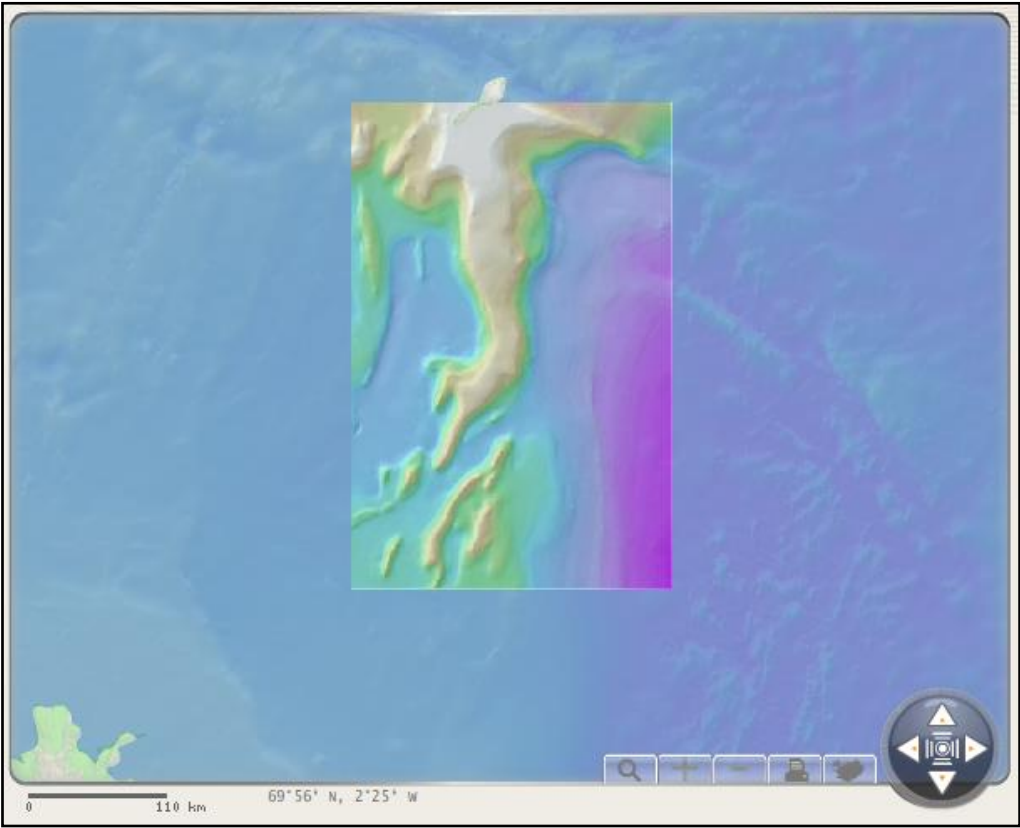


**Figure 14.** Bathymetry grid data layer for the Jan Mayen Ridge within the Iceland Continental Shelf Portal, based on the bathymetry map by Åkermoen (1989).



The international bathymetric database SRTM30plus v/4.0 (Becker et al., 2009) was used until 2013 as the background and large regional scale data set (Figure 15).

The sea current measurements in the Dreki area (see locations on map in Appendix A) were conducted at 3 locations (Mork et al., 2014).

Existing seafloor maps that were produced prior to 2001, such as the first bathymetry map of the area, see Figure 14 (Åkermoen, 1989), were digitized off paper seafloor contour interpretation map displays, and compared to the new post 2001 bathymetry data, in reference to the original structural interpretations of the Jan Mayen Ridges in the 1980's.

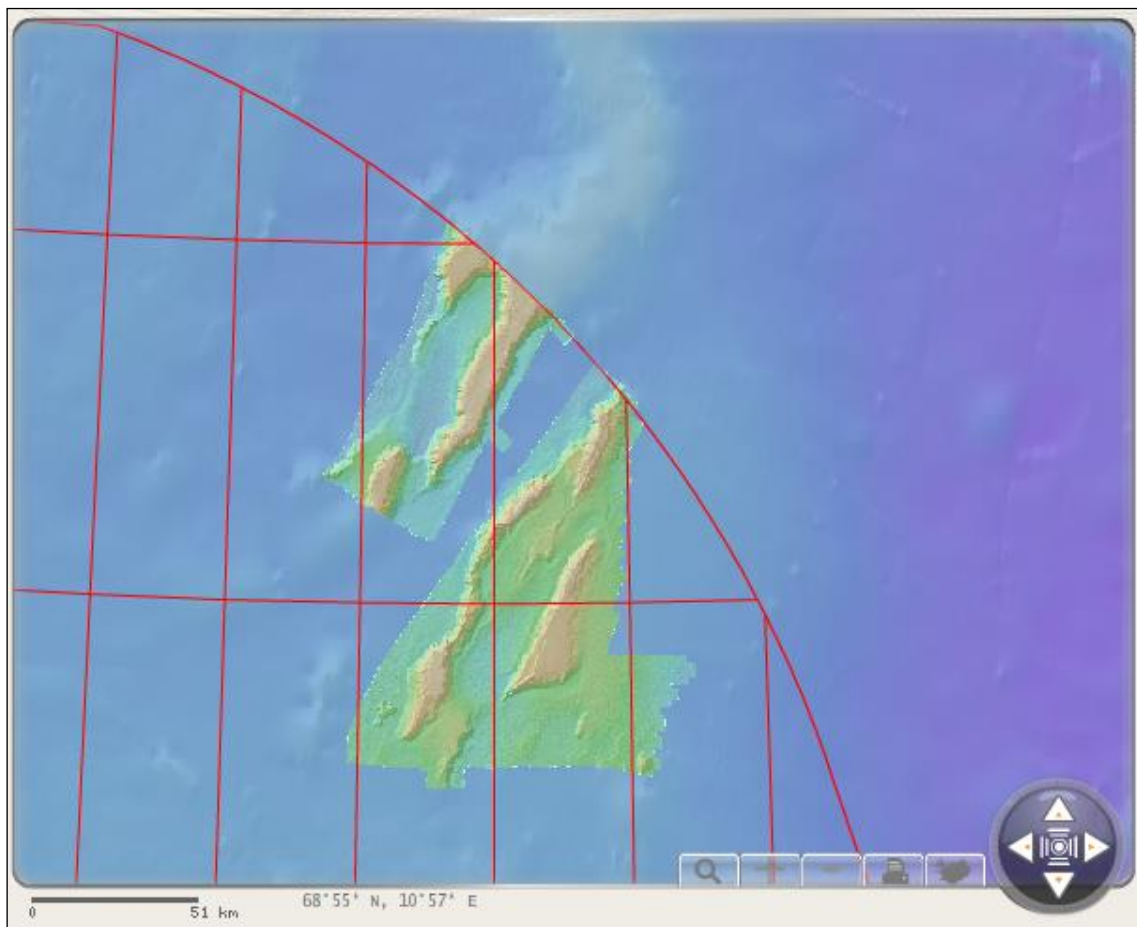


**Figure 15.** Overview of the A8-2008 bathymetry data in the Iceland Continental Shelf Portal.

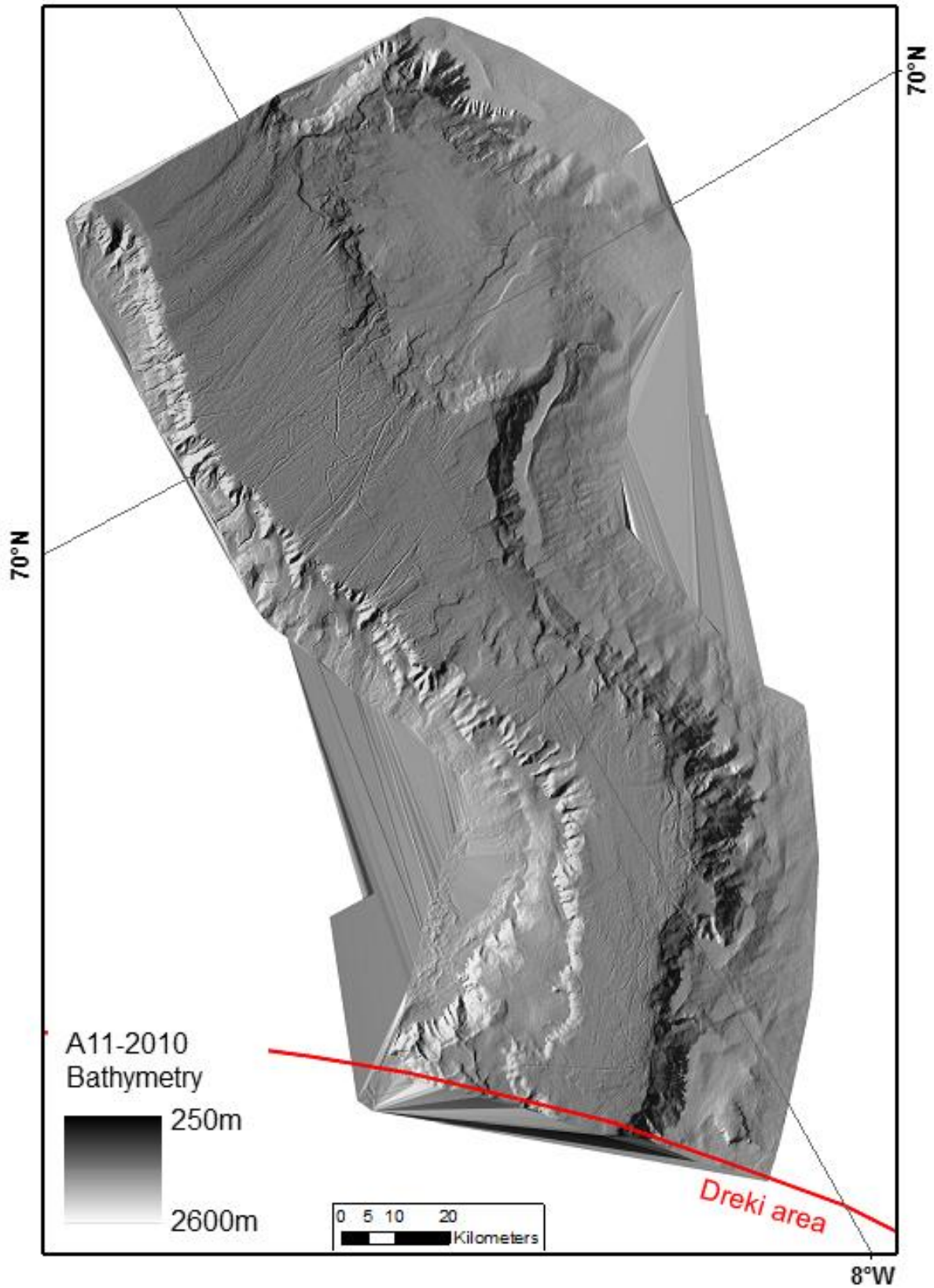


**Figure 16.** Overview map (ISOR, 2010) of the A11-2010 bathymetry data acquired during the seafloor sampling campaign of NEA, NPD & MRI.

### 3.1 Multibeam – initial high resolution data set analysis

Information on the topography and composition of the seabed was collected during the A8-2008 and A11-2010 surveys to produce precise contour-, shading-, 3-D- and bottom-type maps. In total, an area of 10,500 km<sup>2</sup> was mapped, and the depth interval was from 790 to 2210 m. Multibeam bathymetry data was used to map structural trends and features at the seafloor. This high resolution bathymetry data in combination with seismic reflection data enabled us to differentiate strike-slip from normal fault systems and slump faulting along the steep escarpments of the microcontinent's ridges, pockmarks, iceberg plough marks, slide scars, and slumping features.

An interpretation project was carried out between July and October of 2015, with the goal of mapping selected geological and geophysical features visible in the data gathered by this survey, and to give an overview of the findings of the project. Figures are presented in the section to show examples of each type of mapped features. An A2 format sized overview map is also provided in Appendix A.

Two types of data were provided by the Marine Research Institute (MRI) for this project, multibeam bathymetric data and backscatter amplitude data. The multibeam data were provided by MRI as gridded xyz point files at different levels of resolution, 50m X 50 m and 25 X 25 m for the whole area, and 15 X 15 m for the Niflungur area. The seafloor backscatter data were supplied by the MRI at a resolution of 50 X 50 m and are discussed in section 3.2.

Additionally, multi-channel seismic reflection data (Figure 17) from several different surveys were integrated with the multibeam data in Petrel, making it easier to locate and distinguish between different types of faults and slumps.

The Dreki area has two main areas of multibeam data coverage, the main ridge and western flank (WF), and the Southern Ridge Complex (SRC) (Figure 17). The ridge plateaus of the western flank includes plateau-like highs, such as *Lyngvi*, *Buðli*, or *Sörlahryggur*, which lie in the depth range 1000 to 1200 m. The surrounding lows, such as the *Niflungur* area, lie in the depth range 1600 to 2000+ m. The SRC lies at a depth between 900 and 1200 m, while most of the surrounding lows lie between 1600 to 1800 m seafloor depths.

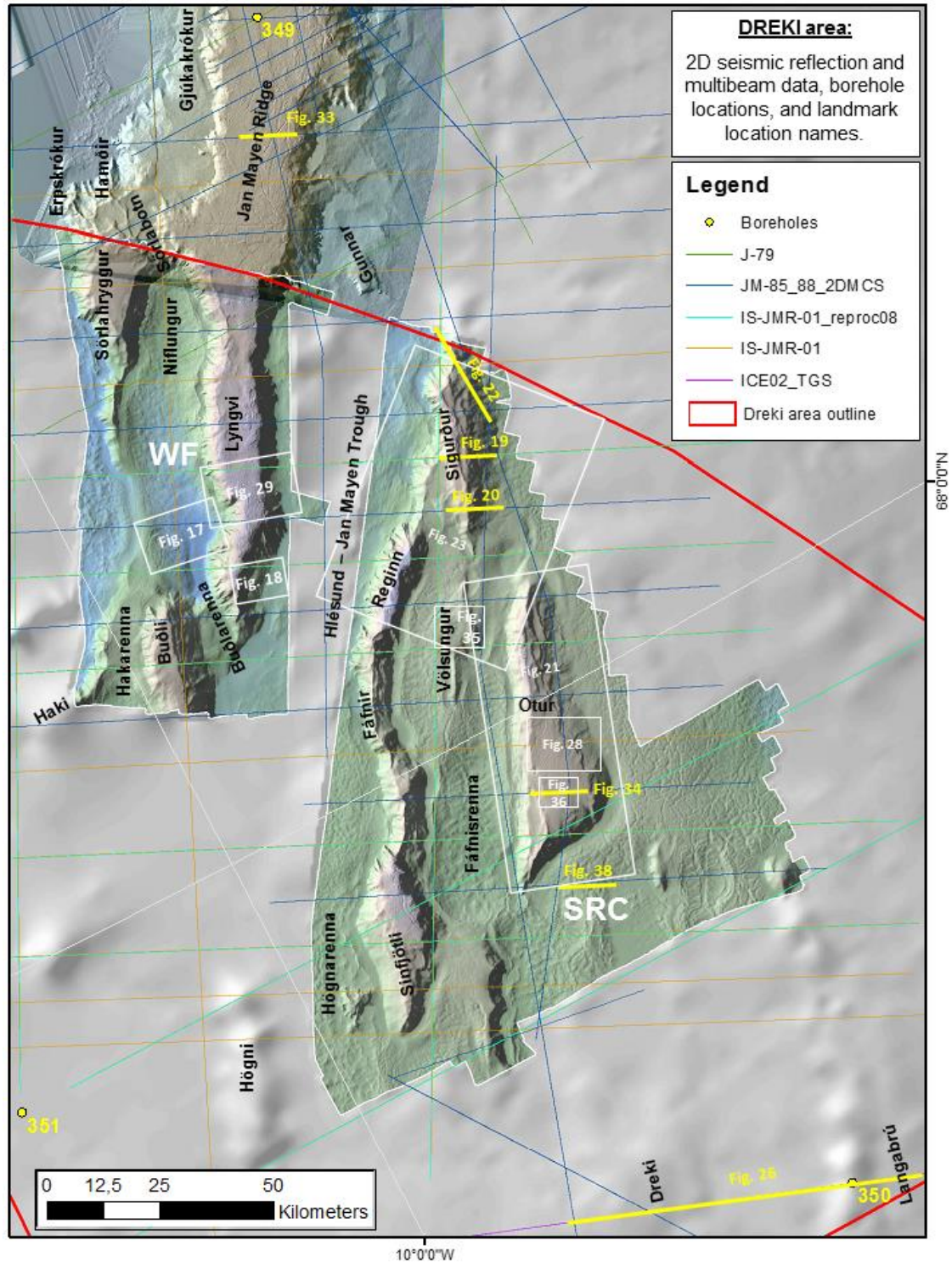


Figure 17. Location map for the A8-2008 & A11-2010 surveys data displays and 2D seismic reflection line locations.



### 3.1.1 Submarine landslides and slump – slump faulting

Slumps and submarine landslides are forms of mass transport, which occur when rock layers or coherent masses of little consolidated materials move down a slope for a short distance. The trigger for these landforms in a submarine environment is often related to earthquakes or overloading along steep slopes and escarpments.

Two clear landslides were detected in the bathymetric data within the Dreki area. The larger one is located 4.5 km to the north of the Buðli Knoll and 5 km to the west of the Lyngvi Ridge and it has an area of approx. 28.35 km<sup>2</sup> (see Figure 18). The smaller one is located on the eastern flank of the southernmost part of the Lyngvi Ridge and has an area of approx. 3.98 km<sup>2</sup> (see Figure 19). Numerous landslides have been found across the Norwegian area (Appendix A & H), especially towards the northern area of the Jan Mayen Ridge that is also more affected by the active Jan Mayen Fracture Zone and the volcanic system of the Jan Mayen Island.

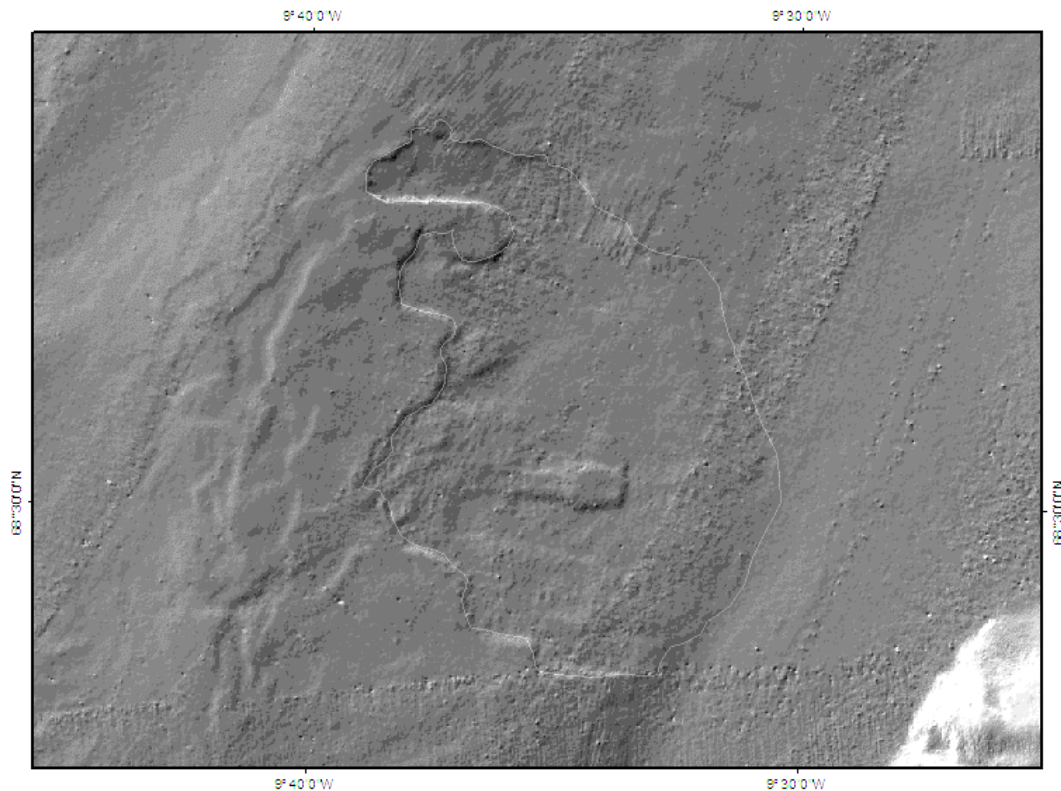


**Figure 18.** The larger of the two landslides has an area of approx. 28.35 km<sup>2</sup> and is located to the north of Buðli Knoll (15 m x 15 m multibeam data resolution). For location, see Figure 17.

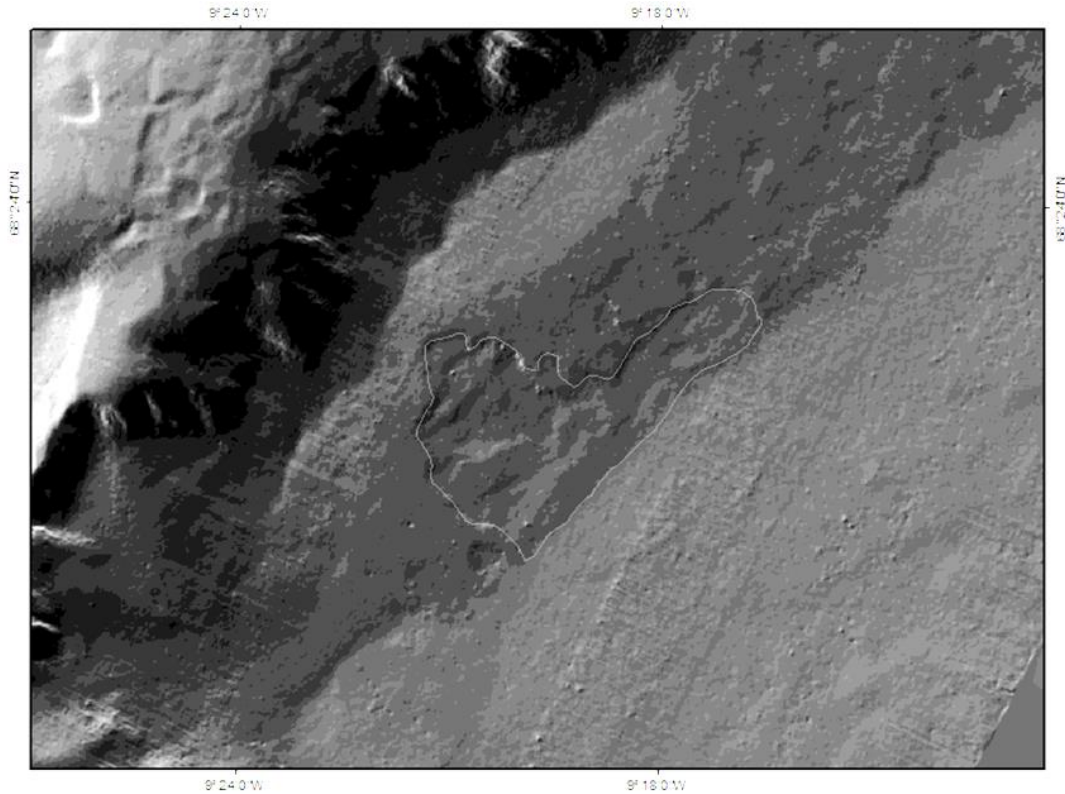


**Figure 19.** *The smaller landslide, with an area of approx. 3.98 km<sup>2</sup>, is located on the eastern flank of Lyngvi's southern tip (15 m x 15 m multibeam data resolution). For location, see Figure 17.*

Slumps associated with slump faulting, have been found along the ridges of the JMMC, here primarily connected to the gravitational effects of unstable cliff / escarpment edges alongside the extensional sub-basins (see Figure 20 to Figure 22). These escarpment areas are important to understand in connection with the selection of seafloor sample that target the autochthon bedrock. This will be discussed in more detail in section 4.2 in regards to the certainty of the acquired seafloor samples.

It proved difficult to distinguish between gravitational and extensional slumps on the overview maps. Thus, most of the work in separating those was done in Petrel, where seismic data were used to correlate faults with slumps on the surface. Gravitational slumps are prevalent in the Dreki area. All of the ridge slopes contain some gravity slumps and the steepest slopes, namely on the Lyngvi Ridge, are covered in them. Extensional slumps were also found on the Sigurður, Reginn and Sinfjötli knolls, and the Fáfñir and Otur ridges for the Dreki area.

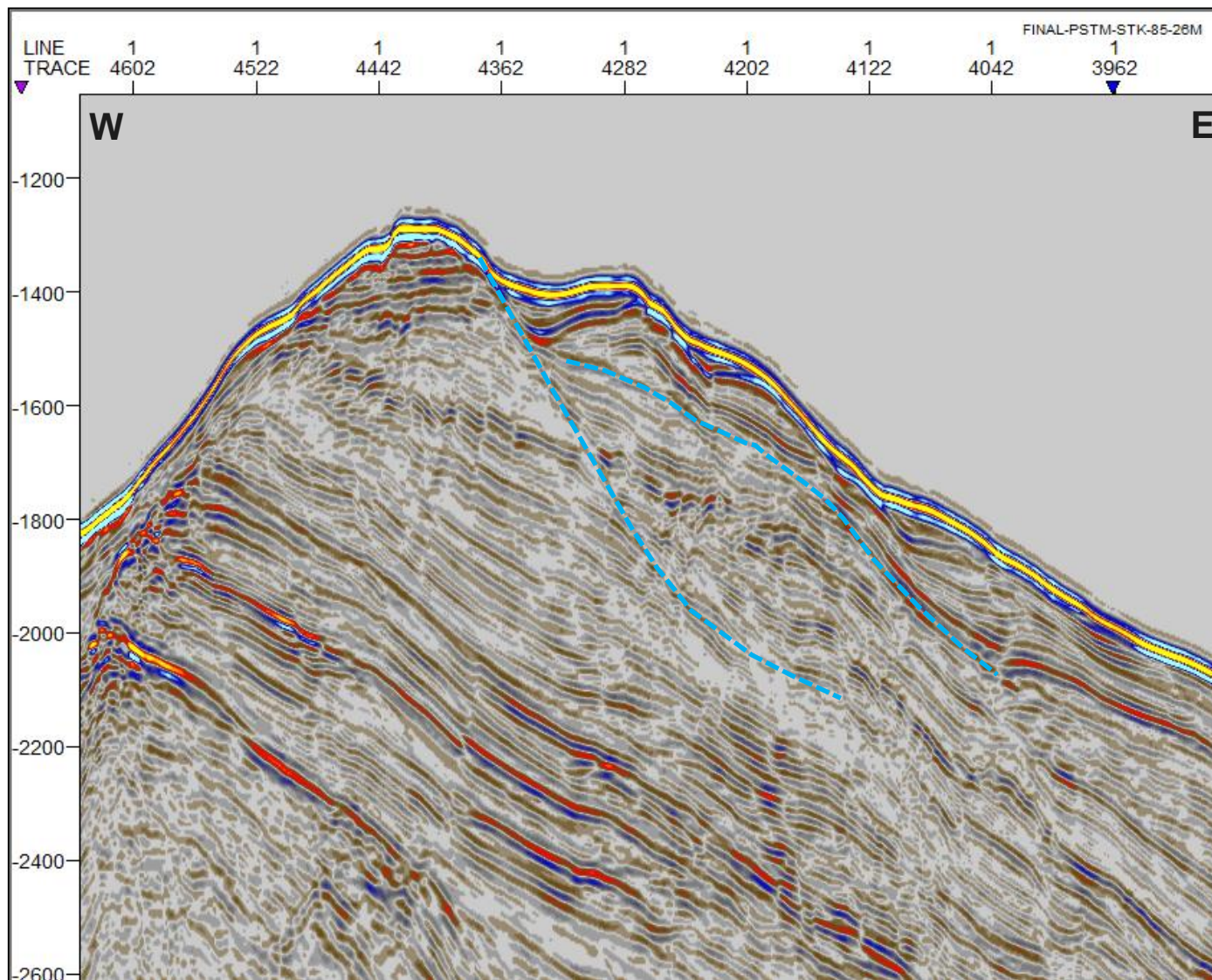


**Figure 20.** Seismic profile showing gravitational slumping (blue dotted line) on Sigurður Knoll near CDP 4360. W-E seismic reflection data profile IS-JMR-01-0040, vertical exaggeration at 5. For location, see Figure 17.



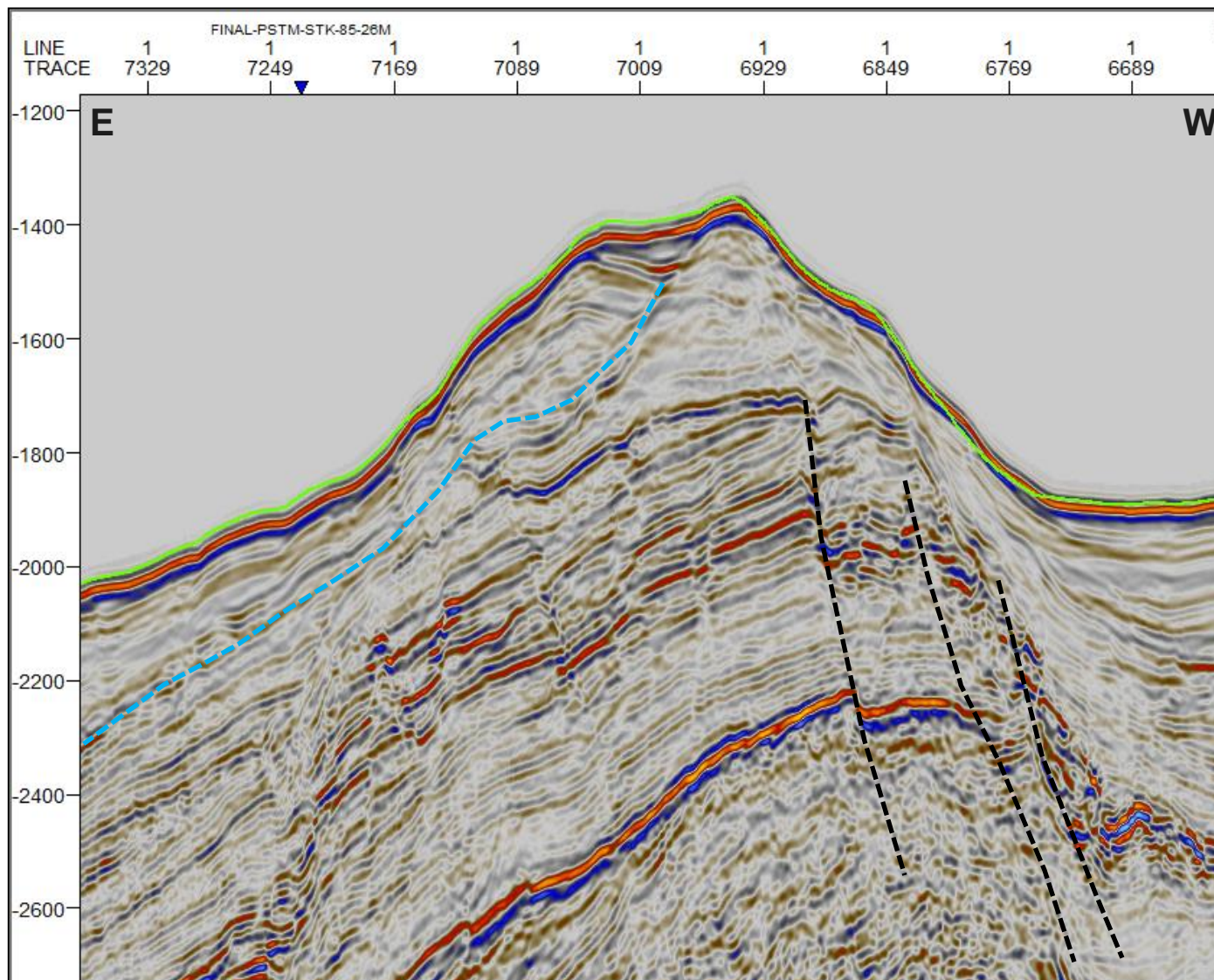


**Figure 21.** Seismic profile of Sigurður Knoll showing slumping (blue dotted lines) due to subsidence along the eastern flank of the JMMC from CDP 7000 to the east. Normal faulting (black dotted lines) can be seen and were caused due to a westward extension within the Jan Mayen Trough. E-W seismic reflection profile JM-85-18, vertical exaggeration at 5. For location, see Figure 17.



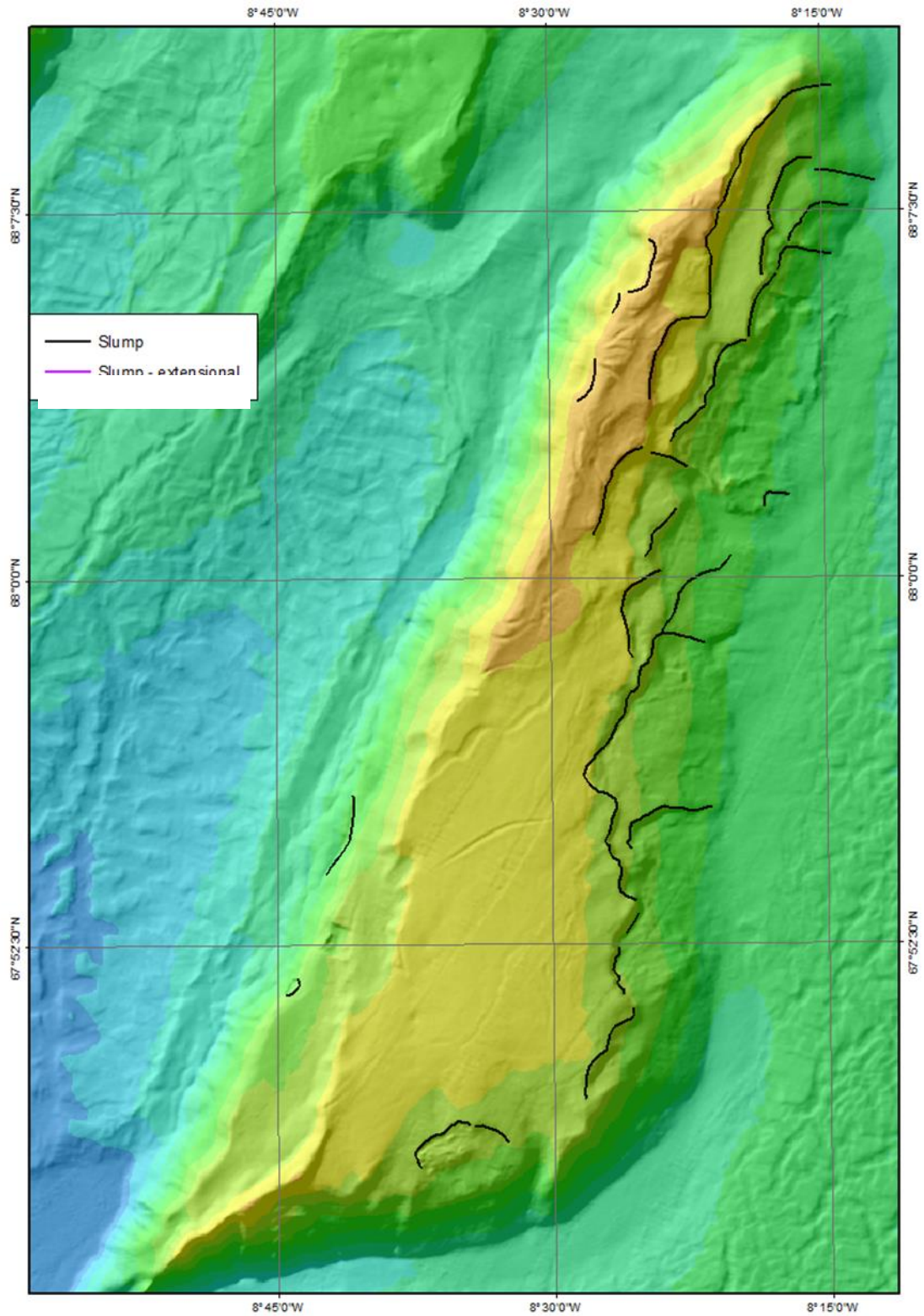


**Figure 22.** The eastern flank of Otur Ridge is dominated by slumps and their seafloor surface edges are here marked with black lines (50 m x 50 m multibeam data resolution). For location see Figure 17.

### 3.1.2 Normal faulting

Normal faults are generally related to extensional processes, either formed due to pure extension in between separating ridges, or occur locally within the extensional domains of structural strike-slip systems (here also referred to as transpressional).

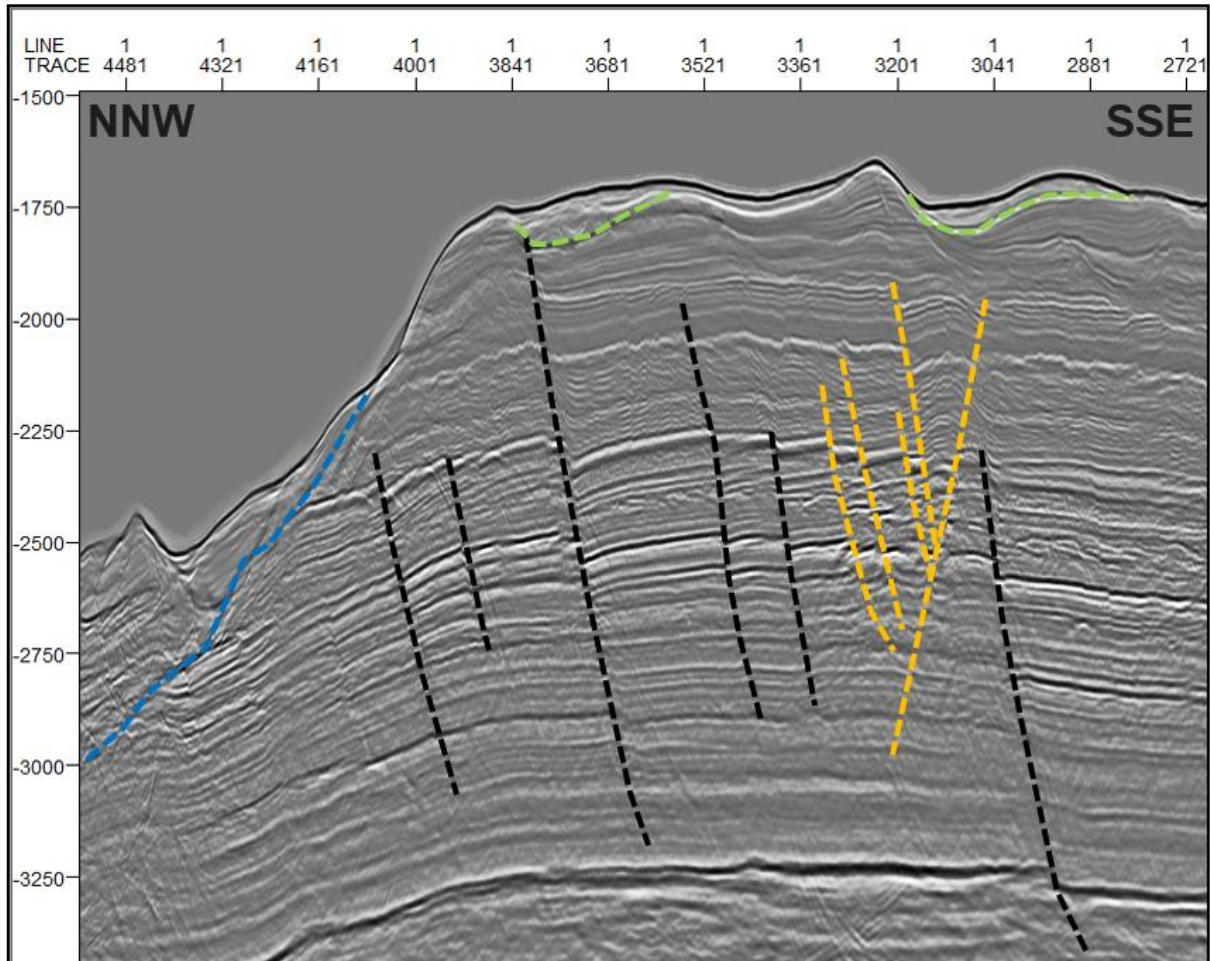


**Figure 23.** Seismic profile showing normal faulting (black dotted lines), slightly transpressional fault sets (orange dotted lines), slump faulting and sliding plain (blue dotted line), or scouring and sediment drift surfaces (green dotted lines) on top of the Sigurður Knoll, along 2D seismic reflection profile JM-11-0020-NPD2011 (Z-scale 4.6). For location, see Figure 17.

Most of the observed smaller normal faults do not reach the seafloor and are buried in the stratigraphic sections below surface. Still, the pattern of extensional faulting observed on the seafloor give a good overview of the overall segmentation of the Jan Mayen Ridges, especially for the Southern Jan Mayen Ridge Complex (Appendix A & I), striking N-S to NE-SW.

The cross-section in Figure 23 and map display in Figure 24 show one example area of two different sets of normal faults. Most of the normal faults that were easily distinguishable in seismic profiles across the main sub-ridge do not reach up to the seafloor.



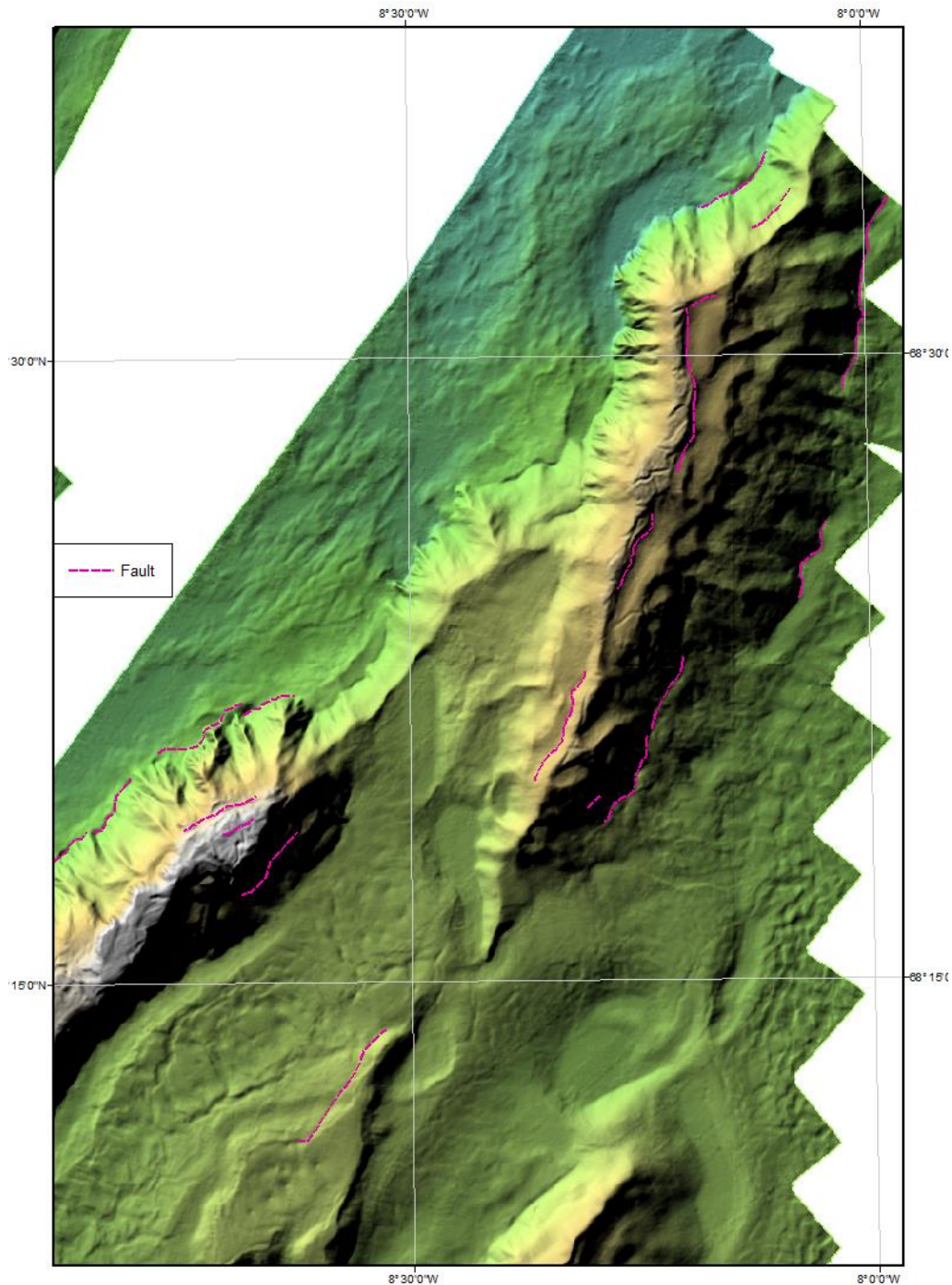


**Figure 24.** Normal faults (pink lines) on the Sigurður (NE) and Reginn (SW) knolls (50 m x 50 m multibeam data resolution). For location, see Figure 17.

### 3.1.3 Strike-slip faulting

The transfer systems and its associated strike-slip fault segments tend to strike NW-SE for the Jan Mayen ridges located along the eastern flank connected to the regional structural elements that form the Ægir Ridge and the Eastern Jan Mayen fracture zone (Figure 25, Figure 26 & Appendix A).

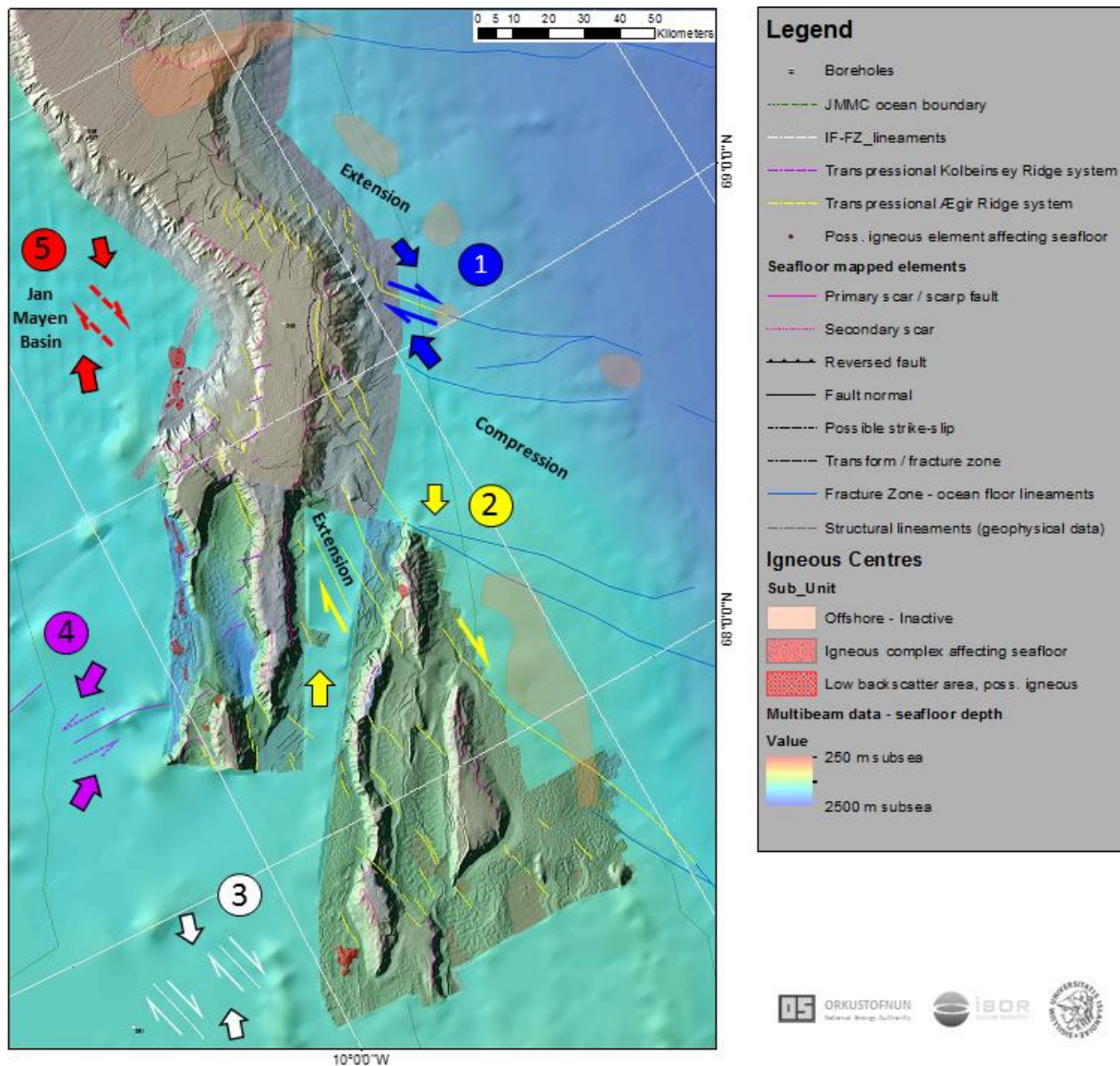


**Figure 25.** Regional transfer systems that affected the flanks of the JMMC during at least 5 stages. Stages 1 (blue) and 2 (yellow) were oblique openings of the Ægir Ridge system; stage 3 (white) was an oblique rifting along the Iceland-Faroe fracture zone; stage 4 (purple) an oblique opening of the pre-Kolbeinsey Ridge system from the southwest to the northeast, and finally stage 5 (red), the forming of the Jan Mayen pull-apart basin during the separation of the microcontinent throughout the Lower Miocene.

The microcontinent is also affected by SW-NE striking strike slip faults along the southwestern and western flank of the microcontinent (purple stage on Figure 25), that are most likely linked to the opening processes of the initial separation of the microcontinent from the East Greenland margin (Blischke et al., 2016), and finally the opening of the Jan Mayen basin as a pull apart basin that separated the northwestern section of the microcontinent from the East Greenland coast, here specifically the area of the Liverpool Land basin just north of the Scoresby Sund area along the central East Greenland coast.



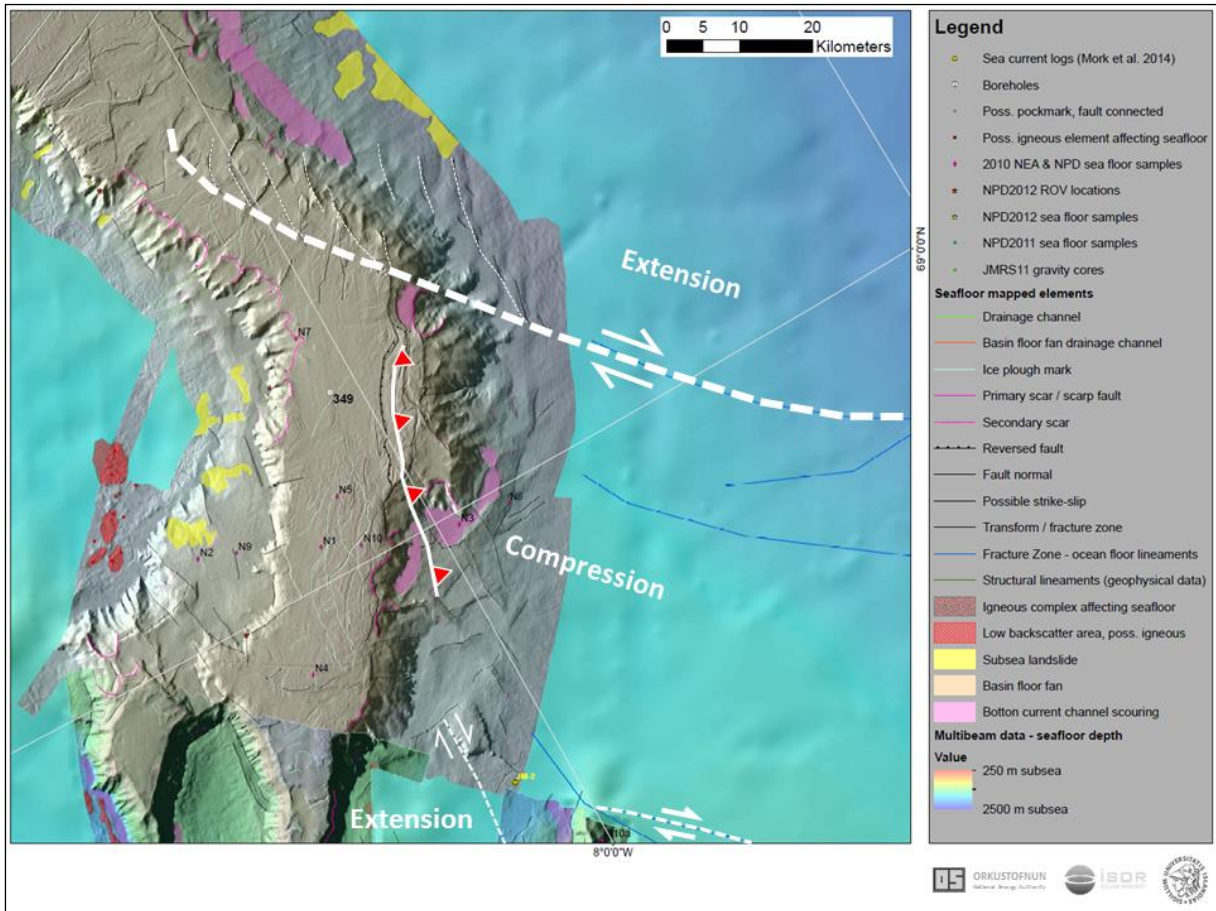


**Figure 26.** Regional transfer systems affecting the central area of the microcontinent. The reverse fault (white line with red triangles) is well mapped at the lower Eocene top basalt horizon on seismic reflection data that apparently reaches all the way up to the seafloor at its northern limit. The normal fault pattern to the north of the strike-slip fault zone (thick WWN-EES white dashed line) has similar characteristics to a horse tail fault patterns that have been described by Brogi (2011).

The compilation of many mapped faults and fault patterns for the project area, suggest that the main boundaries of the Dreki area at its northern and southern extent are formed by strike-slip / transfer zones.

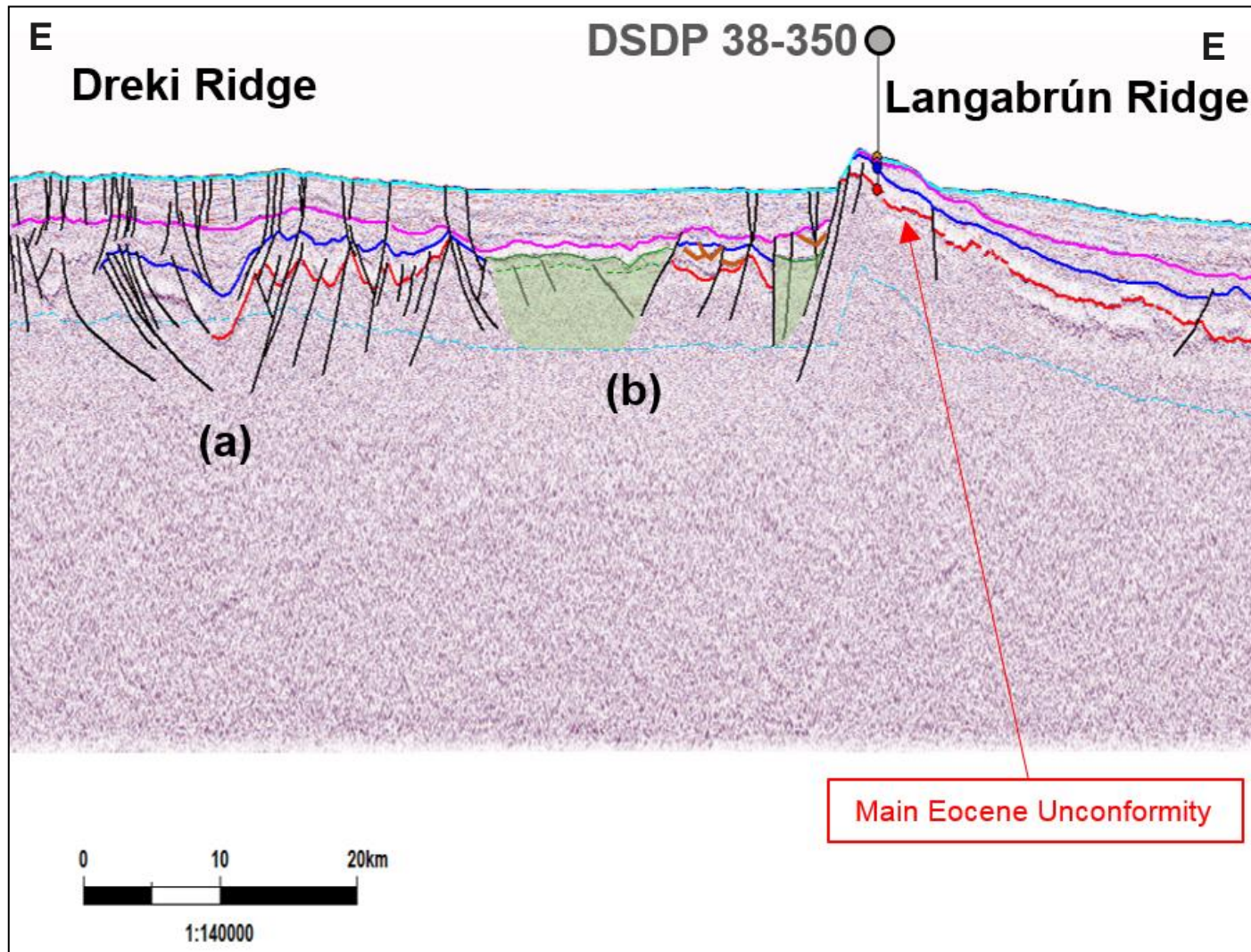


**Figure 27.** Borehole DSDP 38-350 tie-line showing fault trends that indicate at least 2 structural events, the first during the Mid-Late Oligocene (blue marker) affecting the underlying Eocene formations (red marker), which is linked to transform system (Blischke et al., 2016) (a), and the normal extensional faulting (b) around and since the Early Miocene (pink marker) coinciding with increased igneous activity (green marked areas). For location, see Figure 17.

Clear surface indications are not visible at the seafloor, however, lateral fault movements could have been present in earlier geological times (Figure 23 and Figure 27). The northernmost edge of the JMMC along the Jan Mayen fracture zone (JMFZ) is a complex fracture zone and transfer system as well.

A direct comparison with the regional strike-slip fault zone to the south of the JMMC is the Tjörnes Fracture Zone, along the central north Iceland coast line (Brandsdóttir et al., 2002; 2004). The Tjörnes fracture zone has several segments that are visible as large seismically active zones, e.g. the right-lateral Húsavík lineament and transform zone, which forms a pull-apart basin structure visible on 2D seismic reflection data along its extension side of the strike-slip system to the north, and compression and reverse features at its opposite end onshore. The TFZ links the two mid-oceanic ridge (MOR) systems, offshore to the west the Kolbeinsey MOR and onshore to the east the Northern Volcanic Zone (NVZ) (Tibaldi et al., 2016).

#### Channelling and water current erosion

The seafloor map (Appendix A) shows clearly scouring marks and seafloor erosional effects in its uppermost sediment sections (Figure 23), especially along the steep ridge flanks.

A two year project, recording water current measurements (Figure 28) from three moorings and sea water conductivity, temperature and pressure profiles, were conducted across the Jan Mayen Ridge in 2007 and 2008 and published (Mork et al., 2014) by Norwegian (Institute of Marine Research and Bjerknes Centre for Climate Research) and Icelandic (Marine Research Institute and the University of Akureyri) oceanic research groups.



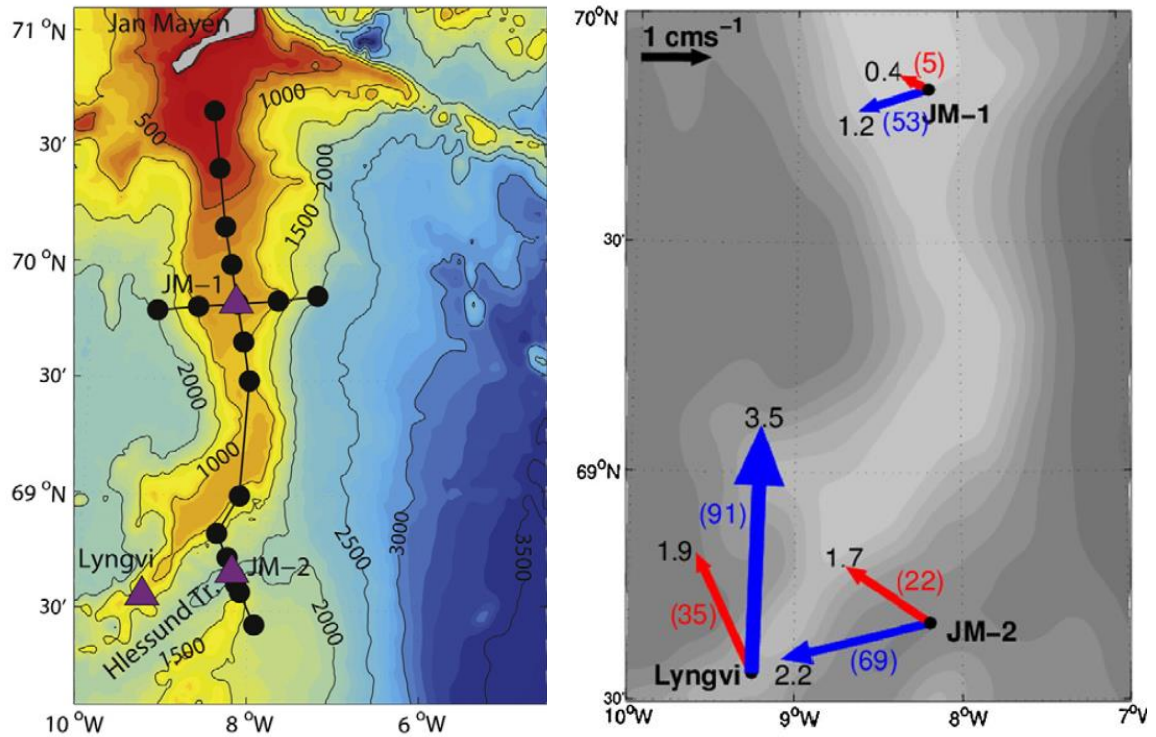


**Figure 28.** Left: Locations of the CTD-stations that record conductivity, temperature at water depth with the associated water depth pressure (black dots), and the three moorings (triangles; JM-1, JM-2 and Lyngvi) across the Jan Mayen Ridge area (Mork et al., 2014). Right: Average velocities (over time) at 50 m depth (red vectors) and near bottom (blue vectors) for the JM-1, JM-2 and Lyngvi moorings (700 m as near bottom current) (Appendix A). The black numbers represent the average speed (i.e. the average magnitude of the velocity, in 10<sup>-2</sup> ms<sup>-1</sup>). The numbers in parenthesis are the stability (%) of the current that is defined as the mean velocity divided by the mean speed (Mork et al., 2014).

The results indicate relatively weak shallow currents, eddy activity, and tidal velocities that are interrupted by frequent intense storms. These storms can generate near-inertial (rotational) motions, affecting at least the uppermost 80 m of the water column. Still, those water current changes do not have a great influence on the ridges themselves. On the other hand, deep water currents have an effect on the top section of unconsolidated sediments, which can be observed especially alongside the steep ridges of the microcontinent (Appendix A and Figure 23). These deep currents appear to be influenced by the wind stress curl over the Norwegian Sea, causing larger flow into the Iceland Sea during winter compared to the summer (Mork et al., 2014).

### 3.1.4 Ice plough marks

Iceberg plough marks were well visible on the bathymetric data, and could clearly be seen on the plateau-like high areas of the main ridges, such as Lyngvi or Otur (Figure 29 to Figure 31). Smaller gouges or scours cover most ridge segments shallower than 1000 m depth at today's sea level. The gouge length varies between several hundred metres and a few kilometres and the width ranges from 50–400 m (Appendix A). Continuous base glacier scrape marks are well



visible at the northernmost extent of the main Jan Mayen Ridge, where water depths are shallower than 200 m, where the top surface of the “flat topped” ridge was directly effected by the base of the moving ice sheet. The ridge areas that lie in deeper water depth areas (>200m), ice plough marks are primarily observed possibly caused by large ice bergs that just “point” scraped to deeper flat tops of the JMR’s, leaving irregular traces after moving across the ridge top areas. These plough marks do not seem to maintain a clear trend in their direction for the southern ridge areas, but show a general SW-NE to S-N trend for the main Jan Mayen Ridge. This dataset has only been interpreted as a first path observation and further studies will be necessary to tie these observations into a regional glaciology context.

The mapped ice plough features were compared to the mapped pockmark-features of the study by Gunnarsson et al. (1989). The proposed pockmark features that were mapped in 1989 lie within the multibeam (A11-2010) data set area (Figure 31; Appendix A) and were compared to the 2D seismic reflection survey of 2001 (InSeis) and reprocessed JM-85 & JM-88 seismic reflection data sets (Spectrum) as well (Figure 17). That review made clear that all the marked 1989 features lie on top of the Jan Mayen Ridge (JMR) plateau and are related to iceberg plough marks and erosional processes. Icebergs tend to carry 7/8 to 8/9 of their mass under the water level (Holly Gordon, Canadian Geographic Magazine, 2006). Assuming that a large iceberg in the Northern Arctic can reach 75 m up to 175 m above the sea, it is well possible that some of those reached the surface of the JMR Plateau with a depth range between 200 m to 1000m.

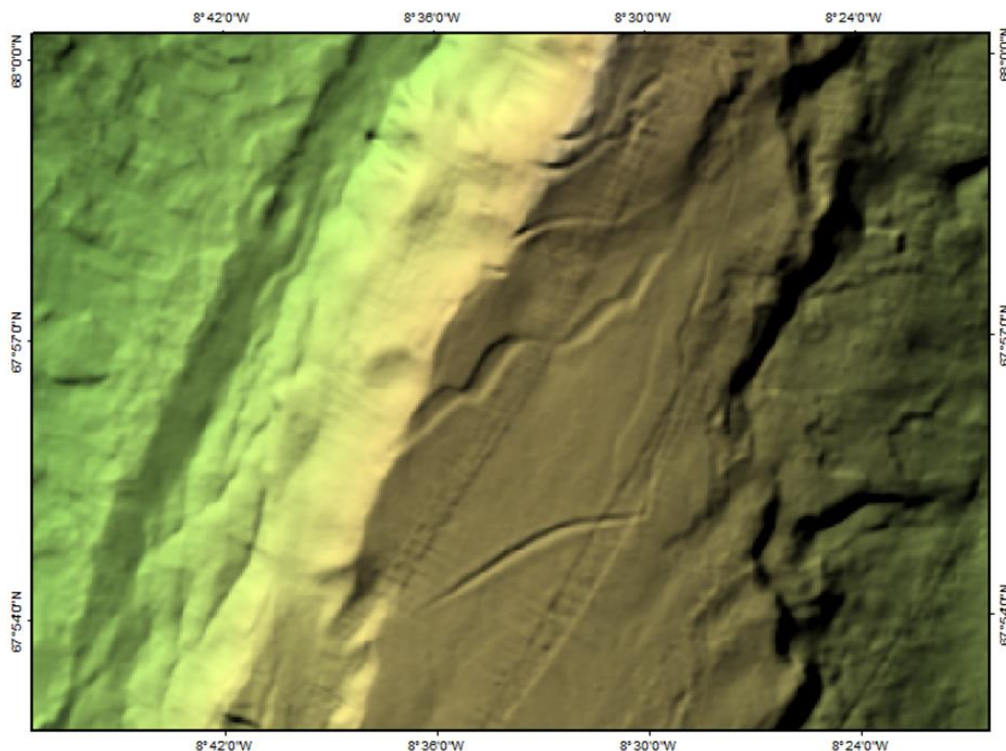


**Figure 29.** *Very large ice plough marks on the Otur Ridge plateau, the largest of which has a maximum width of around 400 m (50 m x 50 m multibeam data resolution). For location, see Figure 17.*

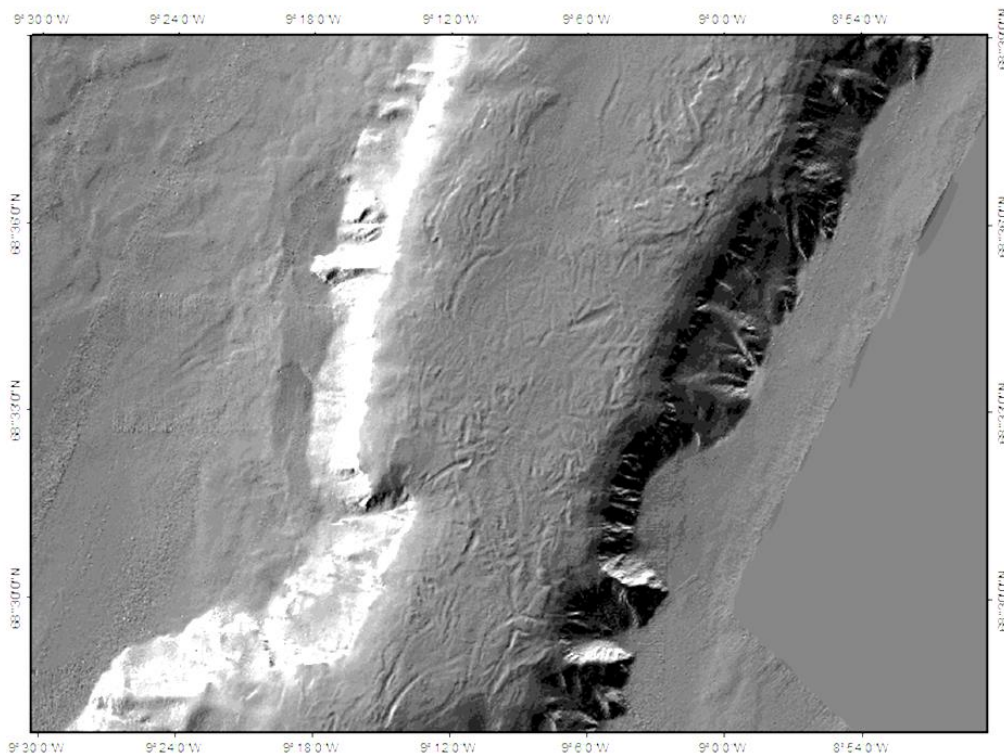


**Figure 30.** *The Lyngvi Ridge plateau has a high density of ice plough marks (15 m x 15 m multibeam data resolution). For location, see Figure 17.*

### 3.1.5 Pockmarks

No proven pockmarks were detected on the ridge plateaus in the 2008 and 2010 multibeam bathymetric data, and possible pockmark structures identified in the 1989 study (Gunnarsson et al., 1989) are more likely related to ice plough and erosional marks (Figure 31 & Figure 32).

A typical pockmark can be seen in Figure 33 from the Central North Sea. During the 1989 seismic reflection survey interpretation process, many possible pockmark-like depressions were flagged in the area, largely following the plateau of the main Jan Mayen Ridge (Figure 32 & Figure 34). Most examples from the JMR ridge plateau appear to be of different shape and character.

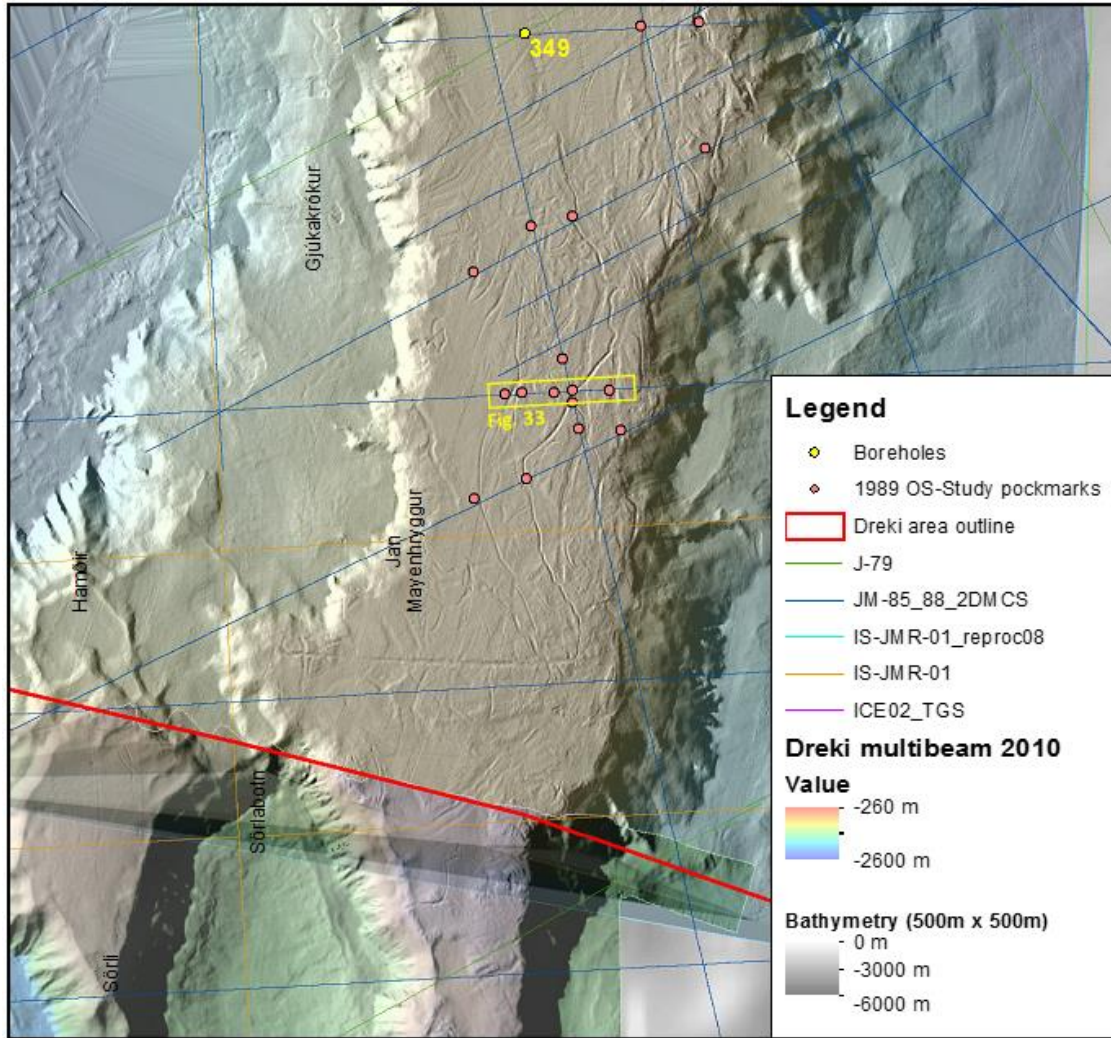


**Figure 31.** A11-2010 multibeam data review in comparison to the 1989 point features assumed to be pock marks, which are related to ice plough and erosional marks.



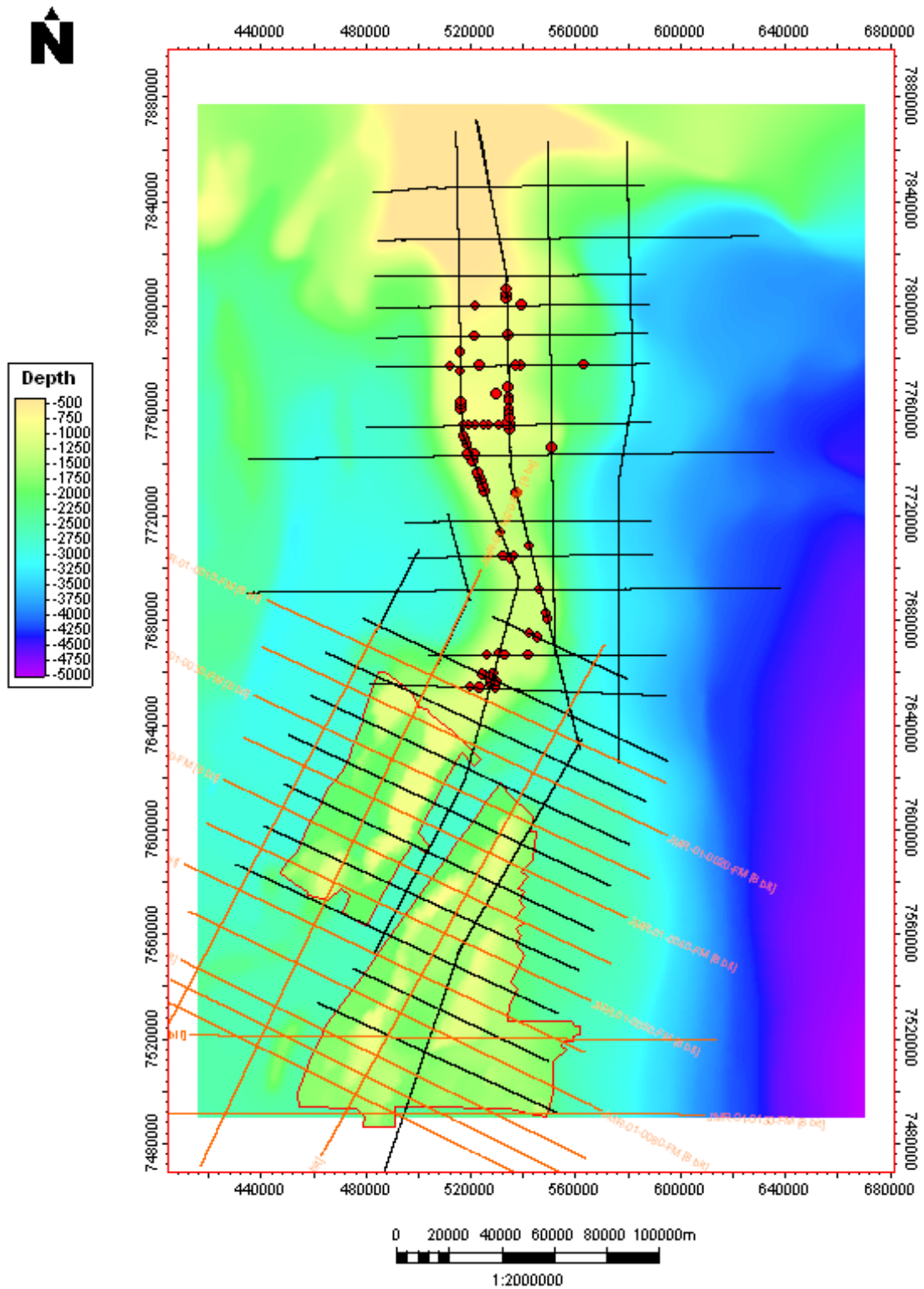


**Figure 32.** Possible pockmark locations based on the original 1985 2D multi-channel seismic reflection data and coarse gridded bathymetry data (Gunnarsson et al., 1989).



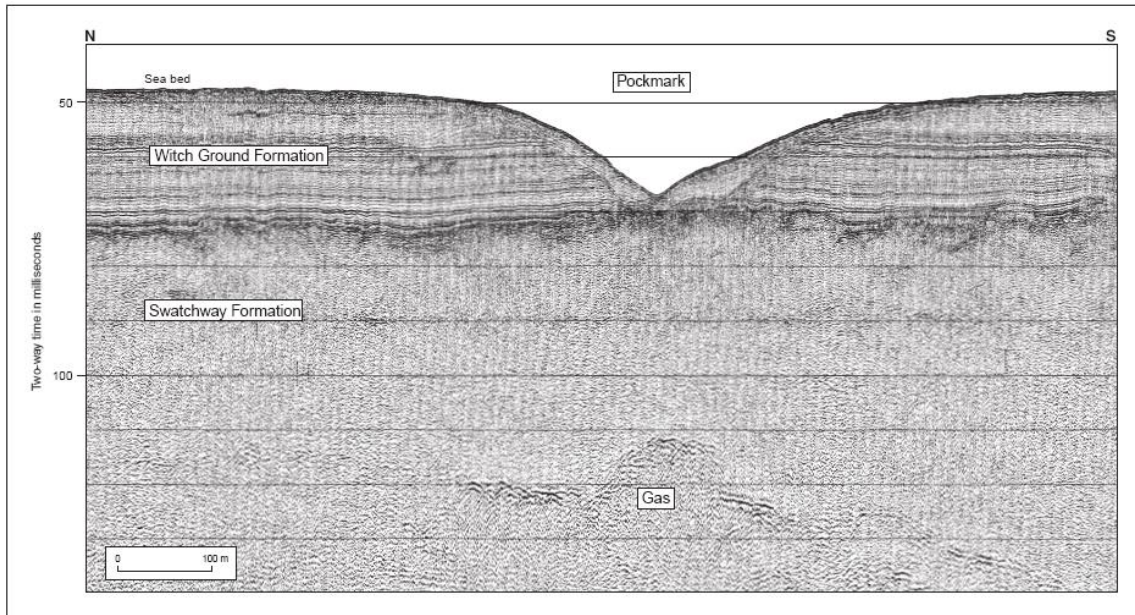


**Figure 33.** Seismic section example over a pockmark. A high-resolution, single-channel seismic section acquired over a large pockmark (Judd et al., 1994).

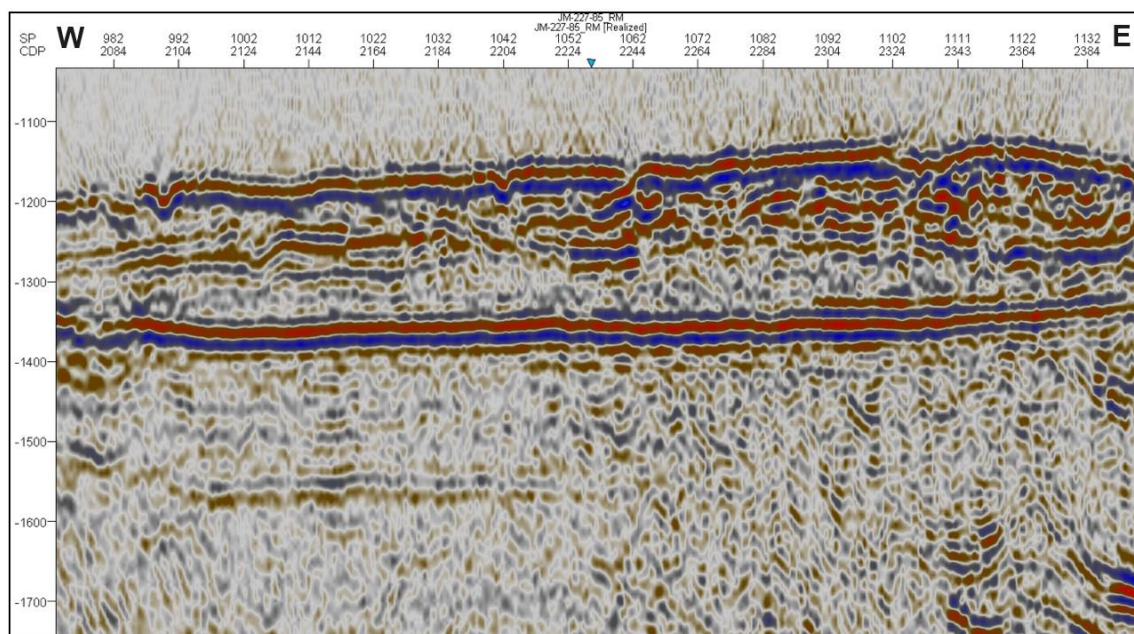


**Figure 34.** Line JM-85-14, 5 pockmarks on top of the Jan Mayen Ridge were interpreted on this line but the data quality makes an interpretation inconclusive, especially with the deeper apparent faulting and possible slumping at the edge of the structure. For location, see Figure 30.

A few sites in the multibeam data were identified as containing possible pockmarks. It is likely that some of those depressions are the result of faulting activity (Figure 35 to Figure 37), rather than the escape of gases or melting of hydrates. For the JMR area the interpreted possible pockmarks often have a different shape to them, which also could be related to the multi-channel seismic data that cannot image a pockmark feature as well as the high-resolution, single-channel seismic.

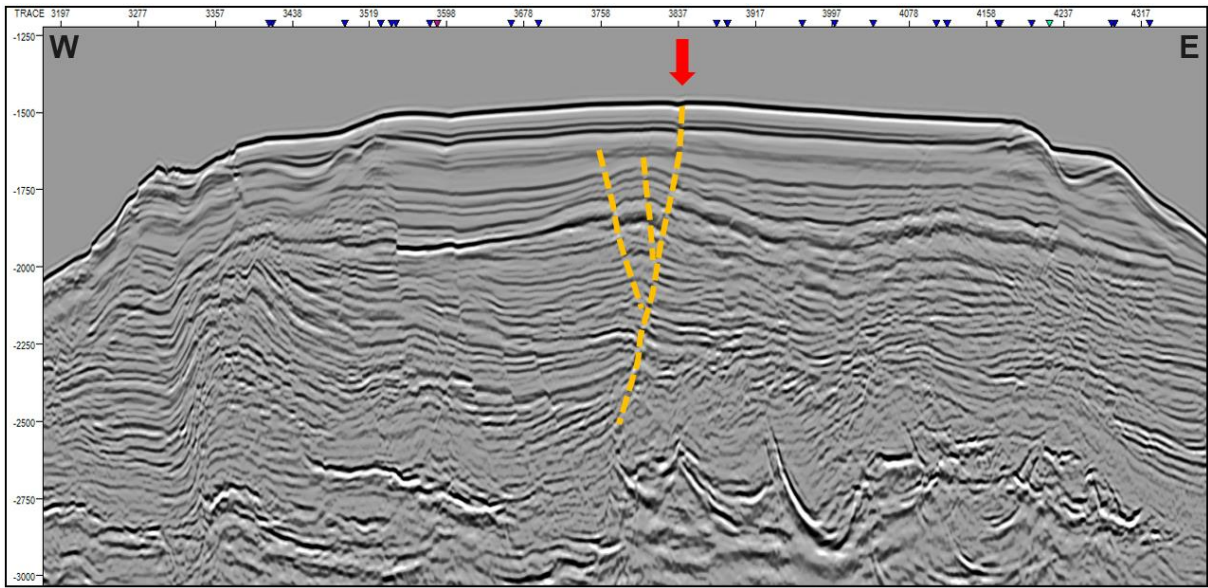


**Figure 35.** Sea floor surface marks (red arrow) showing primarily a small scale popup-fault structure (orange dotted lines) at the centre of the ridge. This fault feature relates to a pockmark like feature around trace 3837. Most other observed seafloor features are related to dragging traces on top of the plateau, normal faults and scouring. For location, see Figure 17.

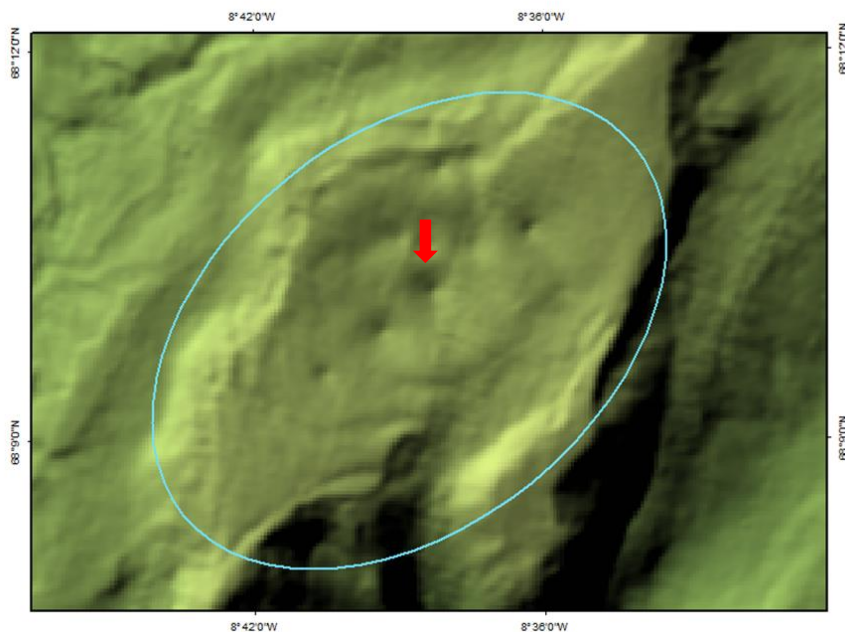


**Figure 36.** Pockmark-like depressions on the ridge structure in Fafnisrenna Channel (50 m x 50 m multibeam data resolution). For location, see Figure 17.



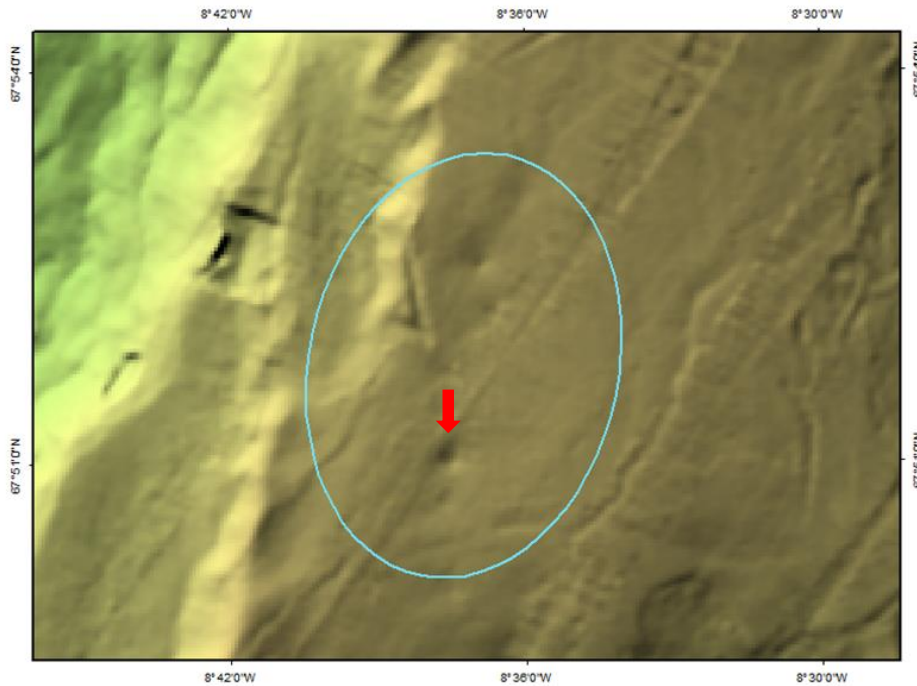


**Figure 37.** Pockmark-like depressions on Otur Ridge (50 m x 50 m multibeam data resolution). For location, see Figure 17.

### 3.1.6 Polygonal fault pattern

Polygonal fault patterns are most commonly observed in fine-grained sediments that sometimes can be very permeable and often are associated with oil or gas seeps and also pockmarks (Gay & Berndt, 2006). Polygonal faults can also be an indication of clay / smectite rich sediments that dehydrate and form polygonal fault patterns due to volume decrease of the sediment column (Dewhurst et al., 1999). This fault pattern type occurs in numerous sedimentary basins worldwide, and is most commonly located on passive margins, in on-lapping sedimentary infill units that tend to comprise of the finest grained sediments of the geological strata. The example in Figure 38 shows an analogue case of polygon faulting (dashed yellow box) to example line section for the JMMC in Figure 39. The Figure 38 analogue example of a seismic reflection data line that is tight to borehole records of well 21/2-5, displays the connection of different sediment sequence characteristics within three different geological time stages. The sequences are marked A - pre-Eocene of age with no polygon faulting, B - Eocene to middle Miocene of age with numerous short disrupted reflectors and polygonal faults, typical for the North Sea region, and C - middle Miocene to Recent of age without polygon faulting and continuous seismic reflective horizons, generally undisturbed up to the seafloor.

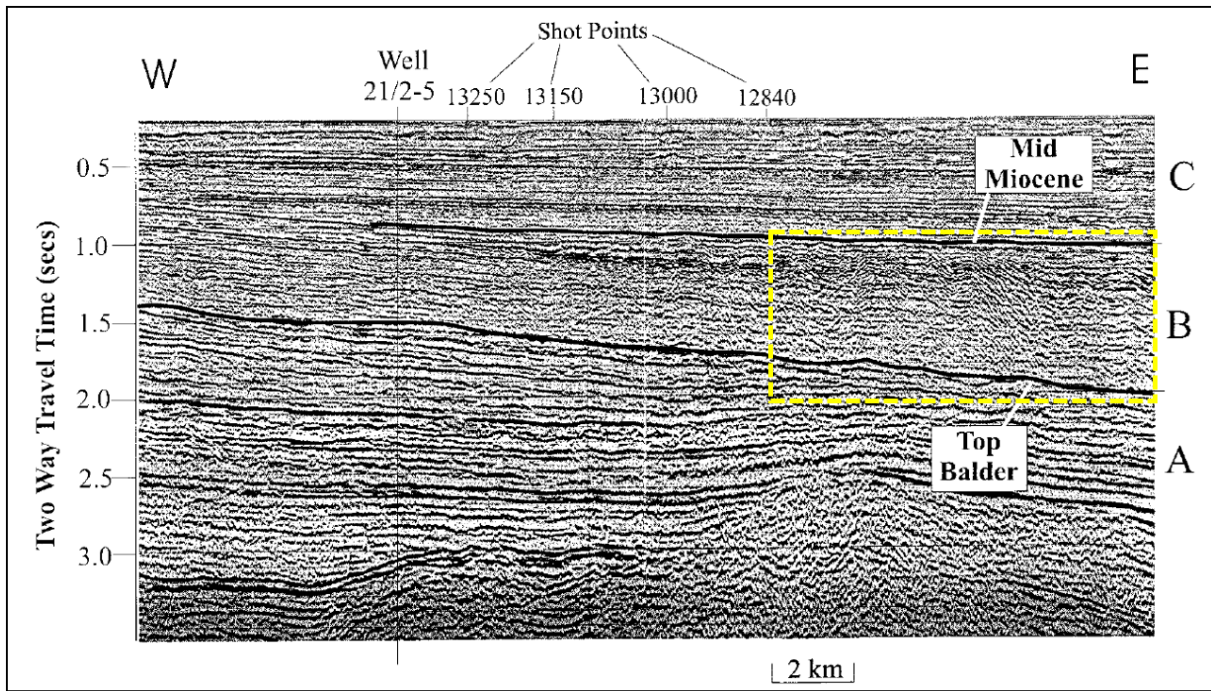


**Figure 38.** Dewhurst et al. (1999) published an analogue case of polygon faulting (yellow box).

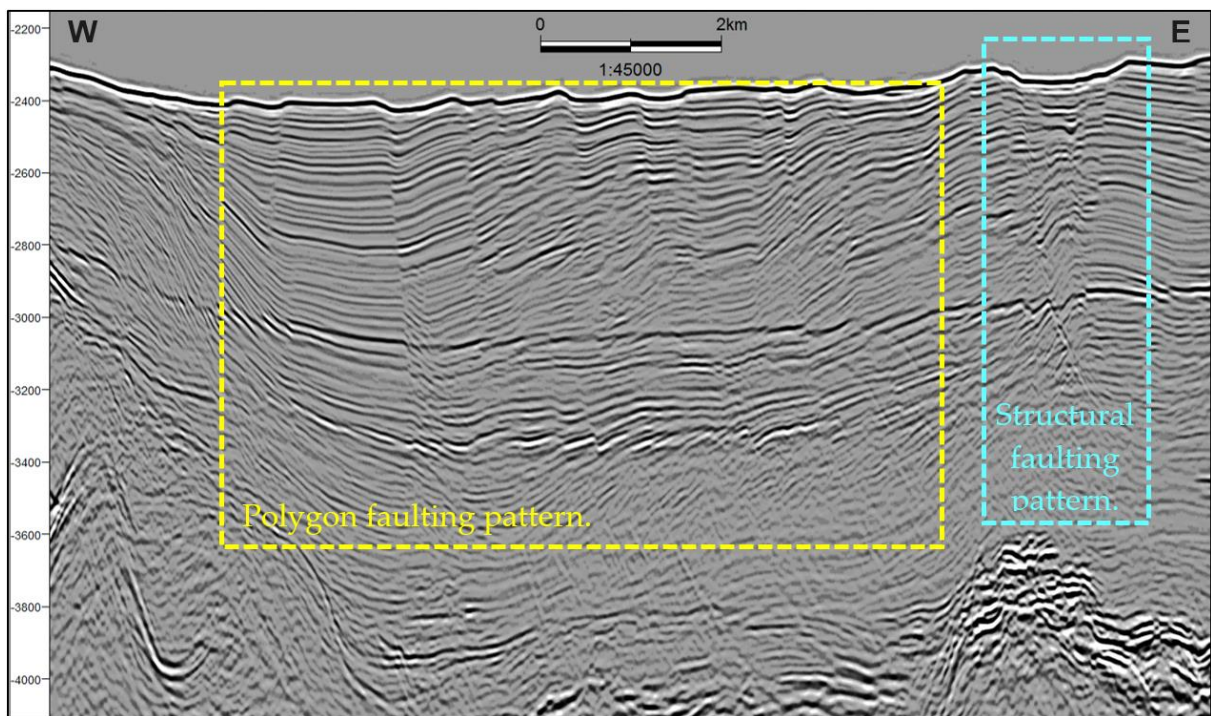


**Figure 39.** JMMC example of polygonal faults (yellow box) vs. structural faults (light blue box) within the southeastern most data extent of the Dreki area, along line IS-JMR-01-80 (vertical scale is in two-way travel time and the exaggeration is 4). For location, see Figure 17.



In the deeper area west of the Jan Mayen ridges, there are plateau areas with well visible “cracks” in the sea floor surface that could related to a polygonal fault system. They are caused by underlying sedimentary layers containing closely spaced small-scale extensional faults forming this polygonal pattern. These patterns were observed on most of the seafloor surrounding the ridges in the survey area, as indicated in Figure 39 and Appendix A & J.

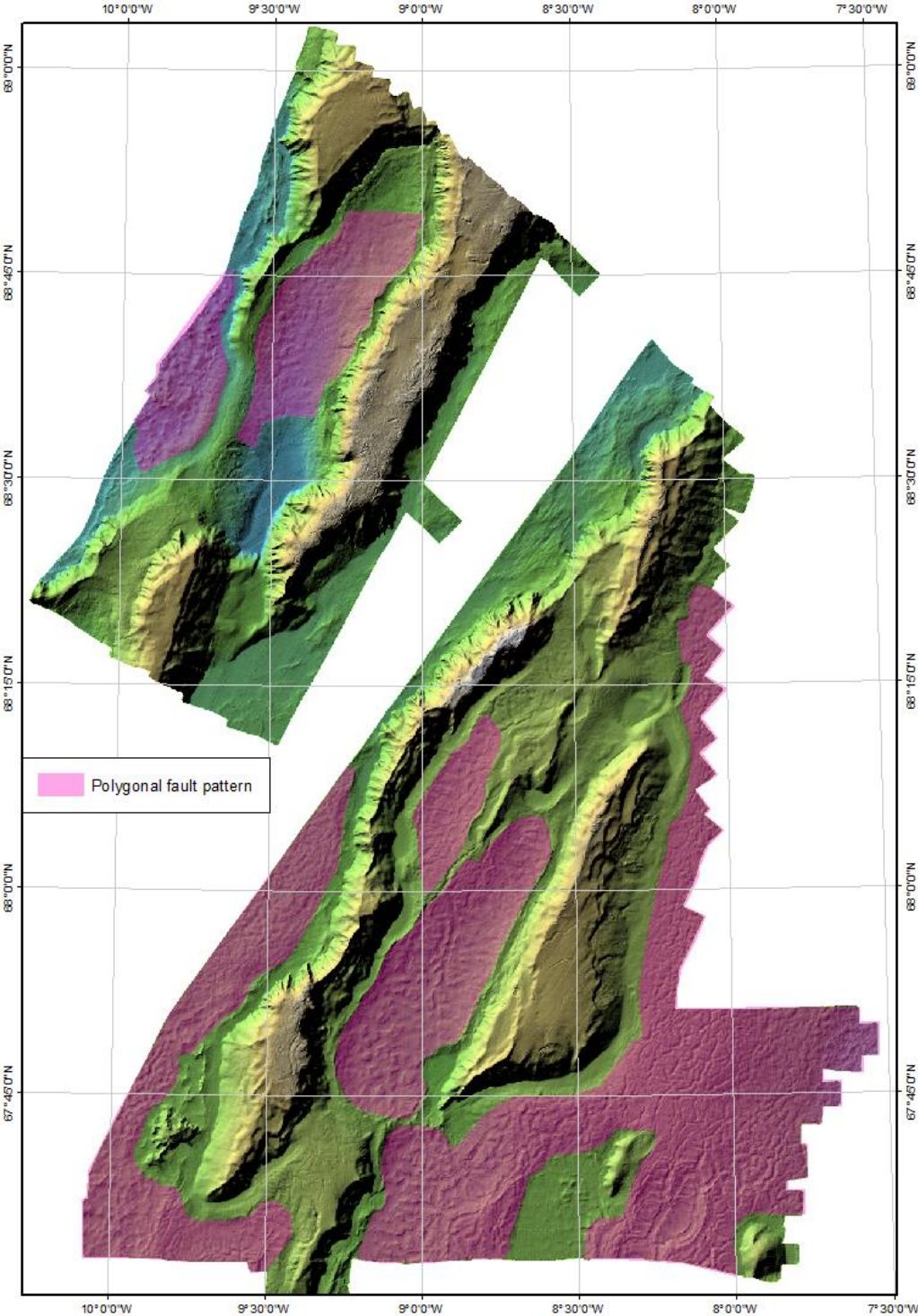


**Figure 40.** Overview map of the polygonal fault pattern areas. 50 m resolution, covering the areas of deep marine sediments that cover the lowest areas in between the ridges and along the flanks.

### 3.2 Multibeam backscatter

In ArcMap, a raster surface was made from the MRI processed multibeam backscatter xyz data (Figure 41). A number of different display parameters for the raster dataset were tested, both in order to highlight areas of potential artificial amplitude areas due to data problems (Figure 42), and to identify high and low amplitude areas (Figure 43 and Figure 44).

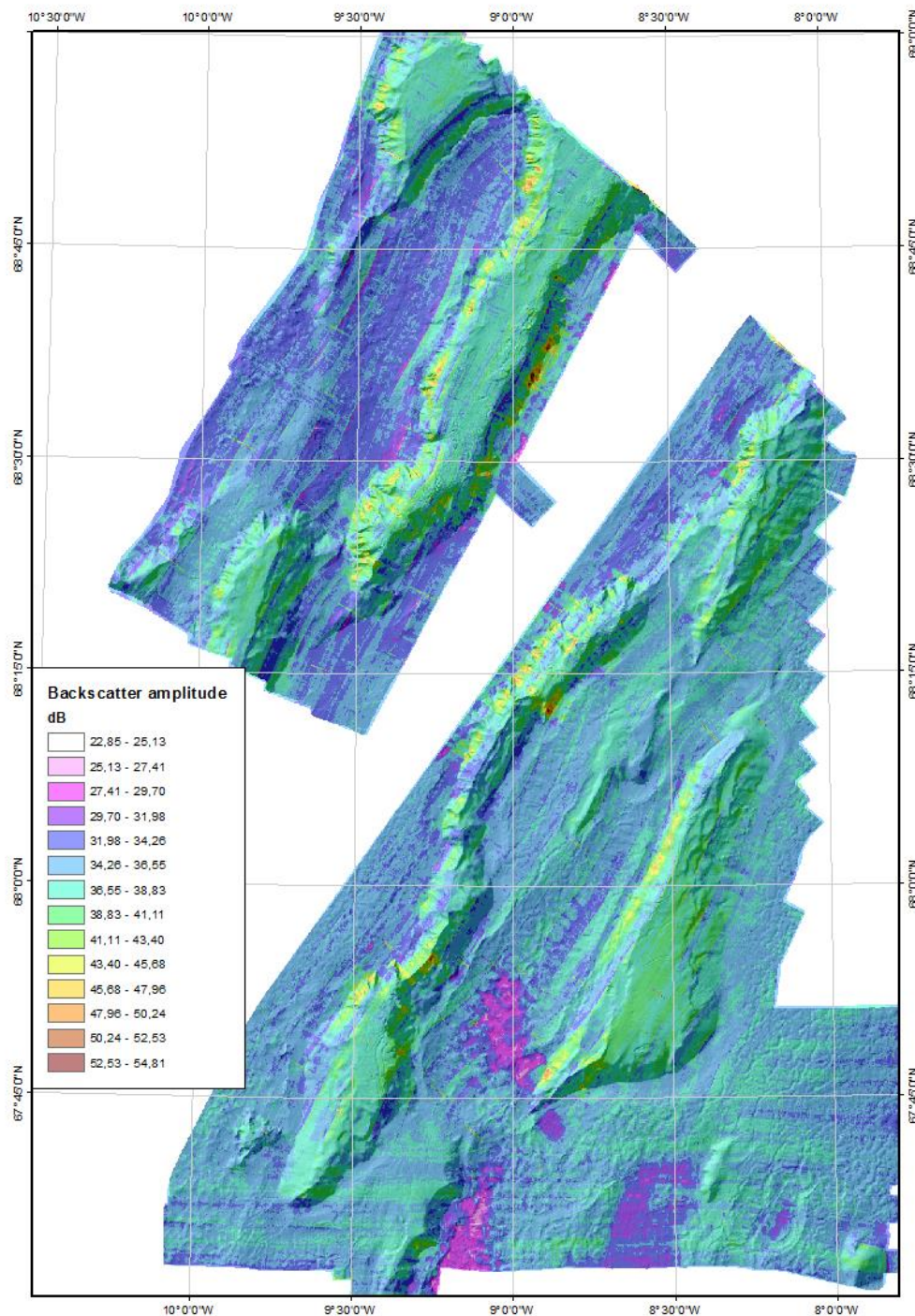
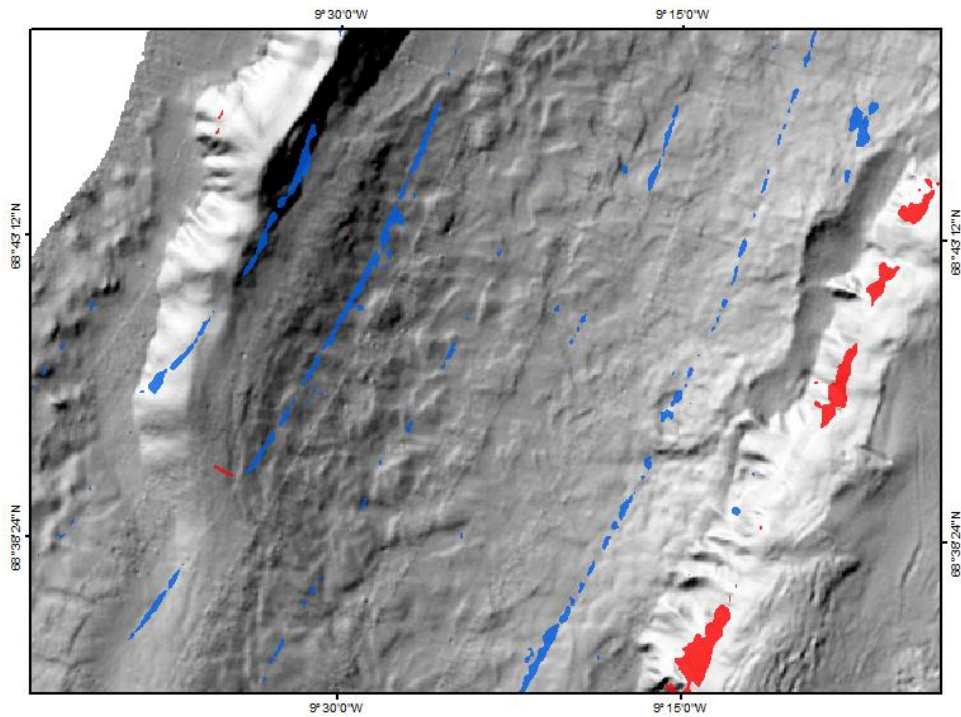
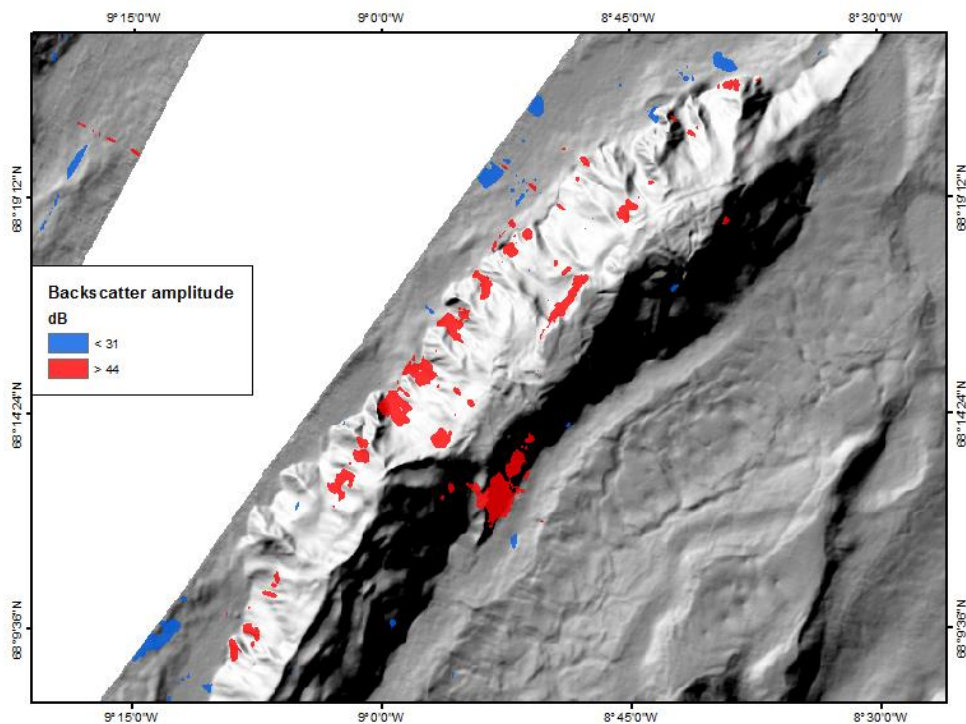


Figure 41. Overview map of the backscatter amplitude (50 m x 50 m resolution).





**Figure 42.** The amplitude data contained linear artefacts correlating with the survey vessel's (inferred) sailing route and possible "edge effects" indicating that there was not enough overlap between the data sweeps (50 m x 50 m resolution).



**Figure 43.** Reginn Knoll showing high amplitude values on its slopes (50 m x 50 m resolution).

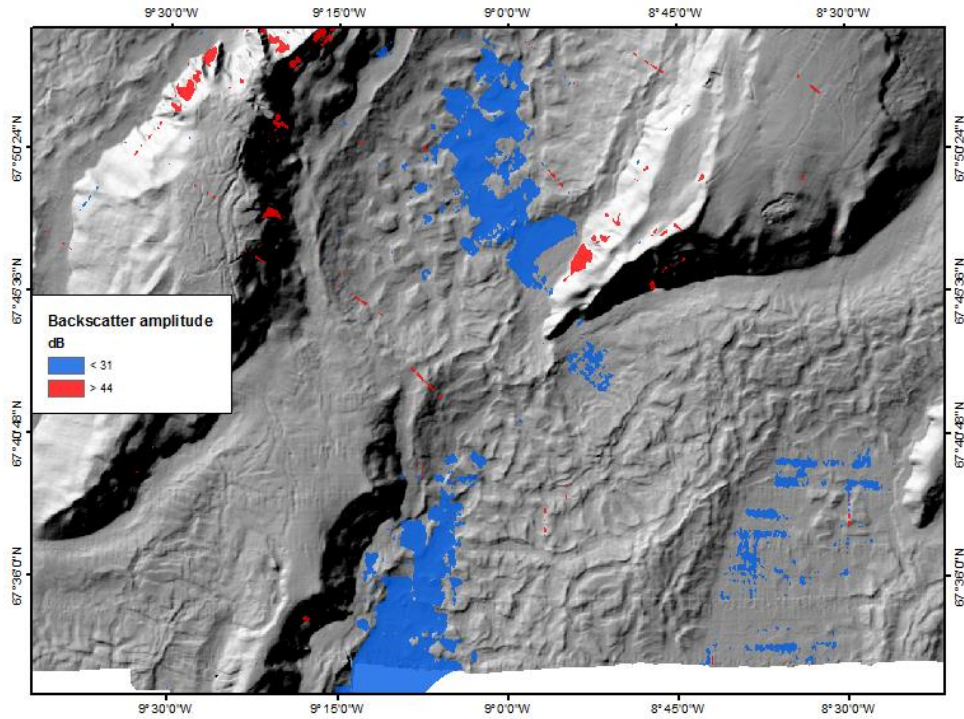


**Figure 44.** *Low amplitude values can be seen clearly in Fáfnisrenna Channel and at the southern margin of the Völsungur area (50 m x 50 m resolution).*

High amplitudes are mostly present along the slopes of the ridges, with the highest values usually coinciding with the steepest sections of the slopes. Low amplitude values are primarily seen in the deep regions in between the ridges, such as within the Sörlabotn Trench and Fáfnisrenna channel, as well as overlapping areas with polygonal fault patterns (Figure 44).

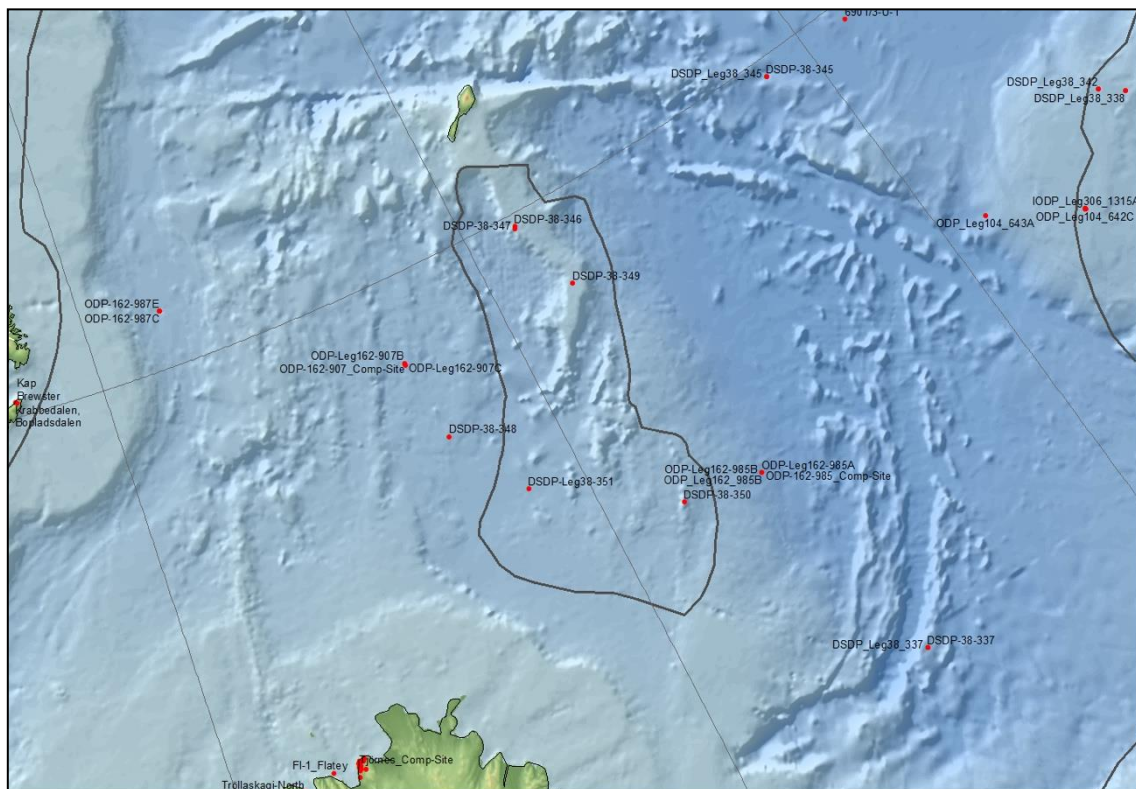


## 4 Borehole and seafloor sampling database

Well data available for the greater JMMC area were acquired through the Deep Sea Drilling Project (DSDP), Leg 38 in the year 1974, and through the Ocean Drilling Program (ODP), Leg 151 in 1993 and ODP Leg 162 in 1995. Also available are sea floor sampling data of four sampling campaigns. The first one was carried out in 1980 by the Russian science academy (formerly Soviet Union), in 2010 by the NEA, NPD and MRI, in 2011 by NPD and TGS-VPBR (Volcanic Petroleum Basin Research), and the latest seafloor sampling survey was conducted by NPD in 2012, see Table 1 and Table 2.

### 4.1 Boreholes

Following is a quick data and interpretation summary of borehole data acquisition for the Jan Mayen microcontinent area, as this is the only “hard” evidence of the present rock formations along the ridges closest to the seabed, besides the geophysical indirect analysis data.



**Figures 45.** Location of the DSDP and ODP boreholes for the East Greenland - Jan Mayen – Norway Basin corridor.

#### 4.1.1 The Jan Mayen Ridge wells - DSDP boreholes, 1974

In 1974, a series of boreholes were drilled in the Jan Mayen area as part of the Deep Sea Drilling Project (DSDP, precursor of ODP and IODP) (Talwani & Udintsev, 1976). The program was primarily designed to test and put constraints on the plate tectonic evolutionary history (Eldholm et al., 1989). During the project, 18 holes were drilled in the Norwegian-Greenland seas. Thereof were five holes, numbered 346–350, drilled at or near the Jan Mayen Ridge (JMR), during Leg 38 of the project. Locations of these holes are shown in Figure 45, demonstrating that wells 346, 347 and 349 are located on the North Ridge, well 350 in the Southern Ridge Complex, and well 348 on oceanic crust of the Kolbeinsey mid-oceanic ridge, see Figure 46 for the well correlation panel. Positions, water depth and total drilled section depth values of the boreholes are listed in Table 4 (Talwani & Udintsev, 1976).

The penetration depths of the boreholes are between 187 and 544 m and water depths range between 700 and 1800 m. Core analyses had showed that the boreholes primarily crossed clay rich or silty sediments. Stratigraphic section biomarkers had been analysed down to Eocene (45.5 Ma), and within the Eocene section of one well (i.e. well 346). The core samples have been analysed for total organic carbon (TOC) as well, reaching up to 4.8%, and showing oil genesis of organic matter at a very early stage. Core analysis based on density and vertical velocity data is available for the wells, which enabled a depth-seismic tie (TWT) to confirm the Top Eocene marker for two wells on the JMR (Talwani & Udintsev, 1976). Unfortunately, the boreholes did not reach the JMR's oldest sedimentary layers, which are considered to be most important in terms of oil and gas resources (Richter & Guðlaugsson, 2007).

**Table 4.** Boreholes in the Jan Mayen area, drilled during Leg 38 of the Deep Sea Drilling Project in 1974 (Gunnarsson et al., 1989).

Hole	Latitude		Longitude		Water depth (m)	Penetration (m)
	Deg.	Min.	Deg.	Min.		
346	69	53.35N	08	41.14W	732	187
347	69	52.31N	08	41.80W	745	190
348	68	30.18N	12	27.72W	1763	544
349	69	12.41N	08	05.80W	915	320
350	67	03.34N	08	17.68W	1275	388

Initially, K/Ar dating of the basalts at the base of well 348 gave an age of 18.8 Ma ( $\pm 1.7$  Ma) (Talwani & Udintsev, 1976), which compares well with magnetic anomalies C6 to C6A (Gaina et al., 2009).

Well 350, on the other hand, shows an inconsistency in regards to the age dating of the basalts at the base of the well, where the K/Ar age dating (Talwani & Udintsev, 1976) ranges between 33.5 Ma ( $\pm 2.8$  Ma) and 50.5 Ma ( $\pm 5.5$  Ma) within a 3 m section of the wells core samples.

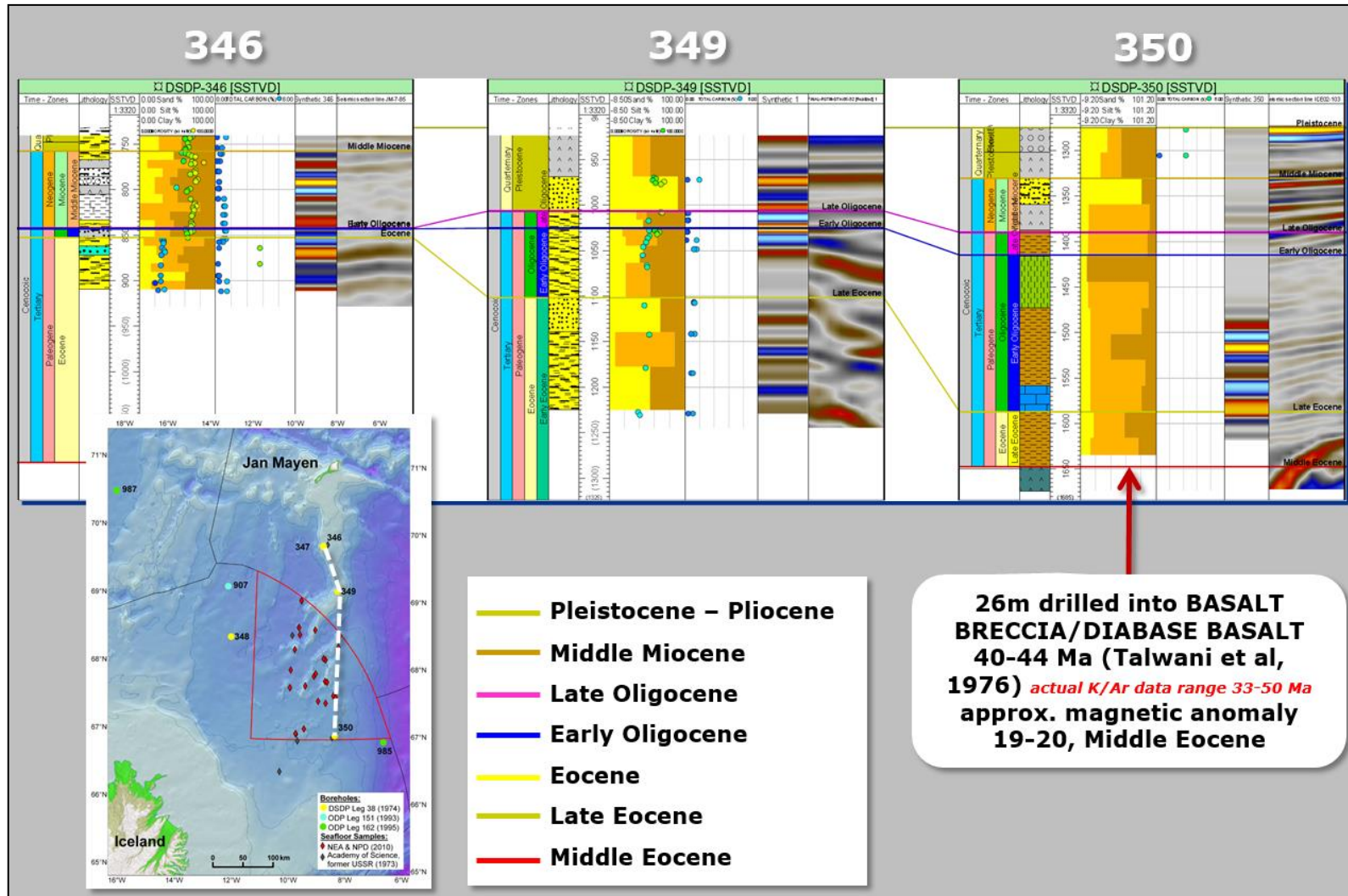


Figure 46. Jan Mayen Ridge well correlation panel tied to the JM-85 seismic data set.

## 4.2 Seafloor sampling and benthic surveys

As well records are quite slim over the JMMC area, so are seafloor samples in regards to outcropping lithology records, source rock potential analysis, and possible hydrocarbon seep records. Five seafloor sampling campaigns have been conducted since 1980, which are further described in this section.

### Soviet sea floor sampling

In 1980, a study on sea floor samples from the North Atlantic was conducted by the Soviet Geophysical Committee of the Academy of sciences of the USSR. The samples were obtained in 1971 and 1973 during a Russian seafloor sampling campaign with a focus on differentiating oceanic crust from continental crust (Geodekyan et al., 1980). The objective of the study was to examine the variation in gas concentrations in sea water and bottom sediments from the North Atlantic, and identify HC-gas anomalies which could possibly be related to hydrocarbon formation. In this study, the near-bottom layer was considered most important. 120 water samples and 28 samples of bottom sediments were used, which had been collected in cruises 10 (1971) and 15 (1973) of the Soviet research vessel R/V Akademik Kurchatov. The stations of gas measurements were located in extremely diverse geo-tectonic zones, such as the Reykjanes and Kolbeinsey rift-type ridges, the Charlie-Gibbs fracture zone, the submerged continental crustal blocks of the Iceland plateau, the Faroe Islands sill and the Vøring plateau, and zones of typical oceanic sediments (Figure 47).

A comprehensive interpretation was made which enabled identification of four gas-geochemical zones, which were considered to be related to processes occurring in the earth's crust, specifically analysing the rapid increase in He migration flow and a correlation of hydrocarbon concentrations with the thickness of the sedimentary strata. It was concluded that the distribution of the gas-geochemical zones implied that the areas lying to the north and north-east of Iceland belong to the continental rather than the oceanic type of the earth's crust. The results of the study corroborated a possibility of catagenesis and hydrocarbon formation in depositional basins of the area with sediments exceeding 1500 m in thickness. For this reason the uplifted crustal blocks including the north-eastern areas of the Iceland plateau and the Vøring plateau, are worthy of investigation for the purpose of oil and gas exploration (Udintsev, 1980).



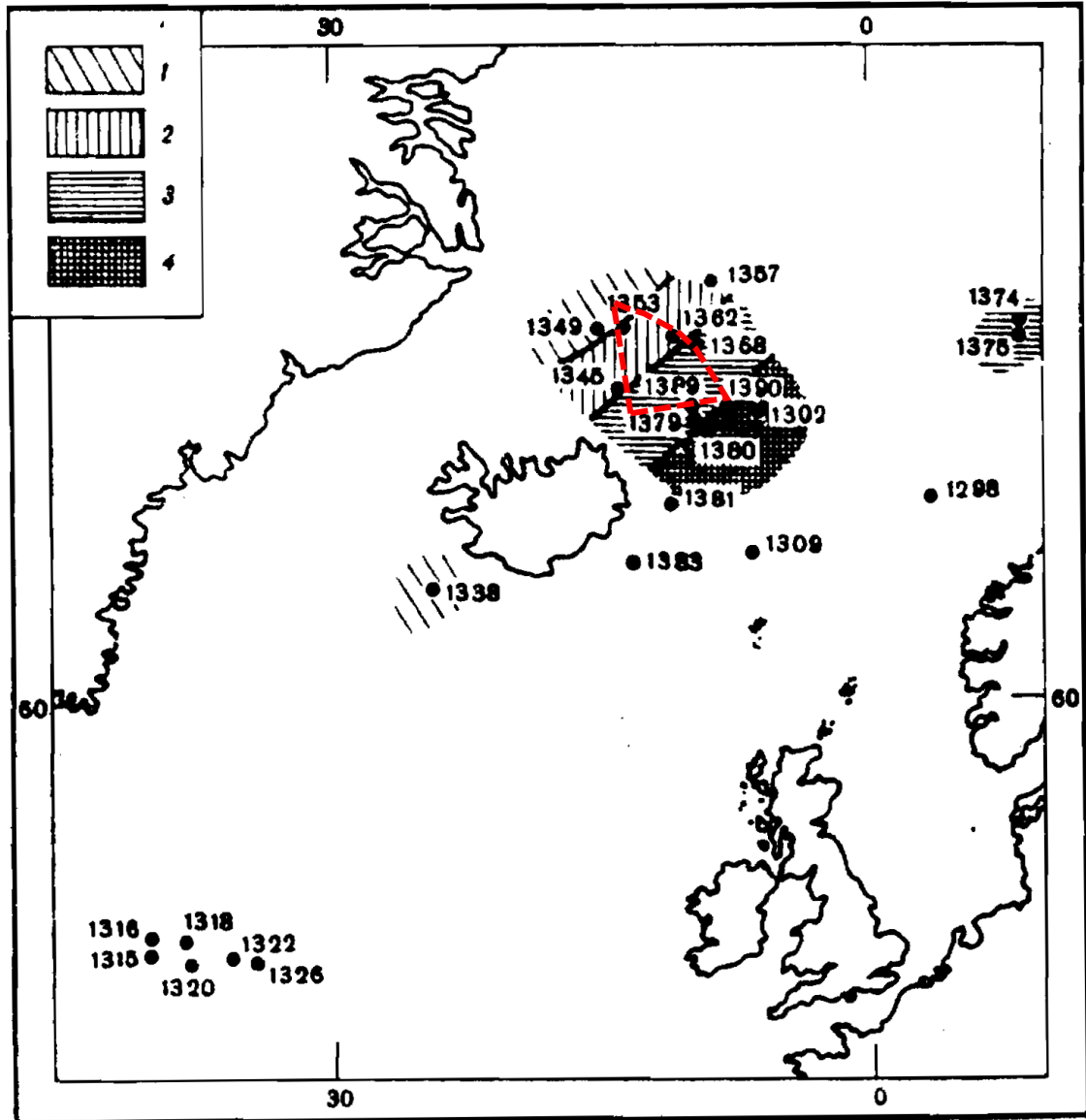
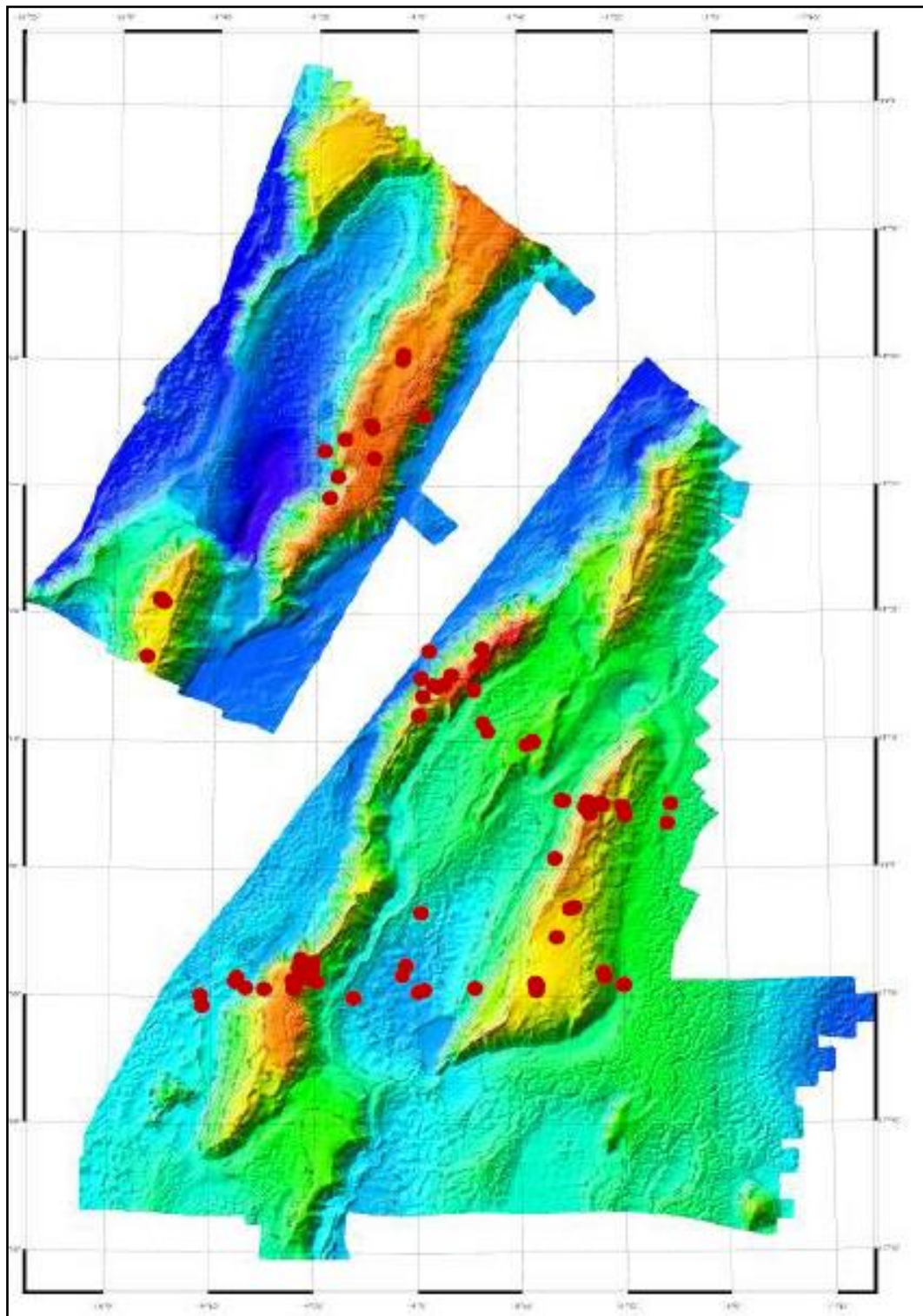


Figure 47. Location map of gas measurements during the 1971 and 1973 surveys (Udintsev, 1980). The legend shows a number code in regards to the mapped content of hydrocarbons (HC) and  $\Delta\text{He}$ , with: 1 – no HC & low  $\Delta\text{He}$ ; 2 – low HC & high  $\Delta\text{He}$ ; 3 – HC and  $\Delta\text{He}$  higher than normal; and 4 – anomalously high HC &  $\Delta\text{He}$  higher than normal. The approximate location of the Dreki licensing area is marked with a dashed red line.

#### MRI benthic survey, 2008 (B11-2008)

A benthic survey was carried out in the Dreki area by the Icelandic Marine Research Institute (MRI) in August 2008. The objective was to obtain general information on the area with benthic communities and habitat research. Samples were taken at 80 locations with depth ranging from 800 to 2000 m (Figure 48). The data were collected using a variety of sampling methods in order to obtain comprehensive information on the broad-scale distribution patterns of the benthic fauna. This included sample collection with four types of towed sledges and an underwater camera system (Helgadóttir, 2008a, b).



**Figure 48.** *Location of samples taken in MRI's benthic survey (Helgadóttir, 2008a).*

#### 4.2.1 NEA-NPD, Dreki Sea floor sampling campaign 2010

NEA carried out a seafloor sampling cruise to the Jan Mayen Ridge in 2010, in cooperation with NPD and MRI (Figure 49). The purpose of the sampling campaign was to map the presence and distribution of suggested oil and gas seepages to identify areas with potential for petroleum reservoirs, which would help to answer the question if the JMR contains an active petroleum system or not. Subsequently, this would also reduce the area to be investigated and focus exploration efforts on regions and structures with active seepage, and predict the oil versus gas potential of prospective structures (Blischke et al., 2010).

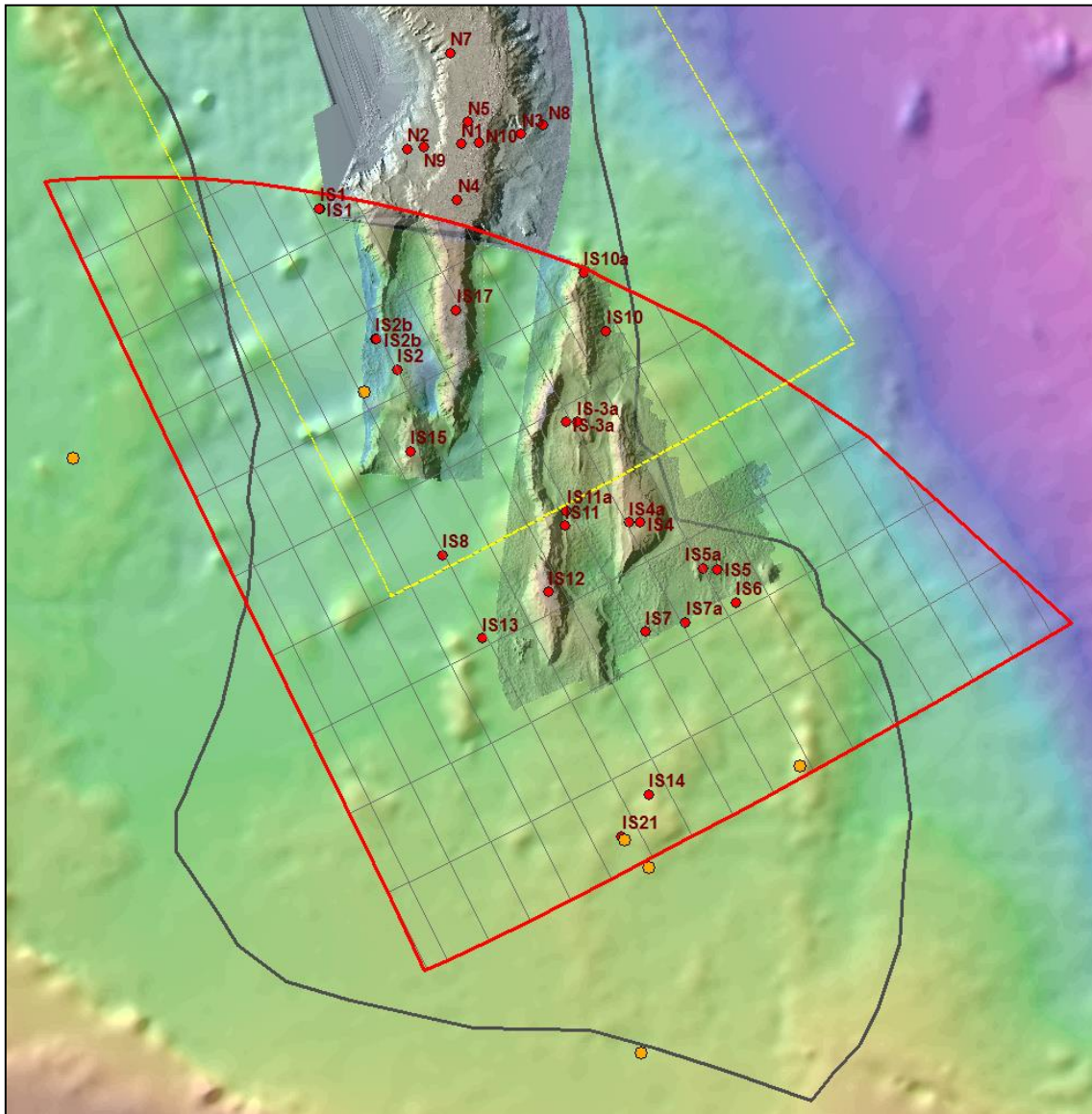


**Figure 49.** Sample sites locations (red points) of the 2010 seafloor sampling campaign, with the Russian seafloor samples for comparison (orange points), and the Dreki licensing area outline (red line).



**Table 5.** A11-2010 Piston coring survey samples (20.08-26.08.2010), supervised and analysed by Fugro Norway.

Id#	Station-name	Latitude	Longitude	Depth-bottom	Barrel-length (m)	Total cored depth (m)	Core-length (m)	Sample-depth (m)
589	N1	69°01.97'N	08°22.69'V	848.76	6	6	3.5	3.2-3.5
590	N2	69°05.74'N	08°46.56'V	1333.8	6	6	2.4	2.10-2.40
591	N3	68°59.06'N	07°55.46'V	1556.1	6	4	2.8	2.5-2.8
592	N4	68°54.31'N	08°37.22'V	862.95	6	5.5	3.9	3.6-3.9
593	N5	69.05.20'N	08°15.09'V	839.35	6	5.7	3.08	2.78-3.08
594	N7	69°16.68'V	08°06.38'V	993.44	6	5.8	4.16	3.86-4.16
595	N8	68°58.44'V	07°43.97'V	1835.2	6	6	3.25	2.95-3.25
596	N10	69°01.17'N	08°15.34'V	817.37	6	6	4.75	4.45-4.75
597	N9	69°04.75'N	08°38.78'V	1234.5	4.5	4.5	2.8	2.45-2.80
598	IS1	69°04.14'N	09°36.43'V	1830.5	4.5	2.5	1	0.65-1
598	IS1	69°04.19'N	09°36.63'V	1841.1	4.5	3.5	2.55	2.2-2.55
599	IS2b	68°39.79'N	09°41.81'V	2030	4.5	3	1.1	0.75-1.1
599	IS2b	68°39.70'N	09°41.45'V	2034.4	4.5	2.5	1.25	0.55-0.9
600	IS-3	68°10.63'N	08°36.82'V	1377.3	4.5	Whole core muddy	<50 cm	no sample
600	IS-3a	68°10.90'N	08°37.45'V	1378.5	4.5	3	0.5	0.1-0.5
600	IS-3a	68°12.30'N	08°41.80'V	1458.6	4.5	3.1	2.4	2.1-2.4
601	IS4a	67°52.15'N	08°38.68'V	1092.1	4.5	3.5	2	1.65-2
602	IS4	67°50.86'N	08°33.87'V	1060.7	4.5	3	1.2	0.9-1.2
603	IS5a	67°38.78'N	08°19.52'V	1503.9	4.5	4	2.55	2.20-2.55
604	IS5	67°37.56'N	08°14.20'V	1589.9	4.5	4	2.75	2.40-2.75
605	IS6	67°31.26'N	08°13.69'V	1560.6	4.5	4	1.65	1.30-1.65
606	IS7	67°33.91'N	08°55.50'V	1661.6	4.5	3	2.4	2.15-2.4
607	IS7a	67°32.37'N	08°37.72'V	1683.6	4.5	2	1.6	1.25-1.6
608	IS12	67°48.17'N	09°25.64'V	929.66	4.5	4	3.35	3.0-3.35
609	IS11	67°56.55'N	09°04.79'V	1658.6	4.5	3	2.4	2.05-2.4
610	IS11a	67°59.03' N	09°01.25'V	1641.6	4.5	Full	3.55	3.2-3.55
611	IS10	68°22.43'N	08°06.05'V	1628.9	4.5	Full	2.95	2.55-2.95
612	IS10a	68°32.78'N	08°01.47'V	1624.3	4.5	2	1.4	1.1-1.4
613	IS9	68°34.37'N	08°41.06'V	1912.5	4.5	0		
614	IS17	68°38.06'N	09°02.31'V	895.43	4.5	3	2.5	2.15-2.5
615	IS2	68°33.52'N	09°39.48'V	1894.5	4.5	3.2	2.2	1.85-2.2
616	IS15	68°20.31'V	09°51.49'V	1070.3	4.5	3	2.25	1.9-2.25
617	IS8	68°02.16'N	10°00.52'V	1912.2	4.5	3	1.95	1.65-1.95
618	IS13	67°46.30'N	10°02.02'V	1727.3	4.5	Full	2.15	1.85-2.15
619	IS14	67°09.45'N	09°27.98'N	1264.6	4.5	3.5	2.8	2.45-2.80
620	IS21	67°04.95'N	09°47.30'V	1505.3	4.5	2	0.25	0-0.25

The sampling campaign was carried out on-board MRI's Árni Friðriksson. The coring equipment consisted of the Benthos Model 2175 piston corer, which can obtain 3 to 5 m long samples. The Woods Hole gravity corer was also in use, which can obtain 0.3 to 0.6 m long samples. The coring samples were sent directly to the Fugro Geolab No AS in Trondheim, Norway, for geochemical analysis (Blischke et al., 2010).

The first objective of the cruise was to collect seafloor samples in order to evaluate hydrocarbon prospects of the North Dreki area in the southern part of the Jan Mayen Ridge complex. The second objective of the cruise was to acquire a high resolution multibeam bathymetric and sub-bottom profiler data on behalf of the NPD & NEA. These instruments were active during the whole survey, including the core phase. (Blischke et al., 2010).

In order to get a as complete as possible geological coverage of the North-Dreki area, various sub-regions were selected for sampling, such as structural highs and lows, volcanic regions and suggested pre-Tertiary sedimentary regions. A total of 39 proposed sites were selected, of which 11 sites were located on the Norwegian side and chosen by the NPD, and 28 sites were selected on the Icelandic side of the Jan Mayen Ridge (Blischke et al., 2010). On the Norwegian side, 9 samples were collected, and for the Icelandic side, 28 samples were collected, of which 3 sample sites were gravity-cored twice, see Table 5.

### **2010 seafloor sampling data and results**

Previous studies, as the Russian seafloor sampling campaign in the 70's and the DSDP and ODP drilling campaigns in the 70's and 80's, have revealed that methane and some higher chained carbon gases were present, but from the DSDP Leg 38 drilling project, it became apparent that the samples had very low TOC (total organic carbon), or between 0.18% and 1.04%. These observations showed samples with marine organic matter in a very early stage of oil generation, but a low source rock potential. The published results by Hood et al. (1976) indicated slightly higher TOC values, with the highest effective content of hydrocarbons (HC) not exceeding 0.22%, therefore, it was concluded that the Tertiary samples did not show potential of source rock quality.

The sampling analysis results for the JMMC area most probably indicate a "background" content of organic matter (OM) of the marine sediments within the area with a TOC range of 0.5% to 1%. This compares well with globally mapped and analysed organic carbon samples of the surface layers of sediments in the world oceans (Bezrukov et al., 1977).

The hypothesis has always been that Mesozoic, or even older sediments, are buried underneath the Cenozoic strata of the JMMC, which could provide the needed source rock unit to make the JMMC a hydrocarbon province. Due to the lack of deep well control, all work so far had to be compared with analogues of the East Greenland margin, the Norwegian margin and the Vøring and the Møre basins. Here especially, the link to the Mesozoic Kimmeridge clay, as one of the main source rock targets, has been of interest and is suspected to be underneath the pre-breakup section, if the Mesozoic strata is present.

As it is important to find direct hydrocarbon indicators (DHIs), the 2010 sampling campaign was conducted, and the main samples were analysed with standard procedures and standard key indicators were processed, calculated and compared to known source rock data from the Norwegian margin.

The results (Ferriday, 2010) of this analysis and comparisons showed that no real indications of oil shows (visual or smell) were observed during coring, but suggests a source maturity of ~0.7% Ro (vitrinite reflectance), i.e. mid-oil window, albeit the restricted number of carbon isotope-analysable gas samples. Most of the gas chromatograph (GC) results did not indicate live oil or gas expulsion, but only immature organic matter. However, the most promising samples with the highest TOC, methane, ethane, and n-alkane concentrations lie in the

Norwegian sector (sample Id: N1, N2 & N3; see location in Figure 49), on the main ridge with a deep, pre-breakup basin structure beneath the Cenozoic strata (Blischke et al., 2016).

Still, analysed headspace gas GC data indicate low yields of practically only methane, the methane of the area probably being of mixed biogenic and thermogenic origin (Ferriday, 2010). Gas data indicates that activity has been consistent in this area over time, but possibly greater in more historic times, and seepages have only been small in absolute terms. The seepage origin could be matured source rocks in the central ridge area, possibly from a hydrocarbon-bearing reservoir. Gas seepage can alternatively occur due to interaction of high reaching sill or dyke intrusive into the local sediments.

Based on the results of the 2010 seafloor sampling study and measurements from the 1971 and 1973 sampling projects, little evidence of to the surface leaking maturing organic matter in form of oil, condensate, or gas can be shown. These results would therefore not support the existence of a working hydrocarbon system, and for the most part possibly indicate small source rock volumes within the post-breakup strata.

#### **4.2.2 NPD seafloor sampling survey, 2011 & 2012**

Seafloor sampling was conducted successfully by the NPD (Sandstå et al., 2012; 2013) in the years 2011 and 2012 (see Figure 50), using a remotely operated vehicle (ROV) in collaboration with the University of Bergen, targeting sampling locations on the Norwegian and the Icelandic sector. In the 2011 survey, the ROV was equipped with a gripper arm, designed to break off rock samples from possible in-situ formation outcrops.



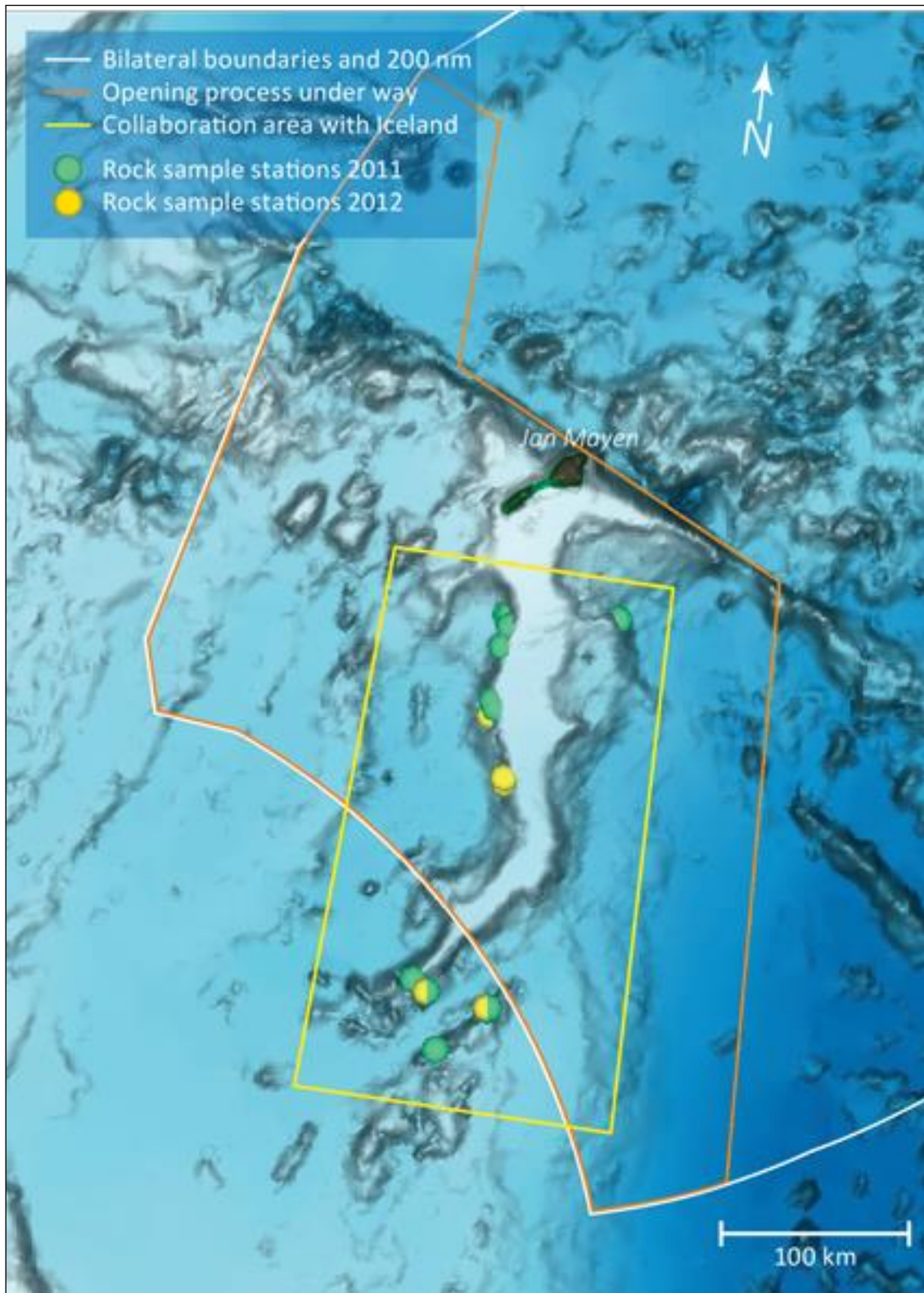


**Figure 50.** NPD sampling stations for ROV surveys in 2011 and 2012, shown in green and yellow, respectively (Sandstå et al., 2012; 2013).

During the 2012 survey, a chain saw was setup onto the ROV to cut samples out of the rock face. As the 2011 sampling campaign brought up the important question of age correlation results, and in-situ versus allochthon samples, especially for the local correlation of the NE Dreki area (Figure 51), some additional samples were taken in that area in 2012. These samples were then compared to the newly acquired 2D reflection seismic data, raising the primary question if the ROV was sampling a slumped block along the fault escarpment or not (Figure 51 to Figure 53), as interpreted by the NPD for this part of the ridge complex (Sandst a et al., 2013).

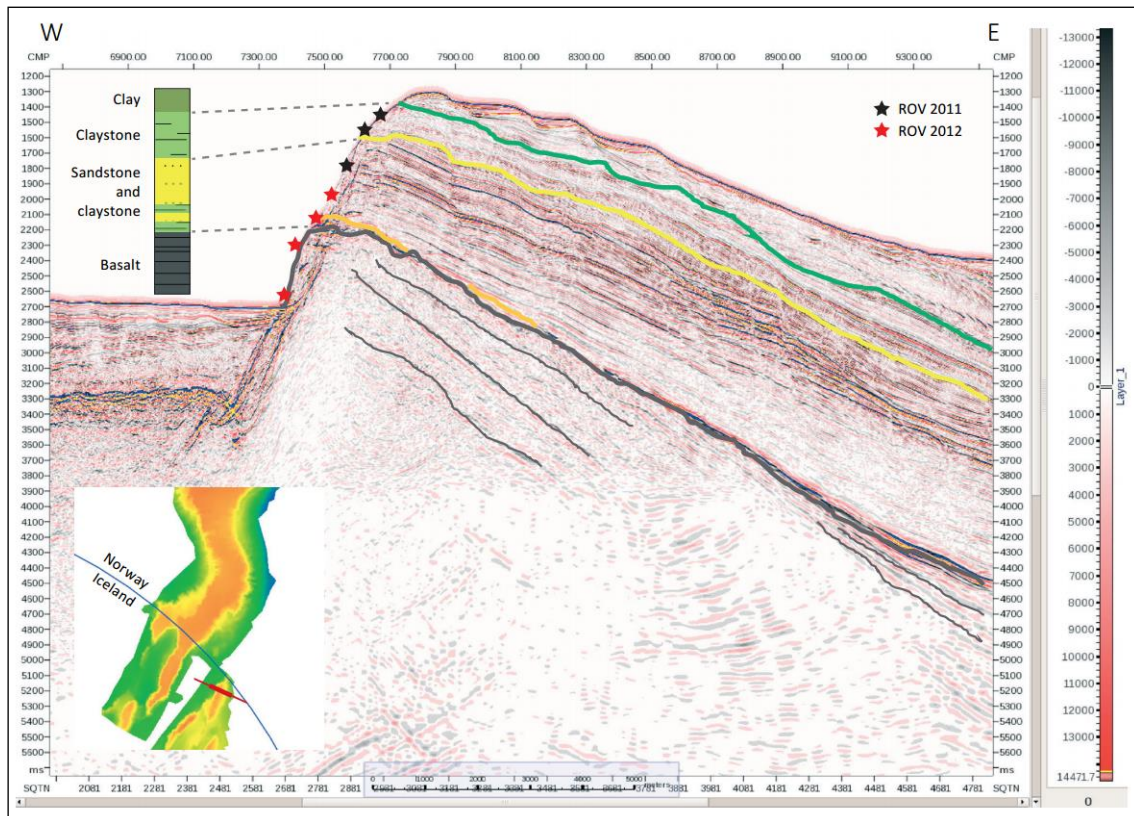


**Figure 51.** *Outcrop correlations within the Icelandic sector of the Jan Mayen Ridge of the 2012 ROV samples and the NPD2011 2D reflection seismic data.*

#### 4.2.3 TGS-VPBR seafloor sampling survey, 2011

VPBR and TGS surveyed between 2008 and 2012 several under-explored areas around Greenland (Baffin Bay, Nuuk West, Ammassalik Basin, and Northeast Greenland shelf) and the southern Jan Mayen Ridge (Figure 52 to Figure 53). Gravity coring and dredging was used to obtain extensive seabed sampling of escarpments and potential hydrocarbon seep sites.

The main focus for the sampling project was to obtain pre-breakup strata, e.g. of Jurassic, Cretaceous, or pre-breakup Paleocene section of the Paleogene. The collected rock samples were dated using biostratigraphy, and analysed for source and reservoir properties.

The sampling profile lies well within the hard outcrop area of the cliff side with high amplitude responses of multibeam data 2008 (see pink shaded area in Figure 52 & insert (a)). Uncertainty

in reference to in-situ sample locations is high for the downslope and westward locations within the sampling profile of dredge and gravity core samples, as the high amplitude rock outcrop responses appear to indicate outcrop in-situ formation, however most likely represent a pseudo-in-situ outcrop, as the entire block has moved down the slope. This can be better seen by viewing this area along a northeast to southwest profile along strike of the Sigurður ridge fault escarpment (Figure 53), it can be shown that the sampled fault escarpment is a system of down-thrown rotated normal fault blocks. Just SSW of this fault block series, a possible igneous complex is exposed at the seafloor, linked to a deep reaching NNW-SSE striking fault system.

This lowermost part of the gravity cored section has therefore to be used with caution, as here the slope base might be covered in slumped, ice-rafted, or even younger igneous material, which might explain VPBR's interpretation to observe Paleozoic up to Cretaceous formations right at the foot of slope for that fault escarpment.

NPD is interpreting the entire section as Paleocene (possibly Lower Eocene) basalt formations. In contrast, the ÍSOR-OS correlation review locates the possible Paleogene – Cretaceous boundary close to the foot of the fault escarpment (Figure 54 and Figure 55). This might support VPBR's claim that an active Jurassic oil seep had been sampled in the uppermost and youngest sediment section covering the large fault escarpment. This would be for the first time that a live hydrocarbon seep that included headspace gas, Gas chromatography–mass spectrometry (GCMS), and biomarkers analysis was detected for the JMMC area. The maturity of that Jurassic oil source was interpreted by VPBR to be within the peak-oil window.



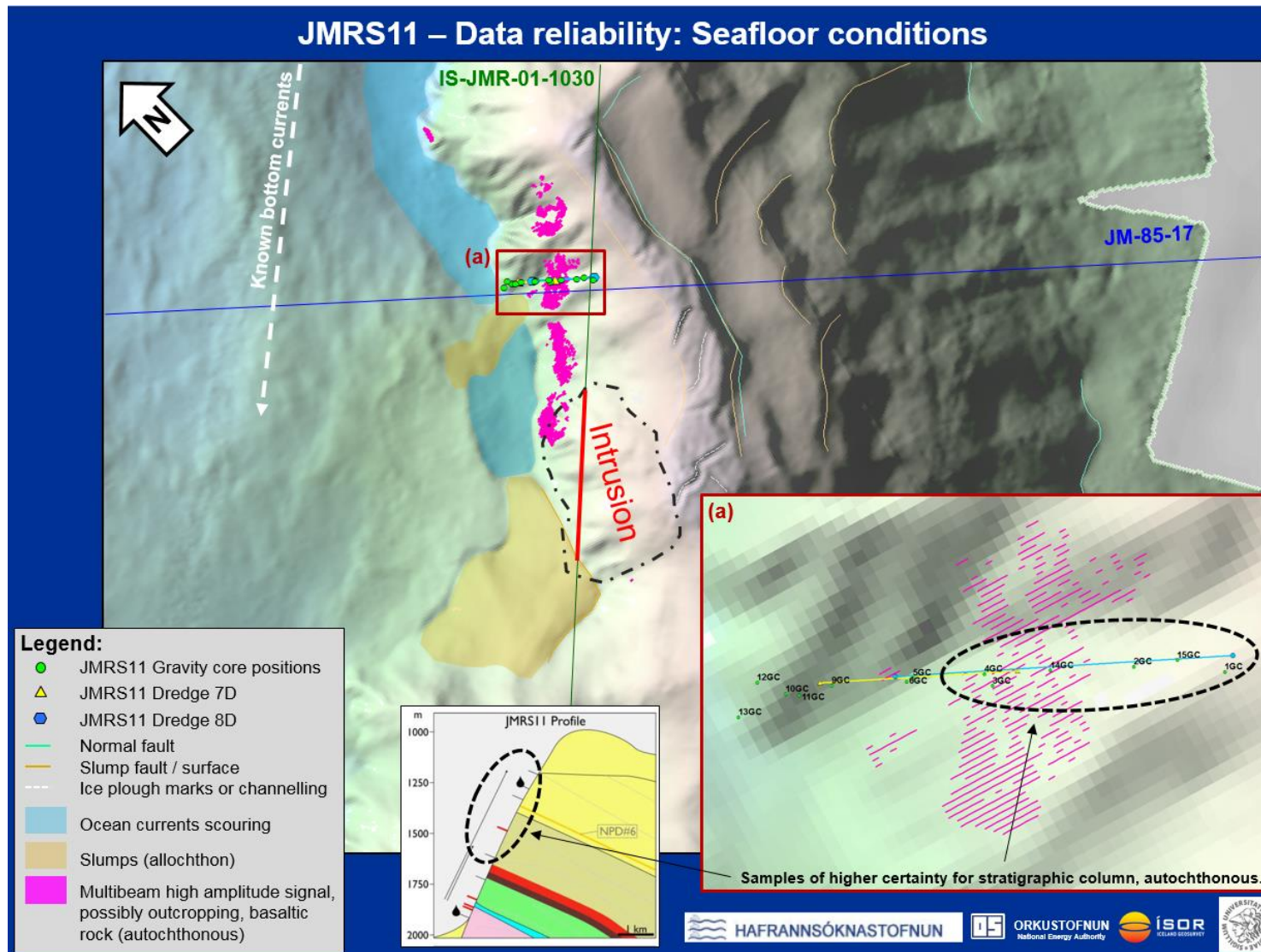
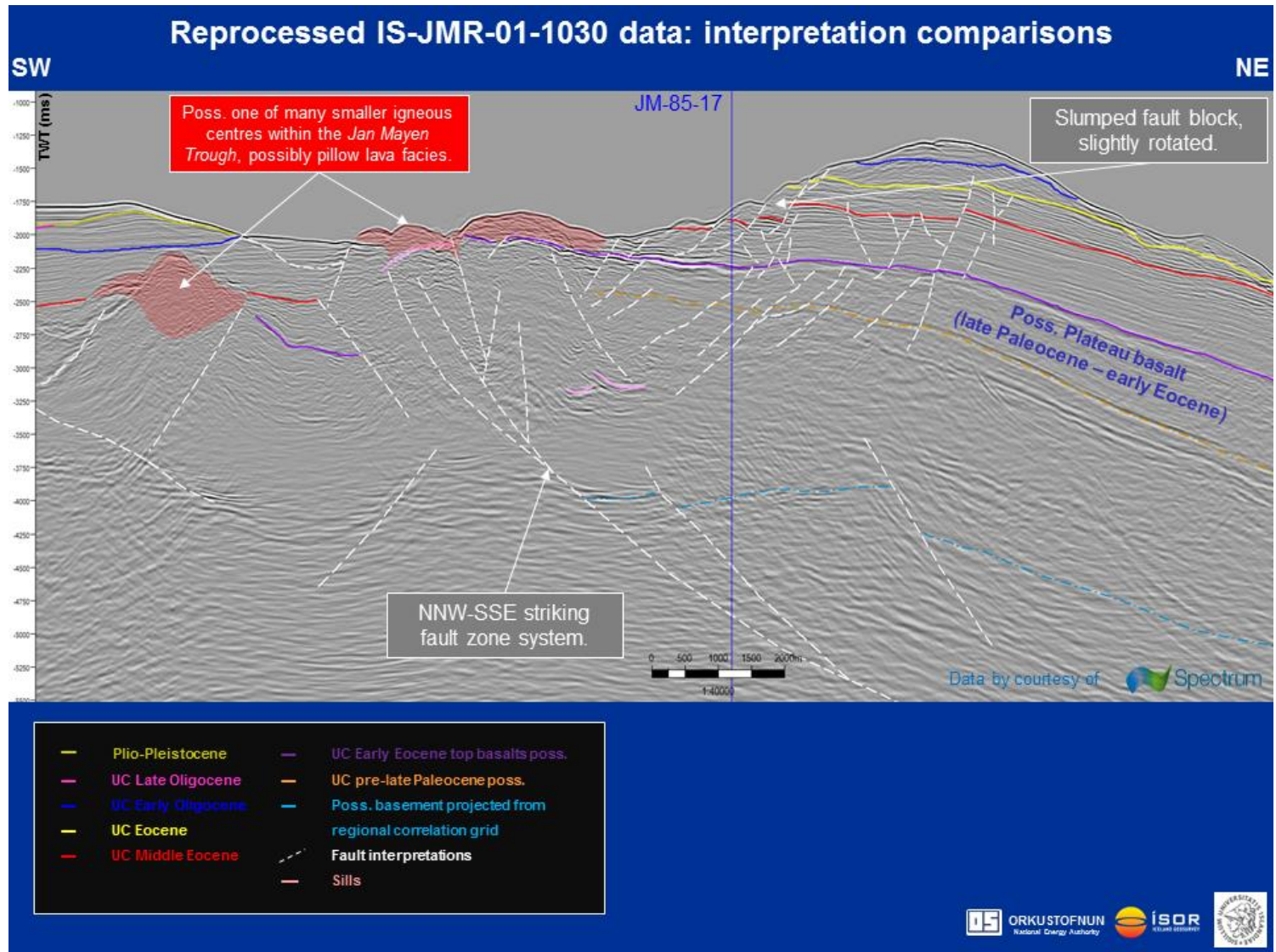
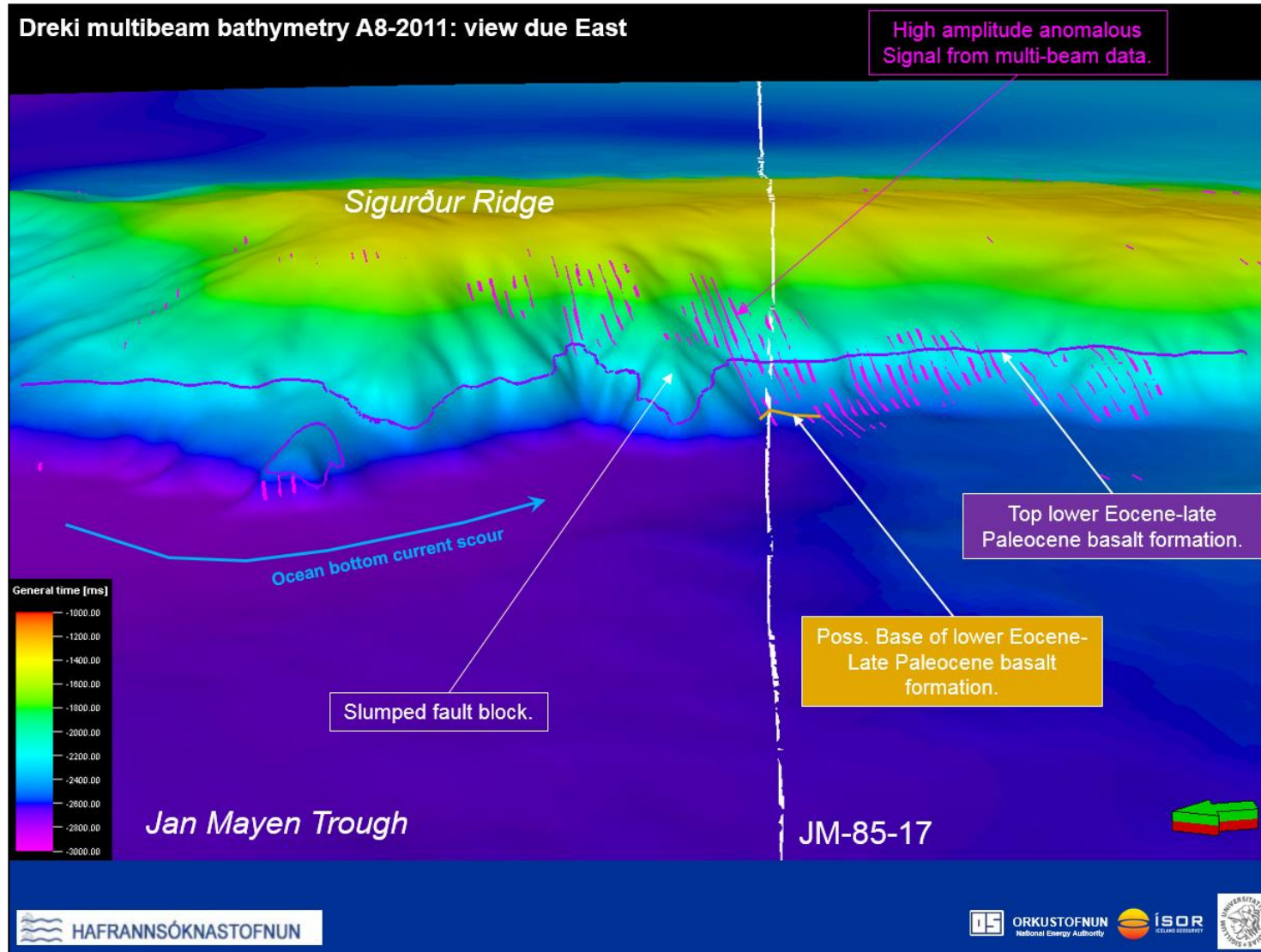


Figure 52. Local setting of the A8-2011 seafloor sampling profile by VPBR-TGS, just south of a slope spur, and possibly a large slumped block.



**Figure 53.** Northeast to southwest 2DMCS profile for the NE Dreki sampling sites NPD-VPBR, see line location in Figure 52.





**Figure 54.** Local setting of the A8-2011 seafloor sampling campaign by VPBR-TGS viewing the sampling site looking east onto the fault escarpment and well visible spur just north of the sampling profile.



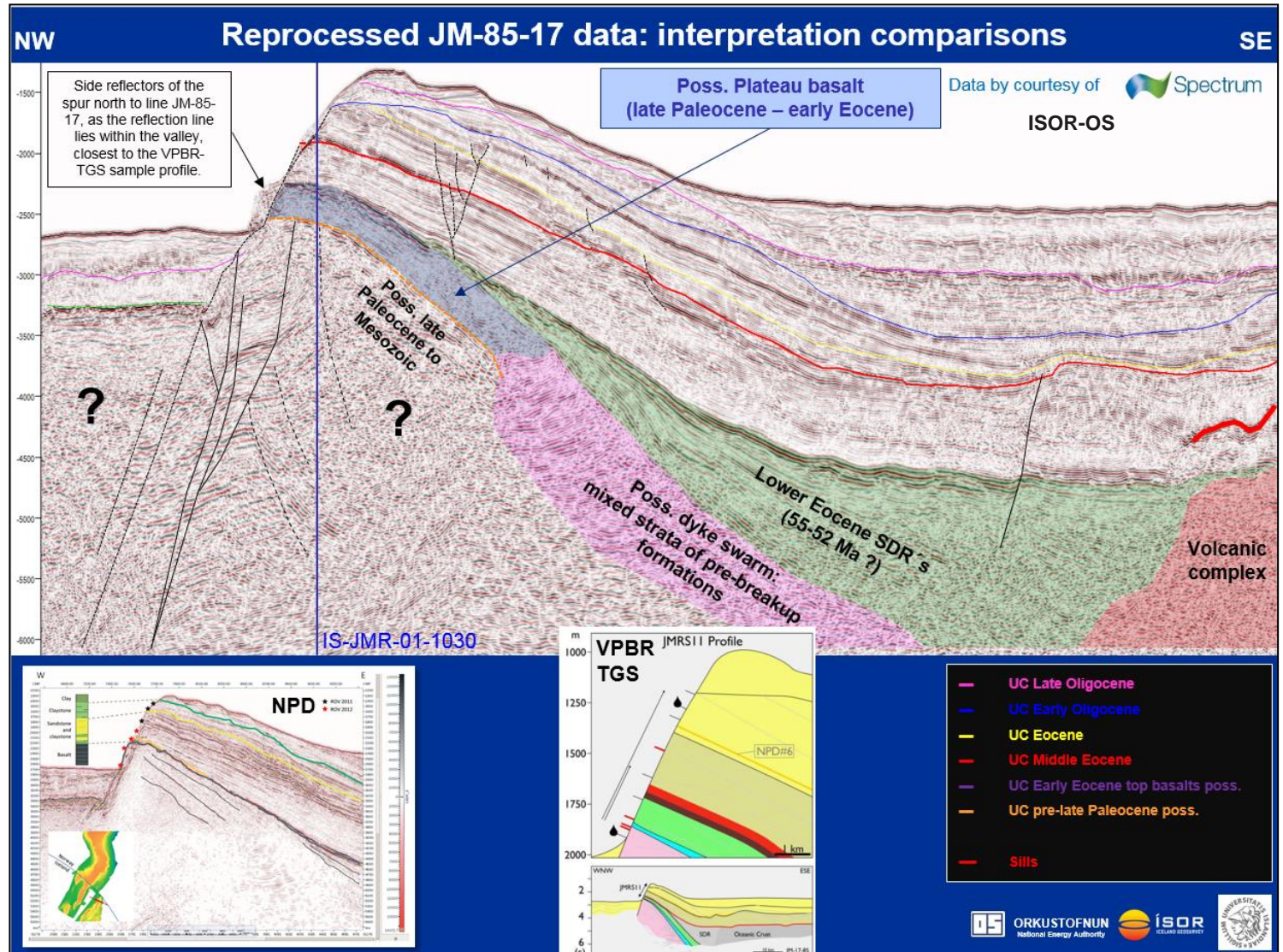


Figure 55. Interpretation comparison for the NPD, VPBR and ÍSOR-OS cases, see line location in Figure 52.

## 5 Conclusion & future recommendation for seafloor research

The purpose of this project stage was to establish a comprehensive digital database and an initial interpretation and description of the seafloor. This goal has been accomplished. This database has served as a basis for international collaboration projects as well, such as the NAG-TEC: Northeast Atlantic Geoscience Tectonostratigraphic Atlas (Hopper et al., 2014), an ongoing PhD project on the JMMC with the University of Iceland (Blischke et al., 2016), collaboration work with the NordMin project consortium (Guarnieri et al., 2016), the EMODnet project (<http://www.emodnet.eu/>), the central East Greenland-JMMC analogue mapping project (Blischke & Erlendsson, 2016) and the temperature modelling project for JMMC (Blischke et al., 2017) that are funded by the Iceland hydrocarbon research fund, and will undoubtedly be of good use in future project applications and collaborations.

Furthermore, a detailed study of the polygon faulting would be of interest, as those appear to occur within the fine-grained and on-lapping infill units at seabed. These should be compared to the Mid-Miocene section in the central lows of the sub-basins observed in the central North Sea that indicate a similar age (Dewhurst et al., 1999).

Future database additions and progresses should be summaries in add-on project reports, as this is a dynamically developing process. All future collaborations and project build up interests will have to be approved by the National Energy Authority – Orkustofnun, and the collaborating institutes, such as the Iceland Marine Institute and the University of Iceland.

In regards to seafloor sampling, there are several selection criteria that have been followed, such as:

- Faulting does extend up to the seafloor.
- Possible chimney-like features are visible in the seismic data.
- Seafloor features as revealed in multibeam bathymetric maps that might indicate possible pockmark sites.
- Indication of deep pre-Paleogene sedimentary sequences close to large fault escarpments.
- Surface slicks located by satellite remote sensing.
- Possible indication of gas in the upper reaches of the sedimentary section, such as unusual amplitude variations and possible bottom simulating reflector.
- Positive HC indications from previous studies.

Specifically the use of ROV's method was used for more accurate sample locating, as the seafloor depth can introduce a large location error, due to ocean currents and long cable sag when gravity coring. However, no clear result could be secured as the interpretation of the latest two survey groups (NPD 2011 & 2012; VPBR 2011) contradict each other, and therefore additional seafloor sampling campaigns could add new information to increase the understanding and certainty of hard rock record for the JMMC area. Eventually will only a stratigraphic borehole solve the question of the age and type of the pre-breakup igneous sedimentary stratigraphy. Future studies should not just involve additional seafloor sampling or sediment type mapping campaigns, but also hazard analysis for slump mechanisms,

shallow or deep drilling campaigns, volcanology-, detailed structural-, or paleo- and present day stress-field analysis.

## **Acknowledgements**

We would like to thank the Marine Research Institute of Iceland (MRI), especially Guðrún Helgadóttir and Páll Reynisson, for making the multibeam and backscatter data available to this study and their support with the review of the multibeam data acquisition process.

We also would like to thank the Norwegian Petroleum Directorate (NPD) for allowing us to use their newest 2D multichannel reflection data sets from 2011 & 2012.

Additionally, we would like to thank Spectrum AS for their continued support, and allowing us to use their reprocessed 2D multichannel reflection seismic data.



## 6 References

- Åkermoen, T. (1989). *Jan Mayen-ryggen: et seismisk stratigrafisk og strukturelt studium*. Cand. scient. thesis, University of Oslo, 174 pp.
- Becker, J.J., Sandwell, D.T., Smith, W.H.F., Braud, J., Binder, B., Depner, J., Fabre, D., Factor, J., Ingalls, S., Kim, S-H., Ladner, R., Marks, K., Nelson, S., Pharaoh, A., Trimmer, R., Von Rosenberg, J., Wallace, G. and Weatherall, P. (2009). Global Bathymetry and Elevation Data at 30 Arc Seconds Resolution: SRTM30\_PLUS, *Marine Geodesy*, 32:4, 355–371.
- Bezrukov, P.L., Yemelyanov, Ye.M., Lisitzin, A.P. and Romankevich, Ye.A. (1977). Organic carbon in the upper sediment layer of the world ocean. *Oceanology*, 17, 561–564.
- Blischke, A. and Erlendsson, Ö. (2016). *Jan Mayen Microcontinent Analogue Study – The Jameson Land Basin. Project Review, Database and Structural Mapping*. Iceland GeoSurvey, ÍSOR-2016/074, 49 pp.
- Blischke, A., Gaina, C., Hopper, J. R., Péron-Pinvidic, G., Brandsdóttir, B., Guarnieri, P., Erlendsson, Ö. and K. Gunnarsson (2016). The Jan Mayen microcontinent: an update of its architecture, structural development and role during the transition from the Ægir Ridge to the mid-oceanic Kolbeinsey Ridge. *Geological Society, London, Special Publications*, 447, first published on September 8, 2016, doi:10.1144/SP447.5.
- Blischke, A., Gunnarsson, K. and Arnarsson, Th.S. (2010). *Site location planning for the sea-floor coring campaign of the southern Jan Mayen Ridge, summer 2010*. Iceland GeoSurvey and National Energy Authority of Iceland, short report, ÍSOR-10090, 54 pp.
- Blischke, A., Millett, J.M., Iyer, K. and Schmid, D.W. (2017). *Temperature modelling of the Jan Mayen Micro Continent: quantifying the thermal influence of igneous activity associated with a dual rift system on a potential hydrocarbon system. Project mid-term status summary*. Iceland GeoSurvey, short report, ÍSOR-17063, pp. 11.
- Brandsdóttir, B., Detrick, R., Helgadóttir, G., Kjartansson, E., Richter, B., Riedel, C. and Larry Meyer (2002). *Tectonics of the Tjörnes Fracture Zone and Southern Kolbeinsey Ridge, N-Iceland. Multibeam Bathymetric Surveys 2002–2004*.
- Brandsdóttir, B., Hooft, E., Mjelde, R. and Murai, Y. (2015). Origin and evolution of the Kolbeinsey Ridge and Iceland Plateau, N-Atlantic. *Geochemistry, Geophysics, Geosystems* 16, 612–634.
- Brandsdóttir, B., Richter, B., Kjartansson, E., Riedel, C., Dahm, T., Helgadóttir, G., Detrick, R., Magnússon, Á., Ásgrímsson, Á., Pálsson, B.H., Karson, J.A., Sæmundsson, K., Mayer, L., Calder, B. and Driscoll N. (2004). Tectonic details of the Tjörnes Fracture Zone, an onshore-offshore ridge-transform in N-Iceland. *Eos Trans. AGU* 85 (47), F1071.
- Breivik, A.J., Mjelde, R., Faleide, J.I. and Murai, Y. (2012). The eastern Jan Mayen microcontinent volcanic margin. *Geophysical Journal International*, 188 (3), 798–818.
- Breivik, A. J., R. Mjelde, J. I. Faleide, and Y. Murai (2006). Rates of continental breakup magmatism and seafloor spreading in the Norway Basin-Iceland plume interaction, *Journal of Geophysical Research*, 111 (B07102), doi: doi:10.1029/2005JB004004.

- Brogi, A. (2011). Variation in fracture patterns in damage zones related to strike-slip faults interfering with pre-existing fractures in sandstone (Calcione area, southern Tuscany, Italy). *Journal of Structural Geology* 33, 644-661.
- Dewhurst, D.N., Cartwright, J.A. and Lonergan, L. (1999). The development of polygonal fault systems by syneresis of colloidal sediments. *Marine and Petroleum Geology* 16, 793-810.
- Erlendsson, Ö. (2010). *Seismic Investigation of the Jan Mayen Ridge - with a close study of sill intrusions*. 111 pp., Aarhus Universitet.
- Ferriday, I.L. (2010). *Surface Geochemical Survey for Orkustofnun: JAN MAYEN RIDGE A11 AREA 2010*. Proprietary Study prepared for Orkustofnun by Fugro Geolab Nor AS, PO Box 5740, 7437 Trondheim, Norway.
- Gay, A. and Berndt, C. (2006). Role of polygonal faults on sedimentary fabric of unconsolidated sediments: implications for compaction and fluid migration. *EGU, Geophysical Research Abstracts, Vol. 8*, 03077.
- Geodekyan, A.A., Verkhovskaya, Z.I. Sudin, A.V. and Trotsiuk, V.Ya. (1980). Gases in seawater and bottom sediments. Chapter 10 of: *Iceland and Mid-Oceanic Ridge, Academy of Sciences of the USSR Soviet Geophysical Committee*. Published in English by "The National Research Council", Reykjavík, Iceland, October 1980.
- Gairaud, H., Jacquart, G., Aubertin, F. and Beuzart, P. (1978). The Jan Mayen Ridge synthesis of geological knowledge and new data. *Oceanological acta 1978, Vol. 1, No. 3*, 335-358.
- Gernigon, L., Blischke, A., Nasuti, A. and Sand, M. (2014). *Conjugate volcanic rifted margins, spreading and micro-continent: Lessons from the Norwegian-Greenland Sea*. ÍSOR, Orkustofnun, Norwegian Petroleum Directorate, Norwegian Geological Service, Trondheim, Norway, NGU2014.028, p. 49.
- Gernigon, L., Blischke, A., Nasuti, A., and Sand, M. (2015). Conjugate volcanic rifted margins, seafloor spreading, and microcontinent: Insights from new high-resolution aeromagnetic surveys in the Norway Basin. *Tectonics* 34, 907-933.
- Grønlie, G., Talwani, M. and Chapman, M. (1979). Geophysical studies in the Norwegian-Greenland Sea. *Norsk Polarinstitutt, skrifter nr. 170*, Oslo 1979.
- Guarnieri, P., Brethes, A., Rasmussen, T.M., Blischke, A., Erlendsson, Ö. & Bauer, T. (2016). CRUSMID-3D Crustal Structure and Mineral Deposit Systems: 3D-modelling of base metal mineralization in Jameson Land (East Greenland). Copenhagen: Nordisk Ministerråd, 2017., 182 p., DOI: 10.6027/TN2016-562 (<http://norden.diva-portal.org/smash/get/diva2:1066963/FULLTEXT02.pdf>).
- Gunnarsson, K. (1995). *Towards the planning of the 1995 Iceland Plateau project*. Orkustofnun, short report, KG-95-03, 26 pp.
- Gunnarsson, K., Sand, M. and Gudlaugsson, S.T. (1989). *Geology and hydrocarbon potential of the Jan Mayen Ridge*. Orkustofnun, Reykjavík, OS-89036/JHD-07 and Norwegian Petroleum Directorate, Stavanger, OD-89-91, 156 pp.
- Helgadóttir, G. (2008a). *Preliminary results from the 2008 Marine Research Institute multibeam survey in the Dreki area, with some examples of potential use*. Iceland Exploration Conference 2008, Reykjavík, Iceland.

- Helgadóttir, G. (2008b). *The Marine Research Institute's Cruises in the Dreki Area in the Summer of 2008*. Iceland Exploration Conference 2008. The Marine Research Institute, Iceland.
- Helgadóttir, G. and Reynisson, P. (2010). *Setkjarnataka, fjölgeisla- og lágtíðnidýptarmælingar á Drekasvæði og Jan Mayen hrygg á rs. Árna Friðrikssyni RE 200 haustið 2010*. Prepared for Orkustofnun and Norsku Olíustofnunina, Hafrannsóknastofnunin, Leiðangursskýrsla A201011, hluti 1 og 2, 17. ágúst –15. september 2010, Reykjavík, Ísland.
- Hinz, K. and Schlüter (1979). The North Atlantic – results of geophysical investigations by the Federal Institute for Geoscience and Natural Resources on North Atlantic continental margins. *Erdoel-Erdgas-Zeitschrift*, 94, 271–280.
- Hooft, E.E.E., Brandsdóttir, B., Mjelde, R., Shimamura, H. and Murai, Y. (2006). Asymmetric plume-ridge interaction around Iceland: The Kolbeinsey Ridge Iceland. Seismic Experiment, *Geochem. Geophys. Geosyst.*, 7, Q05015, doi:10.1029/2005GC001123.
- Hopper, J.R., Funck, T., Stocker, M., Ártíng, U., Peron-Pinvidic, G., Doornenbal, H. and Carmen Gaina (2014). *TECTONOSTRATIGRAPHIC ATLAS of the North-East Atlantic Region*. © By the NAGTEC Group, GEUS, Copenhagen, Denmark.
- Johansen, B., Eldholm, O., Talwani, M., Stoffa, P.L. and Buhl, P. (1988). Expanding spread profile at the northern Jan Mayen Ridge. *Polar Research*, 6, 95–104.
- Jónsdóttir, I. and Valdimarsson, Á.F. (2009). *Searching for natural oil seepage in the Dreki area using ENVISAT radar images*. Prepared for Orkustofnun, OS-2009/001. Faculty of Earth Sciences, School of Engineering and Natural Sciences, University of Iceland.
- Judd, A., Long, D. & Sankey, M. (1994). Pockmark formation and activity, U.K. block 15/25, North Sea. *Bulletin of the Geological Society of Denmark*, vol. 41, 34–49.
- Kandilarov, A., Mjelde, R., Pedersen, R.B., Hellevang, B., Papenberg, C., Petersen, C.J., Planert, L. and Flueh, E. (2012). The northern boundary of the Jan Mayen microcontinent, North Atlantic determined from ocean bottom seismic, multichannel seismic, and gravity data. *Marine Geophysical Research* 33, 55–76.
- Kodaira, S., Mjelde, R., Gunnarsson, K., Shiobara, H. and Shimamura, H. (1998). Structure of the Jan Mayen microcontinent and implications for its evolution. *Geophysical Journal International*, Blackwell Science Ltd, 1998, 132, 383–400.
- Mjelde, R., T. Raum, A. J. Breivik, and J. I. Faleide (2008). Crustal transect across the North Atlantic, *Marine Geophysical Research*, 29 (2), 73–87, doi: 10.1007/s11001-008-9046-9.
- Mjelde, R., Aurvåg, R., Kodaira, S., Shimamura, H., Gunnarsson, K., Nakanishi, A. and Shiobara, H. (2002). Vp/Vs-ratios from the central Kolbeinsey Ridge to the Jan Mayen Basin, North Atlantic; implications for lithology, porosity and present-day stress field. *Marine Geophysical Researches*, 23, 123–145.
- Mjelde, R., Eckhoff, I., Solbakken, S., Kodaira, S., Shimamura, H., Gunnarsson, K., Nakanishi, A. and Shiobara, H. (2007). Gravity and S-wave modelling across the Jan Mayen Ridge, North Atlantic; implications for crustal lithology. *Marine Geophysical Researches*, 28, 27–41.
- Mork, K.A., Drinkwater, K.F., Jónsson, S., Valdimarsson, H. and Ostrowski, M. (2014). Watermass exchanges between the Norwegian and Iceland seas over the Jan Mayen Ridge using in-situ current measurements. *Journal of Marine Systems* 139 (2014) 227–240. <http://dx.doi.org/10.1016/j.jmarsys.2014.06.008>.



- Mutter, J.C., Talwani, M. and Stoffa, P.L. (1984). Evidence for a Thick Oceanic Crust Adjacent to the Norwegian Margin. *Journal of Geophysics, Res.* 89 (B1), doi: 10.1029/JB089iB01p00483.
- Olafsson, I. and Gunnarsson, K. (1989). *The Jan Mayen ridge: velocity structure from analysis of sonobuoy data*. Orkustofnun, Reykjavík, OS-89030/JHD-04, 62 pp.
- Peron-Pinvidic, G., Gernigon, L., Gaina, C. and Ball, P. (2012a). Insights from the Jan Mayen system in the Norwegian-Greenland Sea - I: mapping of a microcontinent. *Geophysical Journal International*, 191, 385-412.
- Peron-Pinvidic, G., Gernigon, L., Gaina, C. and Ball, P. (2012b). Insights from the Jan Mayen system in the Norwegian-Greenland Sea - II: architecture of a microcontinent. *Geophysical Journal International*, 191, 413-435.
- Richter, B. and Guðlaugsson, S. Th. (2007). *Yfirlit um jarðfræði Jan Mayen svæðisins og hugsanlegar kolvetnislindir*. Iceland GeoSurvey, ÍSOR-2007/004, 33 pp.
- Sandstå, N.R., Pedersen, R.B., Williams, R., Bering, D., Magnus, C., Sand, M. and Brekke, H. (2012). *Submarine fieldwork on the Jan Mayen Ridge; integrated seismic and ROV –sampling*. Norwegian Petroleum Directorate & University of Bergen, project presentation, Stavanger, Norway.
- Sandstå, N.R., Sand, M. and Brekke, H. (2013). *Ressursrapporter 2013, Kapittel-7 Jan Mayen*. Norwegian Petroleum Directorate, project web publication, Stavanger, Norway.
- Shipley, T., Gahagan, L., Johnson, K., and Davis, M. (editors) (2012). *Seismic Data Center*. University of Texas, Institute for Geophysics. URL = <http://www.ig.utexas.edu/sdc/>
- Talwani, M. and Eldholm, O. (1977). Evolution of the Norwegian-Greenland Sea. *Geological Society of America Bulletin*, 88, 969-999.
- Talwani, M. and Udintsev, G. (1976). *Initial Reports of the Deep Sea Drilling Project*. U.S. Government Printing Office, Washington, 1256 pp.
- Talwani, M., Mutter, J. and Hinz, K. (1981). Initiation of opening of the Norwegian Sea. *Oceanology Acta 1981, N°SP*, 23-30.
- Tibaldi, A., Bonalia, F.L., Einarsson, P., Hjartardóttir, Á.R. and Pasquarè Mariottoc, F.A. (2016). Partitioning of Holocene kinematics and interaction between the Theistareykir Fissure Swarm and the Husavik-Flatey Fault, North Iceland. *Journal of Structural Geology, Volume 83, February 2016*, 134-155.
- Udintsev, C.B. (1980). *Iceland and mid-oceanic ridge – structure of the ocean-floor*. Academy of science of the USSR, Soviet geophysical committee, results and research on the international geophysical project.
- Vogt, P.R., Johnson, G.L. and Kristjánsson, L. (1980). Morphology and Magnetic-Anomalies North of Iceland. *Journal of Geophysics-Zeitschrift Fur Geophysik*, 47, 67-80.

## 7 Additional references

- Amante, C., and B. W. Eakins (2009). *ETOPO1 1 Arc-minute Global Relief Model: Procedures, Data Sources and Analysis, Technical Memorandum NESDIS NGDC-24*, 25 pp, National Oceanographic and Atmospheric Administration.
- Bojesen-Koefoed, J.A., Petersen, H.I., Finn Surlyk, F. and Vosgerau, H. (1997). Organic petrography and geochemistry of inertinite-rich mudstones, Jakobsstigen Formation, Upper Jurassic, northeast Greenland: Indications of forest fires and variations in relative sea-level. *International Journal of Coal Geology, Volume 34, Issues 3-4*, December 1997, Pages 345-370.
- Crosby, A. G. and D. McKenzie (2009). An analysis of young ocean depth, gravity and global residual topography, *Geophysical Journal International*, 178 (3), 1198–1219.
- Dam, G., Surlyk, F., Mathiesen, A. and Christiansen, F.G. (1995). Exploration significance of lacustrine forced regressions of the Rhaetian-Sinemurian Kap Stewart Formation, Jameson Land, East Greenland. *Norwegian Petroleum Society Special Publications, Volume 5*, 1995, 511–527.
- Dam, G. and Christiansen, F.G. (1990). Organic geochemistry and source potential of the lacustrine shales of the Upper Triassic - Lower Jurassic Kap Stewart Formation, East Greenland. *Marine and Petroleum Geology, Volume 7, Issue 4*, November 1990, 428–443.
- Danielson, J. J. and D. B. Gesch (2011). *Global Multi-resolution Terrain Elevation Data 2010 (GMTED2010)*, Open-File Report 2001-1073, 34 pp, United States Geological Survey.
- Ekholm, S. (1996). A full coverage, high-resolution, topographic model of Greenland computed from a variety of digital elevation data. *Journal of Geophysical Research*, 101(B10), 21961–21972.
- Hell, B., and M. Jakobsson (2011). Gridding heterogeneous bathymetric data sets with stacked continuous curvature splines in tension. *Marine Geophysical Researches*, 32 (4), 493–501.
- Jakobsson, M., Mayer, L., Coakley, B., Dowdeswell, J.A., Forbes, S., Fridman, B., Hodnesdal, H., Noormets, R., Pedersen, R., Rebesco, M., Schenke, H.W., Zarayskaya, Y., Accettella, D., Armstrong, A., Anderson, R.M., Bienhoff, P., Camerlenghi, A., Church, I., Edwards, M., Gardner, J.V., Hall, J.K., Hell, B., Hestvik, O., Kristoffersen, Y., Marcussen, C., Mohammad, R., Mosher, D., Nghiem, S.V., Pedrosa, M.T., Travaglini, P.G. and Weatherall, P. (2012). The International Bathymetric Chart of the Arctic Ocean (IBCAO) Version 3.0, *Geophysical Research Letters*, 39 (12).
- Krabbe, H. (1996). Biomarker distribution in the lacustrine shales of the Upper Triassic-Lower Jurassic Kap Stewart Formation, Jameson Land, Greenland. *Marine and Petroleum Geology, Volume 13, Issue 7*, November 1996, 741–754.
- Olesen, O., Brønner, M., Ebbing, J., Gellein, J., Gernigon, L., Koziel, J., Lauritsen, T., Myklebust, R., Pascal, C. and M. Sand (2010). New aeromagnetic and gravity compilations from Norway and adjacent areas: methods and applications, in *Petroleum Geology, From Mature Basins to New Frontiers* (edited by B. Vining and S. C. Pickering), Proceedings of the 7th Petroleum Geology Conference, 559–586, Geological Society of London.

- Parsons, B. and Sclater, J.G. (1977). An analysis of the variation of ocean floor bathymetry and heat flow with age. *Journal of Geophysical Research*, 82 (5), 803–827.
- Polteau, S., Planke, S., Myklebust, R. and Hickman, G. (2013). Seabed Sampling for Stratigraphy and Seep Studies Offshore Greenland and Norway. *75th EAGE Conference & Exhibition incorporating SPE EUROPEC 2013 London, UK, 10-13 June 2013*.
- Richter, B. (2001). *Kjarnaborun í Tjörnissetlögin til að meta þroska lífrænna efna. Áfangaskýrsla 14255*. Orkustofnun, OS-2001/051 29.
- Wessel, P., Smith, W.H., Scharroo, R., Luis, J. and Wobbe, F. (2013). Generic Mapping Tools: Improved Version Released, *Eos. Transactions American Geophysical Union*, 94(45), 409–410.

## Other recourses

<http://earthquake.usgs.gov/learn/glossary/?term=fault>

<http://earthquake.usgs.gov/learn/glossary/?term=surface%20faulting>

<http://landslides.usgs.gov/learn/l101.php>

<http://oceanexplorer.noaa.gov/oceanos/explorations/ex1104/logs/aug12/aug12.html>

[http://topex.ucsd.edu/WWW\\_html/srtm30\\_plus.html](http://topex.ucsd.edu/WWW_html/srtm30_plus.html)

<http://www.boem.gov/Seismic-Water-Bottom-Anomalies-Map-Gallery/>

<http://www.earthmagazine.org/article/slippery-slopes-how-do-we-insure-against-landslides>

<http://www.nature.nps.gov/geology/usgsnps/deform/gchangft.html>

<http://www.nauticalcharts.noaa.gov/hsd/multibeam.html>